Systematic Entomology

Royal Entomological Society

Systematic Entomology (2022), **47**, 113–151 DOI: 10.1111/syen.12522

Phylogeny, evolution, and classification of the ant genus *Lasius*, the tribe Lasiini and the subfamily Formicinae (Hymenoptera: Formicidae)

BRENDON E. BOUDINOT[1,2], MAREK L. BOROWIEC[1,3,4] and MATTHEW M. PREBUS[1,5]

[1]Department of Entomology and Nematology, University of California, Davis CA, U.S.A., [2]Friedrich-Schiller-Universität Jena, Institut für Spezielle Zoologie, Jena, Germany, [3]Department of Plant Pathology, Entomology and Nematology, University of Idaho, Moscow ID, U.S.A., [4]Institute for Bioinformatics and Evolutionary Studies, University of Idaho, Moscow ID, U.S.A. and [5]School of Life Sciences, Arizona State University, Tempe AZ, U.S.A.

Abstract. Within the Formicidae, the higher classification of nearly all subfamilies has been recently revised given the findings of molecular phylogenetics. Here, we integrate morphology and molecular data to holistically address the evolution, classification, and identification of the ant genus *Lasius*, its tribe Lasiini, and their subfamily Formicinae. We find that the crown Lasiini originated around the end of the Cretaceous on the Eurasian continent and is divisible into four morphologically distinct clades: *Cladomyrma*, the *Lasius* genus group, the *Prenolepis* genus group, and a previously undetected lineage we name *Metalasius* **gen.nov.**, with one extant species *M. myrmidon* **comb. nov.** and one fossil species, †*M. pumilus* **comb. nov.** The crown of the *Lasius* genus group is considerably younger than that of the *Prenolepis* genus group, indicating that extinction has played a major role in the evolution of the former clade. *Lasius* itself is divided into two well-supported monophyletic groups, which are approximately equally speciose. We present evidence that temporary social parasitism and fungiculture arose twice independently in *Lasius*. In addition, we recover the paraphyly of three *Lasius* subgenera and propose replacing all subgenera with an informal species group classification: *Lasius* = *Acanthomyops* **syn.rev.**, = *Austrolasius* **syn.nov.**, = *Cautolasius* **syn.nov.**, = *Chthonolasius* **syn.nov.**, = *Dendrolasius* **syn.nov.** Total-evidence analysis reveals that the Baltic-region amber fossil species †*Lasius pumilus* and †*Pseudolasius boreus* are misplaced to genus; we, therefore, create *Sussuido* **gen. nov.** to accomodate †*S. boreus* **comb. nov.** and transfer †*L. pumilus* to *Metalasius*. Further, we transfer †*Sussudio* and †*Glaphyromyrmex* out of the Lasiini, considering the former to be *incertae sedis* in the subfamily, and the latter a member of the Formicini (**tribal transfer**). Two final taxonomic actions are deemed necessary: synonymy of *Lasius escamole* with *Liometopum apiculatum* **syn.nov.** (**subfamilial transfer**), and transfer of *Paratrechina kohli* to *Anoplolepis* (**tribal transfer**, forming *A. kohli* **comb.nov.**).

ZooBank Article LSID: urn:lsid:zoobank.org:pub:016059BA-33C3-43B2-ADAD-6807DC5CB6D8
Author ZooBank LSIDs: Borowiec: urn:lsid:zoobank.org:author:411B711F-605B-4C4B-ABDB-D4D96075CE48.
Boudinot: urn:lsid:zoobank.org:author:919F03B0-60BA-4379-964D-A56EB582E16D.
Prebus: urn:lsid:zoobank.org:author:1A6494C7-795E-455C-B66F-7F6C32F76584

Correspondence: Matthew M. Prebus, Department of Entomology and Nematology, University of California, Davis, CA, U.S.A. E-mail: mprebus@gmail.com

All authors contributed equally.

Introduction

Ant taxonomy is a rapidly transforming field, incorporating studies across data types and systematic methodologies. Built from the synthesis of all species-level and higher taxonomic works on the Formicidae, the morphology-based systematic hypotheses of Brown (e.g., Brown Jr., 1954; see also Keller, 2011) and Bolton (e.g., Bolton, 1990a, 1990b, 1990c, 1994, 1995, 2003) were first tested using parsimony methods (e.g., Ward, 1990, 1994; Agosti, 1991; Baroni Urbani *et al.*, 1992; Shattuck, 1992, 1995; Lattke, 1994; Grimaldi *et al.*, 1997; Agosti *et al.*, 1999; Keller, 2000) followed by likelihood-based and Bayesian phylogenetics (e.g., Felsenstein, 1983, 1988, 2001, 2003). Whereas a minority of ant phylogenetic studies combined morphological and multi-locus data (Ward & Brady, 2003; Astruc *et al.*, 2004; Janda *et al.*, 2004; Ward & Downie, 2005; Maruyama *et al.*, 2008) and/or included fossils as terminals (Prebus, 2017; Barden *et al.*, 2017a), most phylogenetic studies have only utilized data from Sanger-sequenced loci (e.g., Brady *et al.*, 2006; Moreau *et al.*, 2006; Ward *et al.*, 2010, 2015; Ward & Fisher, 2016; Borowiec *et al.*, 2019). More recently, high-throughput sequencing platforms enabled genomic approaches to ant systematics, such as targeted enrichment of ultraconserved elements (UCEs) (e.g., Blaimer *et al.*, 2015, 2016, 2018; Faircloth *et al.*, 2015; Jesovnik *et al.*, 2017; Prebus, 2017, 2021; Branstetter *et al.*, 2017a, 2017b, 2017c; Sosa-Calvo *et al.*, 2018; Borowiec, 2019; Branstetter & Longino, 2019), RADseq (Fischer *et al.*, 2015; Darwell *et al.*, 2019; Liu *et al.*, 2020), and transcriptomics (Jesovnik *et al.*, 2016, Romiguier *et al.* 2018). Here, we employ an array of phylogenetic methods, including traditional comparative morphology, total-evidence divergence dating (Ronquist *et al.*, 2012a, 2016), phylogeographic analysis (Bouckaert *et al.*, 2014; Matzke 2013), ancestral state estimation (Paradis *et al.*, 2004; Paradis & Schliep, 2018), and species tree estimation (Mirarab & Warnow, 2015) to holistically address the phylogeny, evolution, and classification of the genus *Lasius* Fabricius, its tribe Lasiini Ashmead, and the subfamily Formicinae Lepeletier de Saint-Fargeau (see Table 1 for a summary of our questions and methods).

Lasius is a northern temperate ant genus that is important in terms of its relative ecological impact and as a model for studying social insect biology. For example, *Lasius* was a frequent choice in both early and recent work on pheromone communication (Bergström & Löfqvist, 1970; Holman *et al.*, 2013), dominance hierarchy, competition, and succession in ant communities (Pontin, 1961; Traniello & Levings, 1986; Markó & Czechowski, 2004; Parr & Gibb, 2010), and the evolution of social parasitism (Hasegawa, 1998; Janda *et al.*, 2004), among other topics (Hölldobler & Wilson, 1990; Quque & Bles, 2020). *Lasius* ants are particularly known for well-documented symbioses with honeydew-producing insects and for temporary social parasitism. The latter phenomenon is a mode of colony foundation for many species of *Lasius*, and involves parasite queens invading nests of other *Lasius*, killing the host queen and using subordinated workers to raise the first batch of their own workers. This is followed by attrition of the host and eventually a colony consisting solely of parasite conspecifics. Social parasitism is known in species currently classified in subgenera *Austrolasius* Faber, *Acanthomyops* Mayr, *Chthonolasius* Ruzsky, and *Dendrolasius* Ruzsky (Hölldobler & Wilson, 1990; Buschinger, 2009; Raczkowski & Luque, 2011). Certain species of the subgenera *Chthonolasius* and *Dendrolasius* are known to use ascomycete fungi to bind masticated wood and soil to reinforce nest walls. This association is considered an example of fungiculture because the ants provide the fungi with honeydew and prevent overgrowing by competing fungal species (Schlick-Steiner *et al.*, 2008).

Historically, *Lasius* was split by Fabricius (1804) from Linnaeus's (1758) all-encompassing genus *Formica* based on features of the mouthparts; Latreille (1809) soon after erected the family Formicidae for the ant genera known at the time. The first tribal classification of the family is attributed to the hymenopterist Amédée Michel Louis Lepeletier de Saint-Fargeau (1835), who recognized *les Formicites*, a precursor to the modern Formicinae. Lepeletier de Saint-Fargeau's classification of ants incorporated information on wing venation (Lepeletier de Saint-Fargeau, 1836). Later investigators relied on natural history, external morphology, as well as internal anatomy, especially that of the proventriculus, which is a valve located between the crop and midgut of ants and other insects (e.g., Eisner, 1957). A relatively stable supra-generic classification of the subfamily emerged around the turn of the prior century (Forel, 1878, 1886, 1912; Emery, 1895, 1925), which was used until the beginning of the 1990s. Agosti (1991) provided a critical reassessment of this system and used new exoskeletal characters to diagnose four informal genus groups in the Formicinae. Expanding on Agosti's scepticism and system, Bolton (2003) divided the Formicinae into a total of 11 morphologically defined tribes, which were placed in the 'lasiine' and 'formicine' tribe groups, with three and six tribes, respectively, plus two unplaced tribes.

Over the past two decades, ant classification has increasingly become reliant on phylogenetic trees inferred from molecular data, with subsequent morphological revisionary work. The Formicinae is no exception: Blaimer *et al.* (2015) provided a comprehensive molecular phylogenetic study of the subfamily, which was used for a morphological reassessment of its tribal classification, emphasizing the hyperdiverse Camponotini Forel (Ward *et al.*, 2016; Ward & Boudinot, 2021). Like Bolton (2003), Ward *et al.* (2016) also recognized 11 tribes, for which the generic composition of most remained largely unchanged. The notable exceptions included tribes Lasiini, Melophorini Forel, and Plagiolepidini Forel, whose scope was substantially revised but for which no updated morphological circumscription was provided. Within the Lasiini, the modern taxonomy of *Lasius* was initiated by Wilson's revision of the genus (Wilson, 1955), for which six subgenera have been recognized (Ward, 2005). Monophyly of the subgenera has not been questioned except for the nominotypical subgenus (Janda *et al.*, 2004; Maruyama *et al.*, 2008; see Fig. 1A–C), but the monophyly of *Lasius* was cast into doubt by Blaimer *et al.* (2015), whose analysis of Sanger data suggested paraphyly

Table 1. Overview of study design, explaining which datasets and analyses were used to answer our primary questions.

Question	Data	Programme	Analysis
Phylogenetic analyses			
1. Is *Lasius* monophyletic?	89 taxa, 959 UCE locus alignments 135 taxa, 11 Sanger loci 55 taxa, 11 Sanger loci	UCEs: ASTRAL-II Sanger: MRBAYES 3.2.6, IQ-TREE	UCE: summary coalescence 135 taxa, 11 Sanger loci: Bayesian tree inference, and maximum likelihood bootstrap 55 taxa, 11 Sanger loci: stepping stone, concordance factor
2. Are the subgenera of *Lasius* monophyletic?	55 taxa, 11 Sanger loci	MRBAYES 3.2.6, IQ-TREE	Bayesian: Bayesian tree inference, stepping stone ML; maximum likelihood bootstrap, concordance factor
3. What are the relationships of fossil Formicinae?	154 taxa: 11 Sanger loci for 135 extant taxa, and 110 binary morphological characters for 136 extant and 18 extinct taxa	MRBAYES 3.2.6	Tree search: (clock vs nonclock; morphology-only vs combined data)
Evolutionary history			
4. Under what palaeoclimatological conditions and where biogeographically did the Lasiini and its internal clades originate?	135 extant taxon, 11 Sanger loci chronogram trimmed from 154 taxon tree generated in Question 3	BIOGEOBEARS	BIOGEOBEARS: several models (with and without +J)
5. What was the evolutionary sequence of transformation for taxonomically important characters and life-history traits?	135 taxon chronogram from Question 4, 5 binary morphological characters and 1 ternary morphological character; 21 taxon chronogram trimmed from Question 3, 2 binary life-history traits	R (*ape*)	*ace* with ER (equal rates) versus SYM (symmetrical rates) versus ARD (all rates different) models
Taxonomy			
6. What are the morphological states that define the Lasiini and focal clades therein?	Qualitative comparisons (various) Morphometrics (104 specimens, 56 spp.)	Qualitative: n/a Quantitative: R (ggplot)	Qualitative: Key + Tabulation Quantitative: Plotting

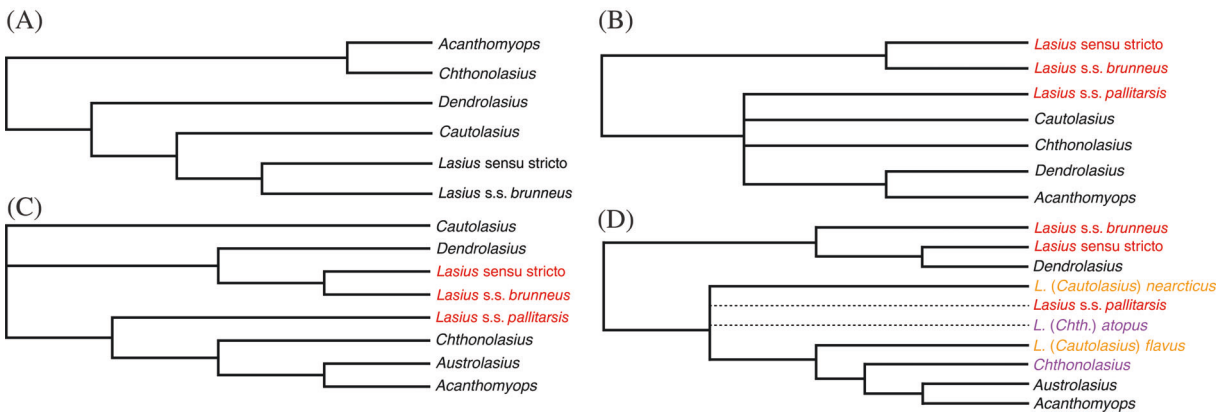

Fig. 1. Comparison of phylogenetic hypotheses for *Lasius*; red indicates paraphyly of *Lasius* sensu stricto, orange of *Lasius* (*Cautolasius*) and violet of *Lasius* (*Chthonolasius*). (A) Intuition-based topology from Wilson (1955). (B, C) combined morphological and mitochondrial topologies of Janda *et al.* (2004), and Maruyama *et al.* (2008). (D) Consensus topology from the current study; see Table 4 for Bayes factor tests of our constraint analyses.

of the genus with respect to *Myrmecocystus* Wasmael. The situation is equivocal, however, as a more recent study using UCEs and a limited taxonomic sampling of the genus recovered *Lasius* as monophyletic (van Elst *et al.*, 2021).

In this contribution, we focus on the genus *Lasius* and the tribe Lasiini, integrating molecular and morphological methods to address several questions about their classification and evolution (Table 1). In addition to the monophyly of *Lasius* and its subgenera (Table 1, *Questions 1 and 2*), we are also interested in the fossil history of the genus and the Lasiini (e.g., Mayr, 1868; Wheeler, 1915; Wilson, 1955; LaPolla *et al.*, 2013; Barden *et al.*, 2017a), from both taxonomic (Table 1, *Question 3*) and evolutionary perspectives (Table 1, *Questions 4 and 5*). We propose a revised morphological definition of *Lasius*, the Lasiini, and a number of newly recognized nodes on the formicine phylogeny, resulting from explicit integration of morphology of both extant and fossil lineages into our phylogenetic analyses. We also provide a systematic, illustrated key to the extant genera of the tribe (Table 1, *Question 6*). Our overarching hope is to encourage the reconciliation of morphological and molecular systematics.

Materials and methods

Study design

Our study addresses six questions outlined in Table 1. A summary of methods is provided below with additional details available as supplementary text. In brief, our objective is to holistically evaluate the phylogeny and evolution of extant and extinct *Lasius* and Lasiini in the context of the Formicinae. We employed an array of tools to three datasets comprising a broad sample of the Formicinae and selected non-formicine outgroups: (i) a set of previously published 959 individual UCE locus alignments for 89 extant terminals (Blaimer *et al.*, 2015, *Question 1*); (ii) a set of 11 Sanger loci for 135 extant terminals (*Questions 1*, *3–5*); (iii) a set of 11 Sanger loci for 55 extant terminals in the Lasiini (*Question 2*), and (iv) a set of 114 binary morphological characters for 154 terminals (136 extant and 18 extinct) (*Question 3*). In addition, we tested the polarity of six morphological characters traditionally used in the classification of the Formicinae (*Question 5*). In order to revise the generic classification of the Lasiini and to provide a new key, we comparatively evaluated several qualitative traits, and took six linear measurements for 109 specimens of 56 species (*Question 6*). The two new genera we recognize are registered with ZooBank (LSIDs in respective taxonomic accounts below). All Bayesian inference (BI) and maximum likelihood (ML) analyses were conducted on the CIPRES Science Gateway V. 3.3 (Miller *et al.*, 2010, accessed at http://www.phylo.org/portal2).

Sanger sequence data

New sequence data were generated from a selection of 20 *Lasius* and 2 *Myrmecocystus* species. Our sampling of *Lasius* was designed to encompass the morphological, geographical, and life history variation within the genus (Table 2), spanning all currently recognized subgenera (Wilson, 1955; Bolton, 2003; Ward, 2005), and was partially guided by previous molecular phylogenies (Janda *et al.*, 2004; Maruyama *et al.*, 2008). Notably, we included a species closely related to or conspecific with the aberrant and previously unsampled species, *Lasius atopus* Cole, from California, U.S.A., as well as another unsampled species, *Lasius myrmidon* Mei, described from Greece (Mei, 1998). Although we included only three species of *Myrmecocystus* (one of these taken from existing GenBank data – see below), these were chosen to span the root node of the genus (O'Meara 2008, van Elst *et al.*, 2021). We also included data from all genera recognized in the *Prenolepis* genus group (LaPolla *et al.*, 2010, 2012), the majority of formicine genera, and a sample of formicoid outgroups. Voucher specimens from DNA extractions made for this study are deposited in the University of California Bohart Museum of Entomology collection (UCDC) and collection data associated with these specimens can be found in Table 2 and on AntWeb at http://antweb.org/.

We used the DNeasy Blood and Tissue Kit (Qiagen Inc., Valencia, CA, U.S.A.) to conduct nondestructive DNA extractions by piercing the cuticle of each specimen, then soaking the specimens overnight in a solution of proteinase K in the lysis buffer provided with the kit. For the remainder of the extraction, we followed the manufacturer's protocol except for eluting the extract with sterilized water rather than the supplied buffer. With these 22 extractions, we amplified and sequenced fragments of eight nuclear protein-coding genes: abdominal-A (*abdA*), arginine kinase (*ArgK*), rudimentary (*CAD*), elongation factor 1α copy F2 (*EF1aF2*), long-wave rhodopsin (*LW Rh*), DNA topoisomerase 1 (*Top1*), ultrabithorax (*Ubx*), and wingless (*wg*). Amplifications of desired gene fragments were performed with primers listed in Table S1 using standard PCR methods described in Ward & Downie (2005). Sequencing reactions were carried out on an ABI 3730 Capillary Electrophoresis Genetic Analyser with ABI Big-Dye Terminator v3.1 Cycle Sequencing chemistry (Applied Biosystems Inc., Foster City, CA, U.S.A.).

Sequence base calling was performed in SEQUENCHER v5.0 (Gene Codes Corporation, Ann Arbor, MI, U.S.A.). Because it has been suggested that arbitrary choice of alleles can bias phylogenetic results in some datasets (Weisrock *et al.*, 2012), we retained ambiguous base calls (R or Y) for any potentially heterozygous sites. To expand our taxon sampling, we downloaded sequences from GenBank. For 18 *Prenolepis* genus-group taxa from LaPolla *et al.* (2010, 2012) we obtained five nuclear loci (*ArgK*, *CAD*, *EF1aF1*, *EF1aF2*, and *wg*); we obtained nine nuclear loci (*abdA*, *ArgK*, *CAD*, *EF1aF1*, *EF1aF2*, *LW Rh*, *Top1*, *Ubx*, and *wg*), and two ribosomal loci (*18S* and *28S*) for an additional 116 formicine and 19 non-formicine taxa from datasets published by Brady *et al.* (2006), Branstetter (2012), Brady *et al.* (2014), Blaimer *et al.* (2015), Chomicki *et al.* (2015), and Ward *et al.* (2015). The final dataset comprised a total of 11 nuclear loci for 135 taxa spanning the Formicinae, and including non-formicine outgroups, with 21 *Lasius* species, 3 *Myrmecocystus* species, and 30 *Prenolepis* genus

Table 2. Voucher specimen collection data for sequences generated de novo.

Species	Specimen code	Locality (year)	Collector
Lasius americanus_nr	CASENT0732004	CA, U.S.A. (2014)	Borowiec, M.L.
*Lasius atopus*_nr	CASENT0234858	CA, U.S.A. (2014)	Boudinot, B.E., *et al.*
Lasius brevicornis	CASENT0234864	CA, U.S.A. (2012)	Borowiec, M.L.
Lasius brunneus	CASENT0234862	Dolny Śląsk, Poland (2010)	Borowiec, M.L.
Lasius carniolicus	CASENT0731085	Dolny Śląsk, Poland (2012)	Salata, S.
Lasius emarginatus	CASENT0234865	Dolny Śląsk, Poland (2010)	Borowiec, M.L.
Lasius flavus	CASENT0234860	Dolny Śląsk, Poland (2010)	Borowiec, M.L.
Lasius fuliginosus	CASENT0234861	Dolny Śląsk, Poland (2010)	Borowiec, M.L.
Lasius latipes	CASENT0234866	CA, U.S.A. (2007)	Ward, P.S.
Lasius myops	CASENT0732040	N Calabria, Italy (2014)	Borowiec, L.
Lasius nearcticus	CASENT0811278	MA, U.S.A. (2008)	Alpert, G.D. & Borowiec, M.L.
Lasius pallitarsis	CASENT0234859	CA, U.S.A. (2014)	Borowiec, M.L.
Lasius platythorax	CASENT0811277	N. Dalmatia, Croatia (2000)	Borowiec, M.L. & Poprawska, M.
Lasius psammophilus	CASENT0811275	Dolny Śląsk, Poland (2009)	Borowiec, M.L.
Lasius sabularum	CASENT0234863	Dolny Śląsk, Poland (2010)	Borowiec, M.L.
Lasius sonobei	CASENT0730575	Hokkaido, Japan (2002)	Ward, P.S.
Lasius spathepus	CASENT0732006	Hokkaido, Japan (2002)	Ward, P.S.
*Lasius subumbratus*_nr	CASENT0731084	CA, U.S.A. (2014)	Ward, P.S.
Lasius turcicus	CASENT0732001	Rhodes, Greece (2008)	Borowiec, L.
Metalasius myrmidon	CASENT0811544	Korinthia, Greece (2013)	Borowiec, L.
Myrmecocystus mexicanus	CASENT0234867	CA, U.S.A. (2014)	Borowiec, M.L.
Myrmecocystus tenuinodis	CASENT0234868	CA, U.S.A. (2004)	Ward, P.S.

Specimen codes link to more detailed collection data on AntWeb (http://www.antweb.org); all specimens were deposited in the Bohart Museum of Entomology (UCDC) except for *L. sonobei*, which was a destructive extraction (collection code: PSW14663, duplicates available).

group species. GenBank identifiers for all sequences used in this study are listed in Table S2.

Morphological data

Worker specimens of extant and extinct species were examined from the American Museum of Natural History (AMMH) and collections housed at the University of California, Davis: the Bohart Museum of Entomology (UCDC) plus the personal collections of Philip S. Ward (PSWC) and the authors (BEBC, MLBC, MMPC). In addition, morphological characters were evaluated from type specimens and other material imaged on AntWeb (http://antweb.org). We constructed two separate datasets for our study: (i) continuous morphometric data to differentiate '*Lasius myrmidon*' and '†*L. pumilus*' relative to other *Lasius* (measurements are defined in Appendix S1, and data are reported in Lasiini_eye_metrics_myrmidon_vs_pumilus.csv, available on Dryad, https://doi.org/10.25338/B8B645), and (ii) discretized binary morphological data to test our assumptions of the taxonomic placement of fossils informative for the Lasiini (characters are defined in Appendix S2, and states scored for each taxon are in Lasiini_w_outgroups_w_fossils_154t_morphology.fasta, available on Dryad, https://doi.org/10.25338/B8B645). For the discretized dataset, worker-based observations were made of 110 morphological characters coded in binary fashion for phylogenetic analysis (character list reported in Appendix S2). These data were scored for 150 terminals in total, of which 18 were fossils and 132 were extant Formicinae. Some of the characters were derived from prior studies, while others were interpreted *de novo* from comparative morphological study across the Formicidae. Each character is treated as a state, which is either observed to be *true* (1) or *false* (0) for a given specimen. Therefore, some complex (multistate) characters were separated into multiple characters, with observed absences and inapplicable states scored as *false*, similar to the 'Composite Coding' method described by Strong & Lipscomb (1999). An effort was made to score characters in a homology-neutral way, that is, each *true* statement is based on the morphological definition, without assuming *a priori* that the state must be homologous when observed across the phylogeny. See the 'Species group classification of *Lasius*' section below for a record of examined *Lasius* species. Overall, the matrix was ~97% complete for extant taxa and ~91% complete for extinct taxa.

Phylogenetic analyses

Alignment and partitioning of Sanger sequence data. We generated two molecular datasets from our initial set of sequences: 'Lasiini_w_outgroups_135t' contains the full taxon set, with 135 taxa spanning the Formicinae, including formicoid clade outgroups (Brady *et al.*, 2006); 'Lasiini_55t' is a subset of 'Lasius_w_outgroups_135t', containing only species from the genera of the Lasiini. For both datasets, individual loci were aligned with the L-INS-I algorithm in MAFFT v7.419 (Katoh *et al.*, 2002; Katoh & Standley, 2013), and exonic regions were inspected in Aliview (Larsson, 2014) to ensure that the

alignments were in frame. The individual alignments were trimmed with GBLOCKS v0.91b (Castresana, 2000), adjusting the default settings to trim less stringently: b1 and b2 were set to half of the total taxon set in each locus (plus one), b3 was set to 12, b4 to 7 and b5 was set to half. After trimming, the ends of each sequence alignment were further trimmed such that the alignment began with the first codon position and ended with the third codon position. If the locus contained introns, the alignment was then split into exonic and intronic regions using AMAS (Borowiec, 2016b). We concatenated the resulting data into the 'Lasius_w_outgroups_135t' and 'Lasiini_55t' matrices, as well as individual gene alignments for each matrix.

As the assumption that evolution of all sequence data is homogeneous is often violated in empirical data (Buckley *et al.*, 2001), we partitioned our matrices into subsets of similarly evolving sites for our concatenated and single gene analyses. To find the optimal partitioning scheme and best substitution models, we used PARTITIONFINDER v2 (Lanfear *et al.*, 2016) on our concatenated molecular datasets as well as the individual gene alignments. As input, we used blocks of data, which represent codon positions within exonic regions of protein-coding loci; introns and ribosomal loci were treated as individual data blocks. We included JC, K80, HKY, symmetrical rates (SYM), F81, and GTR, all with or without $+\Gamma$ or $+$ I, but we excluded models invoking both gamma and proportion of invariable sites (i.e., $+\Gamma+$ I) as it has been shown that interaction of these parameters may cause anomalies in BI (Sullivan & Swofford, 2001; Yang, 2006). To find the optimal scheme, we chose the Bayesian information criterion (BIC) and the 'greedy' algorithm.

Phylogenetic analysis of molecular-only data. We used MRBAYES 3.2.6 (Ronquist *et al.*, 2012b) for BI on concatenated and single-gene alignments (Table 1, *Questions 1–3*) with the model and partition schemes estimated from the PARTITIONFINDER v2 analyses. State frequencies, substitution rates, shape of gamma distribution of substitution rates at sites, and proportion of invariable sites were unlinked and allowed to vary among partitions, while branch lengths remained linked. We ran each analysis for 25 million generations with two runs, four chains each, and we sampled parameters every 2500 generations, leaving burnin at the default 25%. We used the following statistics to diagnose MCMC: PSRF values approaching 1.0, proposal acceptance rates between 20 and 70%, and standard deviation of split frequencies with values of approximately 0.01 or less. In addition, we used the programme TRACER v1.6.0 (Rambaut *et al.*, 2014) to evaluate trace plots and minimum effective sample size values (should be >200) for each parameter in the different runs.

For phylogenetic inference under ML (Table 1, *Question 2*), we used IQTREE v2 (Minh *et al.*, 2020). We used the model and partition schemes estimated from PARTITIONFINDER v2, allowing each partition to have its own rate of evolution (−p), and 1000 ultrafast bootstrap (BS) replicates. Trees for both Bayesian and ML analyses were manipulated with FIGTREE v1.4.2 (Rambaut & Drummond, 2014). In addition, we performed a gene and site concordance factor analyses for each concatenated dataset using the consensus tree and single gene trees from the MRBAYES analyses above as input.

Based on the results from the above ML and BI analyses, we performed stepping-stone analyses of several contrasting topological hypotheses (Table 1, *Questions 1 and 2*). These follow Bergsten *et al.* (2013), who recommended comparisons of analyses under equally constrained topologies (Xie *et al.* 2011) to estimate marginal log-likelihoods in MRBAYES. The hypotheses we tested include: (i) the placement of *Lasius myrmidon* as either with *Lasius* and *Myrmecocystus* or with the *Prenolepis* genus group; (ii) monophyly of *Lasius* with respect to *Myrmecocystus*; (iii) monophyly of *Lasius* s. str. (as presented in Wilson, 1955); (iv) monophyly of *Cautolasius* Wilson; and (v) monophyly of *Chthonolasius* (Figure S1). For these analyses, we ran MrBayes for 25.5 million generations with 2 runs, 4 chains, 50 steps, sampling every 100 generations, and with the alpha shape parameter set to 0.4. We took the mean marginal log-likelihood of the two stepping-stone runs for each analysis, subtracted the likelihood of the alternative hypothesis from the null, then doubled this number. Results of these Bayes factor tests are interpreted after Kass & Raftery (1995), with these specific $2\ln_e(BF_{01})$ ranges: 0–2, 'not worth explaining'; 2–6, 'positive support'; 6–10, 'strong support', and >10, 'very strong support'.

In addition, because *Lasius* was recovered as paraphyletic with respect to *Myrmecocystus* in the Sanger data analyses of Blaimer *et al.* (2015), we employed summary coalescent species tree analysis in ASTRAL-II (Mirarab & Warnow, 2015) with 959 individual UCE locus trees from Blaimer *et al.* (2015) supplied by the lead author as input (the UCE 70% dataset in that study). We did not use the statistical binning pipeline (Mirarab *et al.*, 2014; Bayzid *et al.*, 2015) due to recent criticism (Adams & Castoe, 2019), but instead used individual gene trees as input to ASTRAL-II version 4.10.11, which we ran under default settings.

Phylogenetic analysis of combined data and divergence dating. We analysed a morphology-only data matrix and two combined-data matrices with MRBAYES 3.2.6 to evaluate placement of fossil taxa and to estimate informative priors on relaxed clock models (Table 1, *Question 3*). For morphology-only analysis, we built the 'Lasiini_w_outgroups_w_fossils_morphology_154t' dataset, with 110 morphological characters for 154 taxa. For our first combined-data matrix, we created a 136-taxon dataset containing our partitioned 135-taxon 11-gene matrix and morphological data from extant taxa, adding *Paratrechina kohli* (Forel), which was represented only by morphological data ('Lasiini_w_outgroups_136t'). For our second combined-data matrix, we added morphological data from 18 fossil taxa to the previous matrix ('Lasiini_w_outgroups_w_fossils_154t'). All morphological data were included in a single partition to which we applied the Mk model (Lewis, 2001), accounting for among character rate variation using $+\Gamma$. As rate asymmetry has been shown to have important consequences for morphological analysis (Wright *et al.*, 2016; Klopfstein & Spasojevic, 2019), particularly in the otherwise robust total-evidence dating framework (Klopfstein *et al.*, 2019), the assumption of equal forward

Table 3. Datasets and analyses used for divergence dating.

Dataset name	Purpose of analyses	Data type	Taxa	Clock type
Lasiini_w_outgroups_w_fossils_morphology_154t	Fossil placement comparison	Morphology	Extant & fossil	No clock
Lasiini_w_outgroups_136t	Relaxed clock prior estimation	Combined	Extant taxa	No clock versus strict clock
Lasiini_w_outgroups_w_fossils_154t	Fossil placement comparison, divergence dating	Combined	Extant & fossil	Relaxed clock: IGR versus TK02; uniform clock: IGR versusTK02

and reverse transformations was relaxed by setting the 'symdirihyperpr' to a uniform distribution ('fixed[1.0]') in our input files, thus allowing MRBAYES to estimate asymmetric stationary frequencies (π) across states. To account for ascertainment bias (Lewis, 2001), we set coding for the morphological partition to 'variable'.

With the three datasets above, we performed alternate analyses combining different sets of parameters (Table 3), examining the effect on the placement of fossil taxa when analysing morphological data in isolation in comparison to the results of combined-data analyses in the absence of a molecular clock. To estimate informative priors for the two commonly used relaxed clock models in MRBAYES (IGR and TK02), we followed the methods used in Ronquist *et al.* (2012a) with our Lasiini_w_outgroups_136t dataset. The two clock models with informative priors were then compared against each other using stepping-stone analysis with the Lasiini_w_outgroups_w_fossils_154t dataset. Because the results of the stepping-stone analyses were ambiguous, we analysed the Lasiini_w_outgroups_w_fossils_154t dataset with both clock models for comparison. For the analyses of the Lasiini_w_outgroups_w_fossils_154t dataset, we used the fossilized birth–death branch length (FBD) model (Heath *et al.*, 2014) and a uniform clock for comparison. All analyses included a root node topology constraint (i.e., monophyly of core formicoids enforced), but were otherwise unconstrained. Because our taxon sample does not meet the expectations of the 'diversified sampling' approach (Zhang *et al.*, 2016), we implemented a random sample stratification for FBD analyses. For fossil terminals, uniform distributions were used for stratigraphic ages (New Jersey amber: 94.3–89.3 Ma; Canadian amber: 84.9–70.6 Ma; Baltic amber: 37.2–33.9 Ma; Dominican amber: 20.4–13.7 Ma). The root node prior age was set to the estimated age of the oldest known crown fossil in the Formicidae, an offset exponential distribution with a minimum of 90 and mean of 99 Ma. We ran each analysis for 100 million generations with two runs of four chains each, with sampling every 10 000 generations and the default burnin of 25%. MCMC diagnoses were conducted as for the molecular-only analyses described above.

Historical biogeography. After divergence dating, the post-burnin consensus chronogram resulting from the MRBAYES FBD analysis was trimmed to 55 extant taxa of the Lasiini with the 'drop.tip' function in the R package 'phytools' (Revell, 2012) and used as input for the likelihood-based biogeographic programme BIOGEOBEARS (Matzke, 2013). We used a coarse biogeographical classification following previous studies (e.g., Ward *et al.*, 2015): Neotropical, Nearctic, Palaearctic, Afrotropical, Indomalayan, and Australasian regions, with Wallace's line dividing the last two areas. The maximum ancestral species range size was set to two areas, and the matrices of allowed areas and dispersal constraints were set for three periods: before 60 Ma, 60–30 Ma, and after 30 Ma, reflecting tectonic drift referenced from Scotese (1998). We conducted our phylogeographic analyses using the DEC, DIVALIKE, and BAYAREALIKE models, all with or without +J, but due to criticism of +J (Ree & Sanmartín, 2018), we excluded results that included this parameter from consideration. The script and input files used in this analysis can be found on Dryad (https://doi.org/10.25338/B8B645).

Ancestral state estimation. We employed the *ace* function of the R package *ape* (Paradis & Schliep, 2018) to estimate ancestral states of six traditional morphological characters and two life-history traits (Table 1, *Questions 5 and 6*). These six characters, described in the next paragraph, were scored for the MRBAYES analysis above after trimming fossils from the 154-taxon tree with the 'drop.tip' function in the R package 'phytools', resulting in a 135-taxon phylogeny representing the Formicinae and outgroups, and a 21-taxon phylogeny representing *Lasius*. We contrasted two evolutionary models for five characters and two traits with binary states: equal (ER) and unequal rates (ARD) of forward and reverse transition. For the abdominal segment III character, which had ternary states, we tested SYM in addition to the ER and ARD models. To determine if the more-complex SYM and ARD models had significantly better fit, we conducted pairwise analysis of variance for each character.

We qualitatively reinterpreted the phenotypic diagnostic traits used by Bolton (2003) for classification at the tribe and 'tribe group' level, as well as the form of the proventriculus, a classic character in formicine classification (e.g., Emery, 1925). The six morphological characters that we reconstructed the ancestral states for are: (i) eye placement, with eyes set at or anterior to head midlength as measured from the anterolateral clypeal corners [state 1] or posterior to midlength [state 0]; (ii) metacoxal separation, with coxae either close-set ('formicoform') [state 0] or wideset ('lasiiform') [state 1]; (iii) abdominal sternum III with transverse sulcus at base of helcium [state 1] or without [state 0]; (iv) propodeal

spiracle circular to elliptical [state 0] or slit-shaped [state 1]; (v) abdominal segment III tergosternal suture extending laterally then broadly curving posteriorly or simply linear ('formicoform'/broadly shouldered) [state 0], suture curving forward then narrowly arching posteriorly ('lasiiform'/narrowly-shouldered, low) [state 1] or suture extended dorsally, with free tergite and sternite commencing well away from helcium ('plagiolepidiform'/narrowly-shouldered, high) [state 2]; and (vi) proventriculus asepalous [state 0] or sepalous [state 1]. Character 6, proventriculus form, was scored as generalizations based on Forel (1878), Emery (1888, 1895, 1925), Eisner (1957), and Prins (1983), and therefore may be inaccurate; future anatomical studies should evaluate the plausibility of our generalized scoring. Note that metacoxal separation, as scored, is also a proxy for a long petiolar foramen and U-shaped petiolar sternum cross-section used by Bolton (2003) to define his 'lasiine tribe group'. The two life-history traits for which we reconstructed ancestral states are: (i) temporary social parasitism, absence [state 0] or presence [state 1]; and (ii) fungiculture, absence [state 0] or presence [state 1].

Results and discussion

Alignment and partitioning of the Sanger sequence data

Overall, the 11-gene 135-taxon molecular matrix is 8.3 kbp long and contains 21% missing data, and 2902 variable sites (35%) of which 2449 are parsimony informative (30%). The 11-gene 55-taxon molecular matrix is 8.8 kbp long and contains 39% missing data, 1600 variable sites (18%) of which 1010 are parsimony informative (12%) (statistics calculated with AMAS, Borowiec, 2016b). The PartitionFinder analysis resulted in a best-scoring scheme with 17 partitions for our 135-taxon matrix, and a 12-partition scheme for our 55-taxon matrix (Table S3).

Phylogenetic relationships

Results in this section pertain to *Questions 1–3* of Table 1.

Question 1: Is* Lasius *monophyletic? Answer: The extant fauna of *Lasius* is monophyletic with the exclusion of *Metalasius myrmidon* **gen.nov. comb.nov** (Table 4, Figs 2, 3, 4).

Across all analyses, there is overwhelming support for the placement of *Lasius myrmidon* as sister to the *Prenolepis* genus-group (Table 4). We thus transfer this species to a new genus, forming *Metalasius myrmidon* **gen.nov. comb.nov.,** which we diagnose in the *Taxonomy* section below. With the exclusion of *M. myrmidon*, we find somewhat low topological support for *Lasius* monophyly using standard measures (0.96 posterior probability [PP], 87 ML BS (Fig. 2); 36.6 gene concordance factor [gCF], 42.3 site concordance factor [sCF], (Figure S2). However, genome-scale coalescence analysis recovers *Lasius* monophyly with respect to *Myrmecocystus* (Fig. 3), and a Bayes Factor constraint test using the Sanger loci results in 'very strong support' for monophyly (Table 4). Among the Sanger loci, we found that the source of the nonmonophyly signal was localized to the ribosomal data. Further, our sampling spanned the root of *Myrmecocystus* (O'Meara 2008, van Elst *et al.*, 2021), which was also found to by monophyletic in a focused study on that genus by van Elst *et al.* (2021). For these reasons, we accept the hypothesis that *Lasius* and *Myrmecocystus* are reciprocally monophyletic, with the exclusion of *M. myrmidon*.

Table 4. Bayes Factor results, testing alternative placements of *Metalasius* and the monophyly of the subgenera using the Lasiini_55t matrix.

SS run	Marg. log likelihood H_0	Marg. log likelihood H_1	$2\ln_e(B_{10})$
	Metalasius + *Lasius* g. g.	*Metalasius* + *Prenolepis* g. g.	
1	−29 156.21	−29 092.2	
2	−29 153.15	−29 094.4	
Mean	−29 153.79	**−29 092.79**	−122
SS run	Marg. log likelihood H_0	Marg. log likelihood H_1	$2\ln_e(B_{10})$
	Lasius monophyletic	*Lasius* paraphyletic	
1	−29 068.73	−29 072.46	
2	−29 068.86	−29 072.04	
Mean	**−29 068.79**	−29 072.23	6.88
SS run	Marg. log likelihood H_0	Marg. log likelihood H_1	$2\ln_e(B_{10})$
	Lasius s. str. monophyletic	*Lasius* s. str. paraphyletic	
1	−29 092.4	−29 057.37	
2	−29 094.02	−29 058.11	
Mean	−29 092.91	**−29 057.67**	−70.48
SS run	Marg. log likelihood H_0	Marg. log likelihood H_1	$2\ln_e(B_{10})$
	Cautolasius monophyletic	*Cautolasius* paraphyletic	
1	−29 063.91	−29 054.38	
2	−29 064.12	−29 054.21	
Mean	−29 064.01	**−29 054.29**	−19.44
SS run	Marg. log likelihood H_0	Marg. log likelihood H_1	$2\ln_e(B_{10})$
	Chthonolasius monophyletic	*Chthonolasius* polyphyletic	
1	−29 100.32	−29 047.78	
2	−29 099.17	−29 046.75	
Mean	−29 099.59	**−29 047.13**	−104.92

The mean value for the best-supported hypothesis for each comparison is bolded.

Question 2: Are the subgenera of* Lasius *monophyletic? Answer: Three of the six subgenera of *Lasius* – *Lasius* sensu stricto, *Cautolasius*, and *Chthonolasius* – are not monophyletic (Table 4, Figs 1D, 2, 4) also Fig. 5.

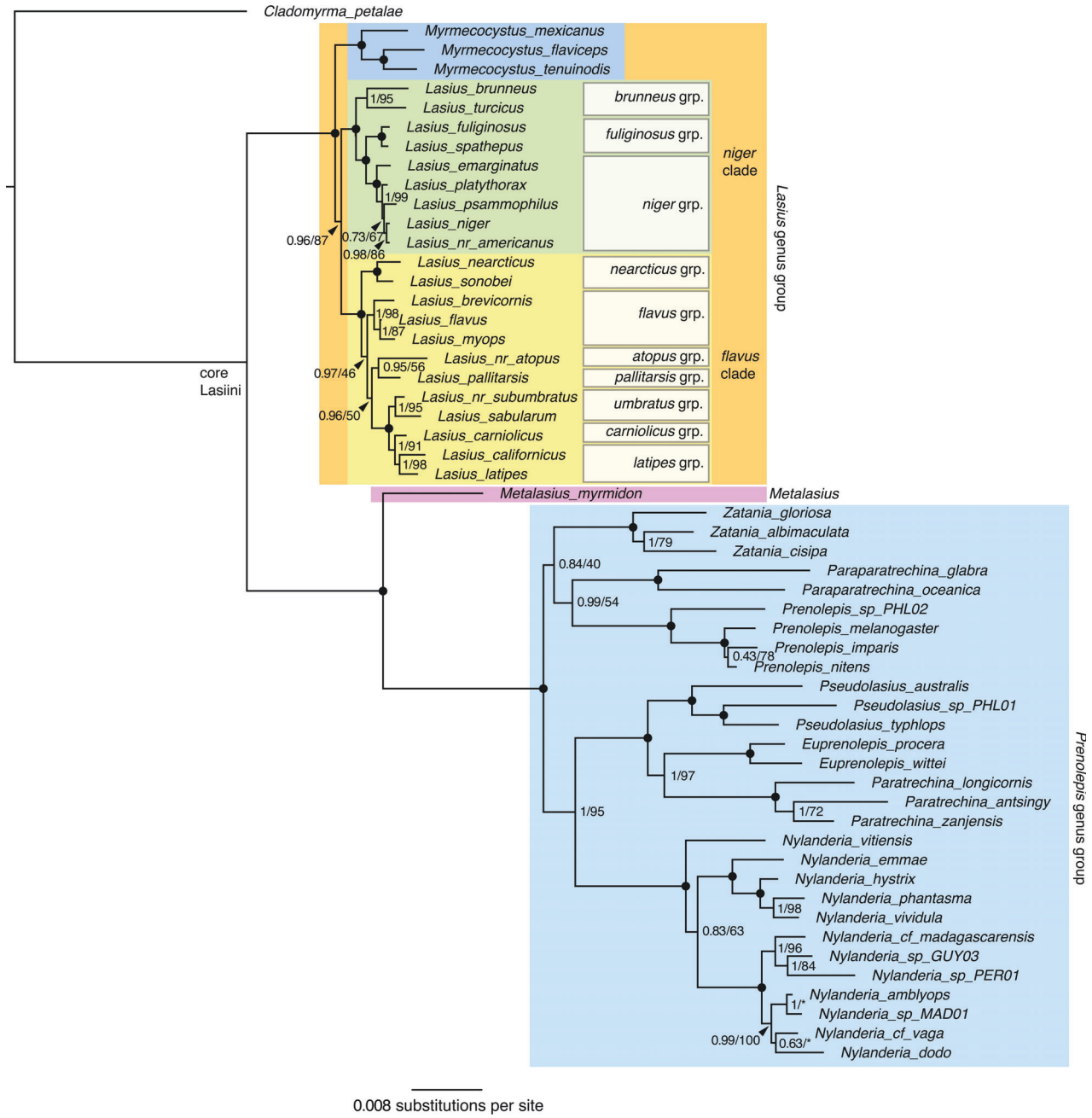

Fig. 2. Molecular phylogeny of the Lasiini inferred from Bayesian analysis of the Lasiini_55t data matrix. Node support values are reported as Bayesian posterior probabilities (BI) versus maximum likelihood bootstrap (ML). Filled circles at nodes indicate full support from both analyses. An asterisk (*) indicates that the topology of the ML analysis diverged from the BI analysis at the given node.

We found that extant *Lasius*, with the exclusion of *Metalasius myrmidon* **gen.nov. comb.nov.**, is divided into two major clades. One clade comprises members of the subgenera *Lasius* s. str. and *Dendrolasius* (together called the '*niger* clade' here), while the other includes all other sampled species (collectively called the '*flavus* clade' here). Critically, we found that the *flavus* clade is diagnosable by an enlarged metapleural gland bulla, constituting a new morphological autapomorphy (see *Key to extant genera of Lasiini* below). Within the *niger* clade, the socially parasitic species classified in *Dendrolasius* are nested within taxa currently considered to belong to *Lasius* s. str., while another *Lasius* s. str. species, *L. pallitarsis* (Provancher), is a member of the *flavus* clade. The aberrant *Lasius* species near *atopus*, currently classified in *Chthonolasius*, is in the *flavus* clade, sister to *L. pallitarsis* with moderate statistical support. Finally, the four *Cautolasius* sampled here are not monophyletic but instead form

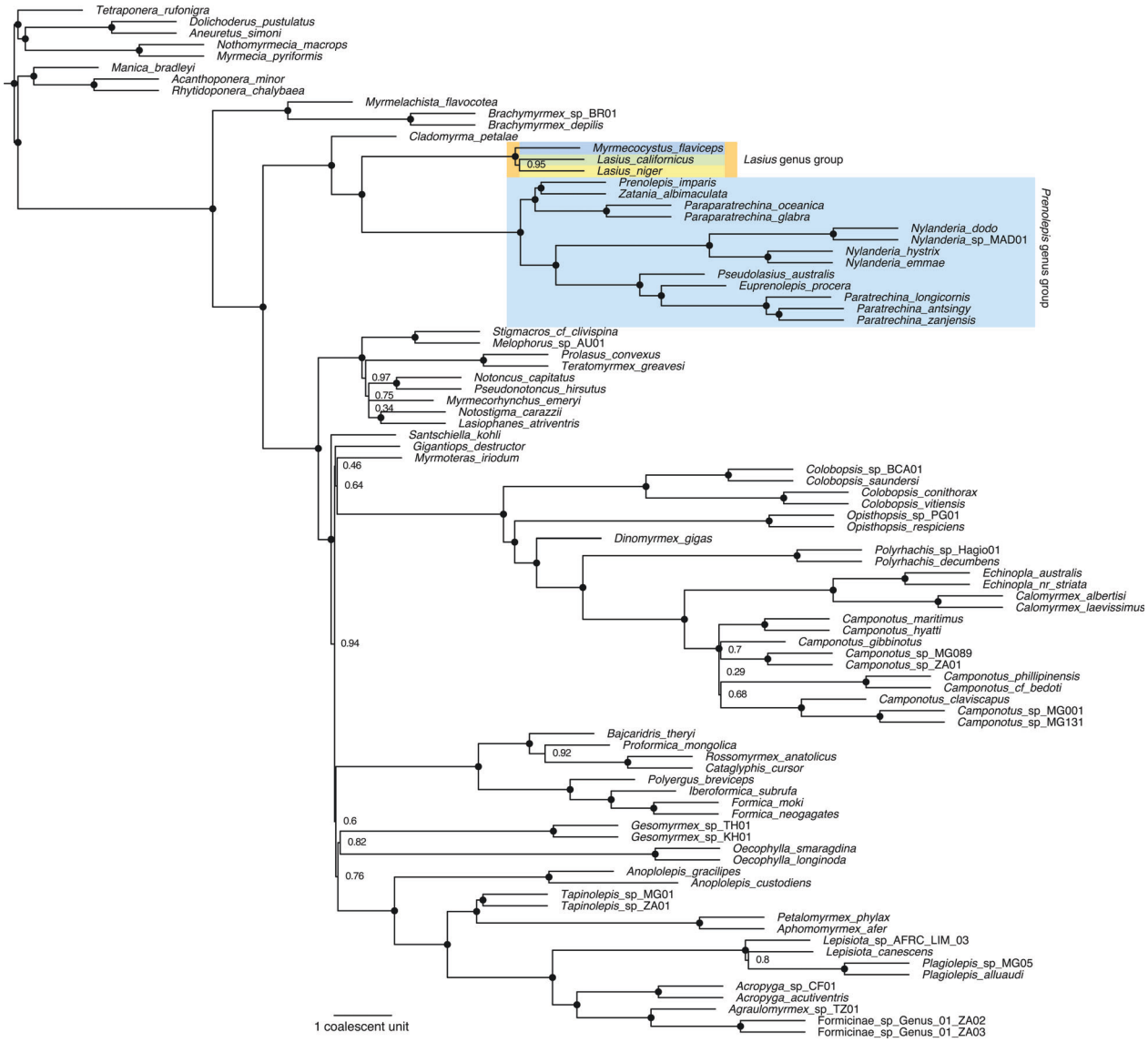

Fig. 3. Summary coalescence species-tree phylogeny from ASTRAL-II analysis of 959 ultraconserved elements from Blaimer *et al.* (2015). Node support values are given as local posterior probabilities (LPP). Filled circles at nodes indicate full support.

two well-supported clades, which we recognize as the *flavus* and *nearcticus* species groups. Because of this phylogenetic arrangement and a continuing trend to abandon subgeneric classification in ants (e.g., Borowiec, 2016a; Borowiec *et al.*, 2021), we propose synonymizing *Lasius* subgenera and recognition of informal species groups instead (see *Taxonomy* below).

Question 3: What are the relationships of fossil Formicinae? Answer: Some previously hypothesized relationships are stable, some are sensitive to model choice, and the taxa †*Lasius pumilus* Mayr, †*Pseudolasius boreus* Wheeler, and †*Glaphyromyrmex* Wheeler require reclassification (Figs 4, S3, S6–S9).

Overall, we find that fossil placement is sensitive to the inclusion or exclusion of a clock model. Under 'clockless' conditions, the fossils were highly nested within the phylogeny (Figures S3 and S6). However, the topology resulting from clockless morphology-only analysis (Figure S3) had both very limited support within the Formicinae and was in considerable conflict with previous and present analyses using molecular data. The outgroup fossils were consistent at the subfamily level, while among our formicine fossils, five of the nine Baltic-region fossil taxa were recovered close to their original attributions (Figs 4, S3, S6–S9): (i) †*Lasius schiefferdeckeri* Mayr may be sister to or nested within the *Lasius* genus group; (ii) †*Prenolepis henschei* Mayr is within the crown of the *Prenolepis* genus group; (iii) †*Formica gustawi* Dlussky is within the crown of the Formicini; (iv) †*Oecophylla brischkei* Mayr is correctly placed to genus; (v) †*Gesomyrmex hoernesi* Mayr is correctly placed to

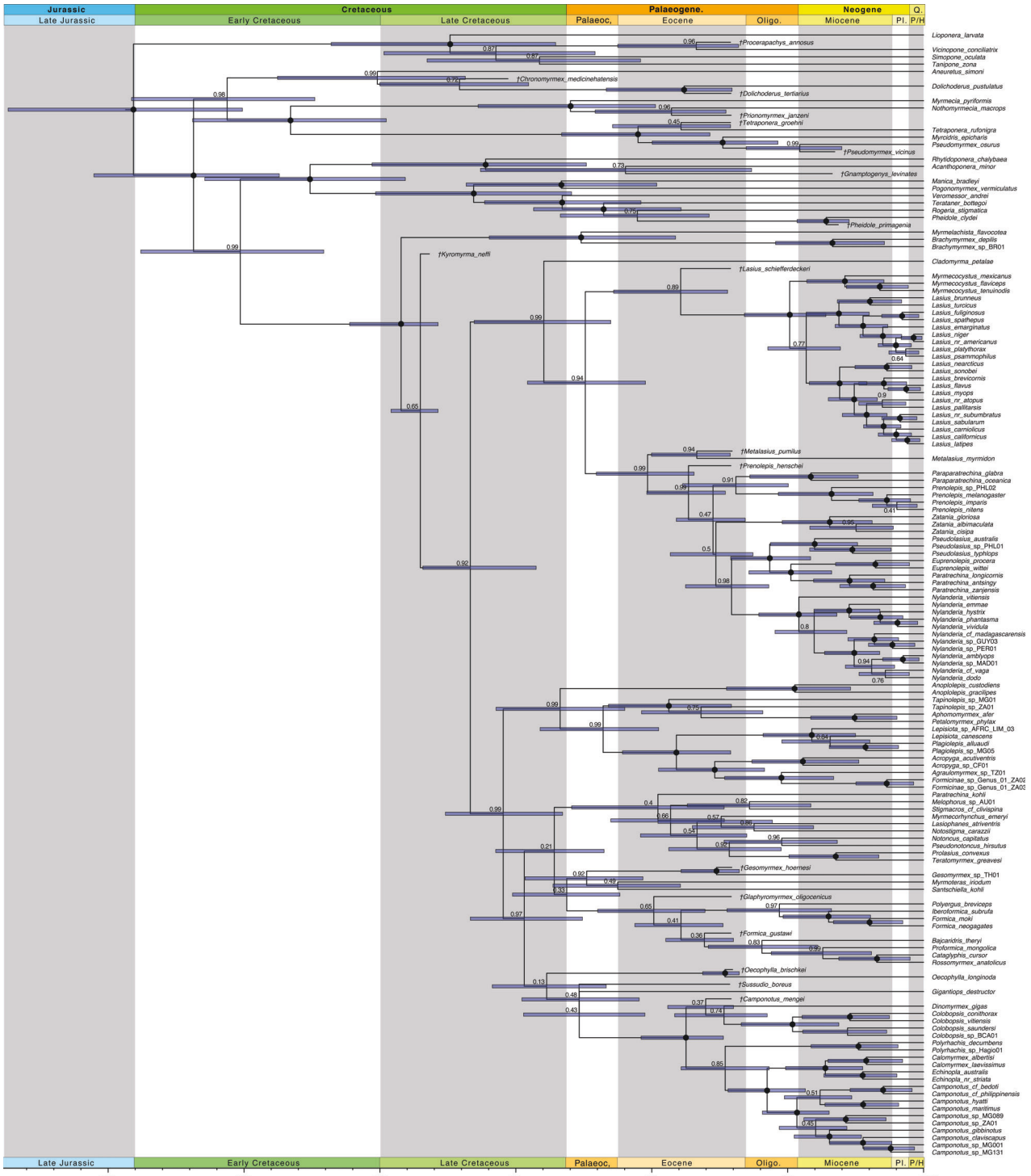

Fig. 4. Results from phylogenetic analysis of the Lasiini_w_outgroups_w_fossils_154t combined morphological and molecular dataset analyzed with MrBayes using the fossilized birth-death branch length prior and the IGR clock variation prior. Fossil taxa are indicated by a dagger preceding the name. Node support values are in Bayesian posterior probability. Filled circles indicate full support. Horizontal blue bars at nodes are 95% highest posterior density (HPD) intervals.

genus and; (vi) †*Camponotus mengei* Mayr is a member of the crown Camponotini.

In contrast, we find that one generic and two tribal transfers are necessary. †*Pseudolasius boreus* Wheeler and †*Glaphyromyrmex oligocenicus* Wheeler, both attributed to Lasiini, are recovered outside of the tribe with very high support across all combined-evidence analyses (0.98–0.99 PP). We transfer the former species to a new genus forming †*Sussudio boreus* **gen.nov. comb.nov.**, which we consider *incertae sedis* within the subfamily (**tribal transfer**), and we transfer †*Glaphyromyrmex* back to the Formicini (**tribal transfer**; see *Taxonomy* below for discussion). With respect to *Lasius*, †*L. pumilus* is recovered outside of the genus, being consistently recovered as sister to *Metalasius myrmidon* **gen.nov. comb.nov.** (Figs 4, S7–S9); for this reason, we transfer the fossil species to the new genus, forming †*M. pumilus* **gen.nov. comb.nov.** (see *Taxonomy* below for diagnosis).

The placements of two key taxa, †*L. schiefferdeckeri* and †*Kyromyrma neffi* Grimaldi and Agosti, were sensitive to the choice of clock model. Under IGR (Figure S7), †*L. schiefferdeckeri* was sister to the *Lasius* genus group (0.90 PP) and †*Kyromyrma* was nested in the crown Formicinae to the exclusion of the Myrmelachistini (0.94 PP). Under TK02 (Figures S8, S9), †*L. schiefferdeckeri* formed a clade with *Lasius* (0.63–0.71 PP) and †*Kyromyrma* was nested in the crown Lasiini (0.91–0.94 PP). Notably, the MCMC performed better under the IGR model relative to the TK02 model. Under TK02, the clock rate parameter sampled poorly, which was reflected in low ESS values for tree height and tree length. This, in addition to the unusually old estimations for the root node (Figures S8 and S9), led us to prefer the IGR model over TK02. Regardless, we conservatively retain †*L. schiefferdeckeri* in *Lasius* and treat †*Kyromyrma* as *incertae sedis* within the Formicinae, in agreement with Ward *et al.* (2016) and Grimaldi & Agosti (2000). We note the striking similarity of †*Kyromyrma* and †*L. schiefferdeckeri* to extant *Lasius* (Figs 8, 9), suggesting possible morphological stasis.

Evolutionary history

Results in this section pertain to *Questions 4* and *5* of Table 1.

Question 4: Where and when did the internal clades of the Lasiini originate? Answer: The Lasiini likely originated and initially diversified in the Eastern Hemisphere, with modern genera present by the mid-Miocene (Figs 4, 5, Table 5).

Our primary divergence dating findings, based on the FBD analysis with and IGR branch length variation model, are as follows (Figs 4, 5, Table 5): (i) The deepest split in the Lasiini (*Cladomyrma* Wheeler + core Lasiini) is Late Cretaceous to Palaeocene; (ii) the split between *Metalasius* **gen.nov.** and the *Prenolepis* genus group crown was probably post-K–Pg and may have been during the Early Eocene Climatic Optimum (part of the Ypresian Epoch, 56.0–47.8 Ma), and (iii) the crown *Lasius* genus group is young compared to that of the *Prenolepis* genus group, being probably Oligocene to Early Miocene in origin, while the crown *Prenolepis* genus group arose in the Late Eocene.

Our date estimate for *Myrmecocystus* (21.5–7.3 Ma, 14.6 Ma mean) concurs with a recent study by van Elst *et al.* (2021) (19.9–10.2 Ma, 14.1 Ma mean therein), but the crown *Lasius* genus group (33.0–18.0 Ma, 24.9 Ma mean) and crown *Lasius* (28.6–15.3 Ma, 21.9 Ma mean) ages are slightly older, likely due to inclusion of the Baltic *Lasius* fossils (26.8–13.5 Ma, 18.4 Ma mean and 23.4–11.4 Ma, 16.3 Ma mean, respectively, in van Elst *et al.*, 2021). Our 95% highest posterior density (HPD) for *Nylanderia* Emery (~30–15 Ma), while overlapping with the 95% HPDs of Blaimer *et al.* (2015) (~38–15 Ma) and Matos-Maraví *et al.* (Matos-Maraví *et al.*, 2018) (~33–25 Ma), does not overlap with that of Williams *et al.* (2020) (~45–35 Ma). We suspect that the variation in *Nylanderia* crown age between these studies is related to how the fossil taxon †*N. pygmaea* was assigned during node calibration. While Blaimer *et al.* (2015) and our study do not include any *Nylanderia* fossils, Matos-Maraví et al. (2018) and Williams *et al.* (2020) included †*N. pygmaea*, with this species assigned to the stem of *Nylanderia* in the former and to the crown of *Nylanderia* in the latter (Jason Williams & John LaPolla pers. comm.). Future studies should address this discrepancy by clarifying the placement of *N. pygmaea* using the combined-evidence/tip-dating approach.

With respect to our biogeographic reconstructions, we find that DIVALIKE is the most likely model for the deep history of the Lasiini (Table 5) although the second-most likely model (DEC) results in largely congruent estimated distributions (see results on Dryad https://doi.org/10.25338/B8B645). Mapping the DIVALIKE inference onto our chronogram and considering the climatological history of Earth (Fig. 5), we propose the following narrative.

The Lasiini originated on the Eurasian landmass around the End Cretaceous, with the core Lasiini originating in the Western or 'Palaearctic' portion of the ancient continent. Subsequently, the *Lasius* genus group experienced some degree of extinction, which pruned the clade down to a single Nearctic ancestor, possibly due to the global cooling of the Oligocene to Pleistocene. Within the crown *Lasius* genus group, *Myrmecocystus* arose as an arid-region-adapted lineage from an extinct *Lasius*-like lineage, as evinced by the ~35 Ma Baltic fossils assigned to *Lasius*. The ancestor of *Lasius* dispersed back to the Palaearctic, and a complicated series of range expansions and dispersal events occurred throughout the Miocene and Pliocene, in a pattern similar to two other ecologically dominant northern temperate ant genera: *Formica* and *Myrmica* Latreille (Jansen *et al.*, 2010; Borowiec *et al.*, 2021). An early dispersal event to the Nearctic from the Palaearctic led to the origin of the distinctive *flavus* clade, wherein a complex series of dispersal events between the Palaearctic and the Nearctic probably occurred across the Bering Land Bridge. Within the *niger* clade, there was at least one dispersal to the Nearctic in the *niger* group.

Whereas the *Lasius* genus group was heavily pruned, the *Prenolepis* genus group began radiating during the second half

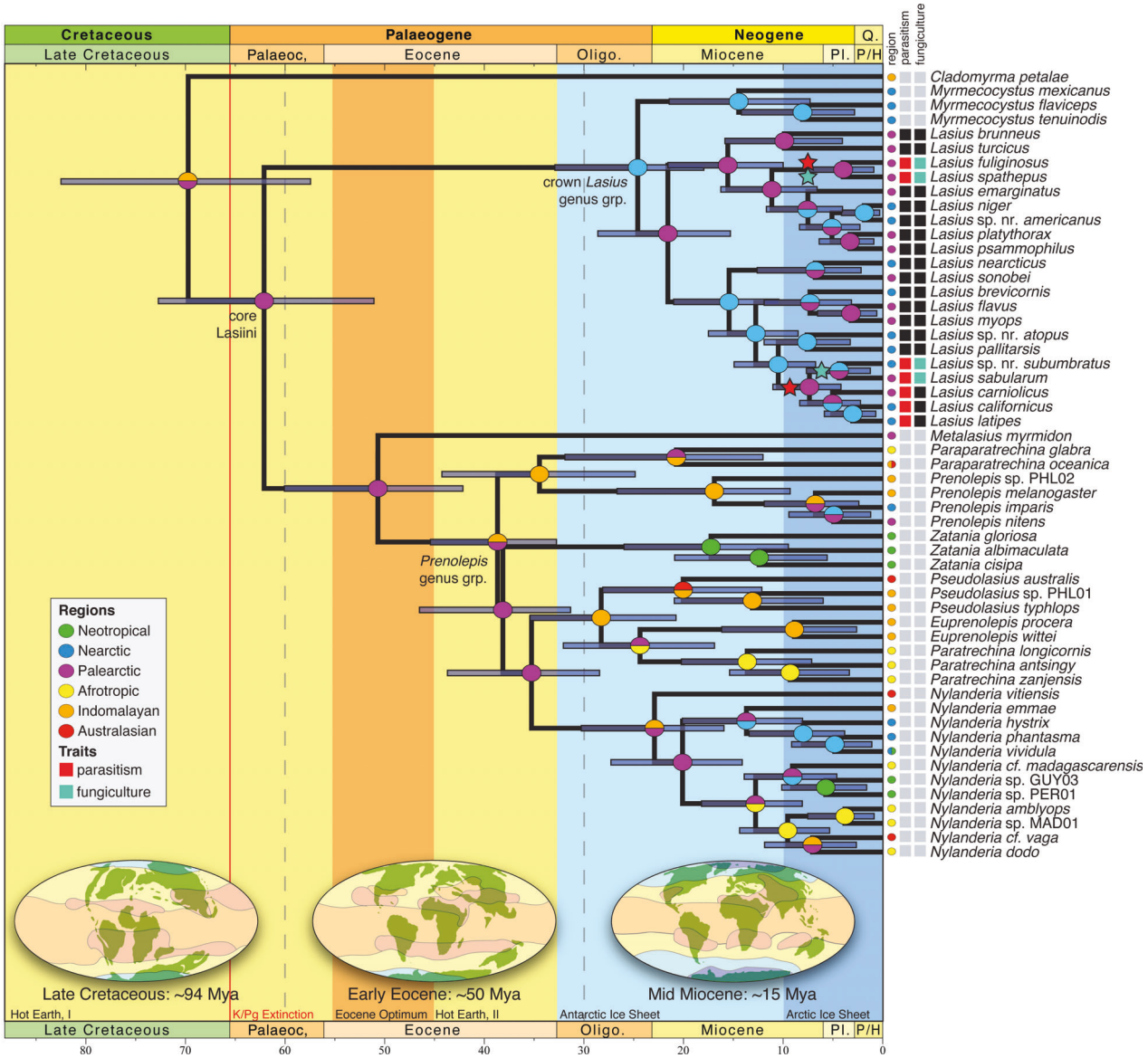

Fig. 5. Results of the BioGeoBEARS and life-history trait ancestral state estimation analyses on a chronogram pruned from the analysis of the Lasiini_w_outgroups_w_fossils_154t combined morphological and molecular dataset. Horizontal blue bars at nodes are 95% highest posterior density (HPD) intervals from the divergence dating. Coloured circles on nodes are inferred inherited biogeographic ranges, with the top half of each corresponding to the upper branch and bottom half with the lower branch; coloured circles at branch tips represent biogeographical coding for terminal; dashed lines at 60 and 30 Ma indicate the boundaries of the three BioGeoBEARS dispersal rate matrix time periods. Coloured boxes at branch tips represent presence or absence of two traits for *Lasius*: temporary social parasitism (black = absence, red = presence) and fungiculture (black = absence, green = presence). Stars on internal branches indicate the evolution of temporary social parasitism (red) and fungiculture (green) The figure background indicates generalized major climatological regimes during Earth's history (Royer *et al.*, 2004; Zachos *et al.*, 2008; Hansen *et al.*, 2013), while the inset globes visually represent palaeoclimate and landmass configuration modified from Scotese (1998).

of the Eocene, with their depauperate sister group surviving to the present day as *Metalasius myrmidon* **gen.nov. comb.nov.** The ancestor of the *Prenolepis* genus group either adapted to, or retained an ancestral physiological optimization for tropical climes, having perhaps expanded into the Indomalayan region following the Eocene Optimum. Subsequently, the *Prenolepis* genus group radiated across the global tropics through a complicated history of transcontinental dispersal. Notably, the crown lineages of the *Lasius* genus group have failed to invade tropical zones, whereas at least two invasions of the temperate zone have occurred in the *Prenolepis* genus group, once each for the *imparis* clade of *Prenolepis* and the *vividula* clade of *Nylanderia*. A third invasion is implied by Matos-Maraví *et al.* (2018) and Williams *et al.* (2020) for

Table 5. Results of divergence dating and historical biogeography reconstruction analyses.

	Divergence dating							Biogeography reconstruction					
	FBD IGR clock		FBD TK02 clock		Uniform IGR clock		Uniform TK02 clock	DEC (lnL −136.77)		DIVALIKE (lnL − 132.24)		BAYAREALIKE (lnL −150.98)	
Node	Mean age (95% HPD)	PP	Mean age (95% HPD)	PP	Mean age (95% HPD)	PP	Mean age (95% HPD)	Range	Likelihood	Range	Likelihood	Range	Likelihood
Lasiini	**70.0 (57.6–82.7)**	**0.99**	97.2 (89.6–106.0)	0.91	80.8 (68.6–91.8)	0.96	100.0 (90.9–112.3)	PI	0.33	**PI**	**0.37**	PI	0.43
Core Lasiini	**62.3 (51.2–72.9)**	**0.94**	88.6 (79.8–97.8)	0.64	72.5 (59.0–85.4)	0.94	92.0 (83.5–102.2)	P	0.42	**P**	**0.56**	PI	0.43
Metalasius + *Prenolepis* g. grp.	**51.1 (42.2–60.2)**	**0.99**	71.0 (60.8–81.9)	1.00	59.9 (48.7–72.8)	0.99	75.6 (65.1–86.5)	P	0.40	**P**	**0.53**	PI	0.48
Prenolepis g. grp.	**39.0 (36.5–50.9)**	**0.47**	53.1 (43.6–62.6)	1.00	50.9 (40.8–61.3)	1.00	57.0 (48.2–66.5)	PI	0.42	**PI**	**0.50**	PI	0.64
Lasius g. grp.	**24.9 (18.0–33.0)**	**1.00**	67.9 (54.9–81.6)	0.99	31.1 (22.4–40.5)	0.99	73.7 (61.9–88.3)	NaP	0.53	**Na**	**0.55**	NaP	0.84
Crown *Lasius*	**21.9 (15.3–28.6)**	**0.77**	63.7 (52.4–75.1)	0.63	27.3 (19.4–35.6)	0.73	64.3 (58.4–82.2)	P	0.72	**P**	**0.71**	NaP	0.87
niger clade	**15.8 (10.0–21.6)**	**1.00**	53.2 (41.2–65.3)	0.70	20.0 (12.7–27.7)	1.00	60.6 (46.1–73.0)	P	0.87	**P**	**0.99**	NaP	0.62
flavus clade	**15.7 (10.4–21.0)**	**1.00**	49.1 (36.7–61.8)	1.00	19.7 (13.2–26.8)	1.00	55.9 (41.1–69.4)	Na	0.71	**Na**	**0.90**	NaP	0.91
Myrmecocystus	**14.6 (7.3–21.5)**	**1.00**	47.9 (33.5–63.1)	1.00	17.8 (8.9–26.9)	1.00	55.8 (40.0–69.8)	Na	0.87	**Na**	**0.97**	Na	0.53

The 'Divergence dating' section compares 95% HPDs for selected nodes given alternative calibration treatments. All ages reported are in units of Ma and are for crown nodes. The 'Biogeography reconstruction' section provides ranges at key nodes along with their likelihood (I = Indomalayan, Na = Nearctic, P = Palaearctic; combinations indicate both regions were occupied). Results in bold are presented in Fig. 4 and Fig. 5.

Table 6. Results of ANOVA tests on alternative ancestral state estimation models.

Model	Log lik.	df	df change	Resid. dev	Pr (>|Chil)
Eyes_ER	−49.43	1	NA	NA	NA
Eyes_ARD	−49.12	2	1	0.63	0.43
Coxae_ER	−26.97	1	NA	NA	NA
Coxae_ARD	−26.24	2	1	1.48	0.22
Prov_ER	−27.56	1	NA	NA	NA
Prov_ARD	−27.29	2	1	0.53	0.47
Spiracle_ER	−28.83	1	NA	NA	NA
Spiracle_ARD	−27.64	2	1	2.38	0.12
Sulcus_ER	−12.74	1	NA	NA	NA
Sulcus_ARD	−12.25	2	1	0.97	0.32
AIII_ER	−42.53	1	NA	NA	NA
AIII_SYM	−39.71	3	2	5.66	0.06
AIII_ARD	−38.36	6	3	2.69	0.44
Parasitism_ER	−7.74	1	NA	NA	NA
Parasitism_ARD	−7.39	2	1	0.71	0.40
Fungiculture_ER	−7.75	1	NA	NA	NA
Fungiculture_ARD	−7.73	2	1	0.03	0.87

the *Nylanderia fulva* clade. Future studies of the biogeography of *Lasius* may benefit from treating biogeographic region as an observed state (character) in the nongenomic (phenotypic) matrix to extract information from the coarse compression fossils in the Nearctic and Palaearctic regions.

Question 5: What were the evolutionary sequence of formicine morphology and life-history traits? Answer: Our analyses recover wide-set hind coxae and sepalous proventriculi as synapomorphies of the Formicinae, and show independent, convergent evolution of social parasitism and fungiculture in *Lasius* (Figs S10–S17, Table 6 & 7).

We determined that the polarity of six characters is particularly important for understanding the morphological evolution of the Lasiini and the subfamily Formicinae. In all cases, the equal rates (ER) transition matrix was found to be the most likely model (Table 6). Empirical Bayesian posterior probabilities are presented for all character states at selected nodes in Table 7, and mapped posterior probabilities are presented in Figures S10–15. Based on our analyses, we predict that the most recent common ancestor of the Formicinae probably had, in addition to the acidopore, the following states: (i) Eyes set at or anterior to head midlength [plesiomorphy]; (ii) wide-set hind coxae [apomorphy]; (iii) absence of a transverse sulcus posterad the helcial sternite [plesiomorphy]; (iv) circular propodeal spiracles [plesiomorphy]; (v) broadly shouldered tergosternal margins laterad the helcium [plesiomorphy], and (vi) a sepalous proventriculus [apomorphy]. Roughly corresponding to expectation (Bolton, 2003), slit-shaped spiracles are estimated to be defining apomorphies of the Formicini, Camponotini and the melophorines *Melophorus* Lubbock and *Notostigma* Emery (Figure S12); other results require further consideration, including those addressing social parasitism and fungiculture, which we provide below.

Of the reconstructed states, the sepalous form of the proventriculus is newly detected as a synapomorphy of the

Table 7. Empirical Bayesian posterior probabilities from ancestral state estimation for selected nodes; numbers may not add up to 1.00 due to rounding error.

	Eyes		Metacoxae		AIII shoulder			Propodeal spiracle		Proventriculus		Sulcus	
Node	Post.	Ant.	Close	Wide	Absent/ broad	Low, narrow	High, narrow	Circle/ ellipse	Slit	Asepal.	Sepal.	Absent	Present
Doryloformicoids (root)	*0.02*	**0.98**	**1.00**	*0.00*	**1.00**	*0.00*	*0.00*	**1.00**	*0.00*	**1.00**	*0.00*	**1.00**	*0.00*
Myrmecioformicoids	*0.00*	**1.00**	**1.00**	*0.00*	**1.00**	*0.00*	*0.00*	**1.00**	*0.00*	**1.00**	*0.00*	**1.00**	*0.00*
Formicinae	*0.02*	**0.98**	*0.08*	**0.92**	**0.72**	*0.06*	0.22	**1.00**	*0.00*	*0.33*	**0.67**	**1.00**	*0.00*
Myrmelachistini	*0.02*	**0.99**	*0.01*	**0.99**	0.06	*0.01*	**0.93**	**1.00**	*0.00*	*0.33*	**0.67**	**1.00**	*0.00*
Lasiini + core Formicinae	*0.05*	**0.95**	*0.07*	**0.93**	**0.69**	*0.11*	0.19	**1.00**	*0.00*	*0.11*	**0.89**	**1.00**	*0.00*
Lasiini	*0.05*	**0.95**	*0.00*	**1.00**	*0.04*	**0.86**	0.10	**1.00**	*0.00*	*0.01*	**0.99**	**1.00**	*0.00*
core Lasiini	*0.07*	**0.93**	*0.00*	**1.00**	*0.01*	**0.89**	0.10	**1.00**	*0.00*	*0.00*	**1.00**	**1.00**	*0.00*
Metalasius + *Prenolepis* g. grp.	*0.03*	**0.97**	*0.00*	**1.00**	*0.01*	**0.85**	0.14	**1.00**	*0.00*	*0.00*	**1.00**	**1.00**	*0.00*
Prenolepis g. grp.	*0.03*	**0.97**	*0.00*	**1.00**	*0.00*	*0.00*	**1.00**	**1.00**	*0.00*	*0.00*	**1.00**	**1.00**	*0.00*
core Formicinae	*0.13*	**0.87**	*0.09*	**0.91**	**0.71**	*0.09*	0.20	**1.00**	*0.00*	*0.11*	**0.89**	**1.00**	*0.00*
Melophorini	**0.98**	*0.02*	**1.00**	*0.00*	**1.00**	*0.00*	*0.00*	**1.00**	*0.00*	**0.90**	*0.10*	*0.00*	**1.00**
formicoform radiation	*0.30*	**0.70**	**0.99**	*0.01*	**1.00**	*0.00*	*0.00*	**1.00**	*0.00*	*0.02*	**0.98**	**0.93**	*0.07*
Formicini	**0.98**	*0.02*	**1.00**	*0.00*	**1.00**	*0.00*	*0.00*	0.03	**0.97**	*0.00*	**1.00**	*0.00*	**1.00**
Plagiolepidini	*0.11*	**0.89**	*0.00*	**1.00**	0.28	*0.16*	**0.56**	**1.00**	*0.00*	**0.95**	*0.05*	**1.00**	*0.00*
Camponotini	*0.01*	**0.99**	**1.00**	*0.00*	**1.00**	*0.00*	*0.00*	*0.01*	**0.99**	*0.00*	**1.00**	*0.00*	**1.00**

For ease of reference, the highest probability state is **bolded** and lowest *italicized* for each node.

subfamily – if the asepalous state in *Myrmelachista* Roger is interpreted as an independent reversal, as implied by our results (Figure S14). Other reversals are also implied for the formicoform radiation (the clade that includes Camponotini, Formicini, and Melophorini, along with the monotypic tribes Gesomyrmecini Ashmead, Gigantiopini Ashmead, Oecophyllini Emery, and Santschiellini Forel; Figure S11), including some Melophorini, Plagiolepidini, and *Myrmoteras* Forel. Overall, this finding contradicts the traditional assumption that the sepalous form arose from the asepalous form within the Formicinae (Emery, 1925; Eisner, 1957), and the hypothesis that the sepalous form is homoplastic within the subfamily (Agosti, 1991; Bolton, 2003). Because our coding was generalized from the literature and was discretized into two (rather than three or more) categories, our results must be treated as tentative. We strongly recommend that future studies expand on the sampling of Eisner (1957), particularly to include Leptanillinae Emery, Martialinae Rabeling and Verhaagh, and more 'poneroids' (sensu Moreau *et al.*, 2006, Brady *et al.*, 2006), and to define new traits of the proventriculus for evolutionary analysis because of its 'social stomach' function (Eisner & Brown Jr., 1958; Wilson, 1971). Moreover, a microanatomical study, perhaps using micro-computed tomography, would be a substantial contribution to this question.

Within the Formicinae, posteriorly set eyes are estimated to have been derived nine independent times (Figure S10), which is a simplistic statement, given that eye position is a continuous and evolutionarily labile trait. This strongly contradicts our intuition that posteriorly set eyes were ancestral, as they are observed in the Leptanillinae (where known), Amblyoponinae Forel, and stem Formicidae (Boudinot *et al.*, 2020; Perrichot *et al.*, 2020). If posteriorly set eyes are truly retained in the various Formicinae, the Ectatomminae Emery s.l., and the Pseudomyrmecinae Smith, then we must appreciate the low likelihood of this scenario and search for corroborating evidence. Ideally, eye position should be modelled as a continuous trait (Parins-Fukuchi, 2018), and ocular and neural anatomy accounted should be accounted for. We expect eye position to be a strongly directional trait, despite the favourability of the ER model in our analyses.

Our estimates indicate that wideset ('lasiine') coxae are an apomorphy of the Formicinae, with a subsequent reversal in the formicoform radiation with losses in *Lasiophanes* Emery, and the ancestor of *Teratomyrmex* McAreavey and *Prolasius* Forel of the Plagiolepidini, as well as *Myrmoteras*. It will be possible to further evaluate the plausibility of this reconstruction through comparative μ-CT analysis of propodeal/petiolar skeletomuscular anatomy. At present, comparative data on 'waist' skeletomusculature is limited (e.g., Hashimoto, 1996; Perrault, 2004).

We detect three independent origins of the 'plagiolepidiform' third abdominal segment among Formicinae (i.e., raised, with free sclerites occurring high; Fig. 7A vs B): Once in the ancestor of the Myrmelachistini, once within the Lasiini (*Prenolepis* genus group), and once in the Plagiolepidini (Figure S15). A fourth independent origin is implied for the Dolichoderinae Forel (Bolton, 2003). Our results support Bolton's (2003) hypothesis that the lasiine condition (i.e., narrowly shouldered but not raised) was a precursor to the plagiolepidiform condition, as elevated shoulders arose well-within the Lasiini. However, whether the narrow and low shoulders of *Anoplolepis* Santschi (Plagiolepidini) are ancestral or a reversal (as must be the case for *Acropyga* Roger) is uncertain. Narrowed shoulders arose three times within the Melophorini (*Stigmacros* Forel, *Lasiophanes*, and the ancestor of *Teratomyrmex* + *Prolasius*). Curiously, 'high and narrow shoulders' are also observed in

Dolichoderinae (e.g., Bolton, 1994), thus comparative anatomical studies focusing on this condition are warranted.

Finally, most of the socially parasitic species within *Lasius* included here (L. 'nr. *subumbratus*', L. *sabularum* (Bondroit), L. *carniolicus* Mayr, L. *californicus* Wheeler, L. *latipes* (Walsh)) form a strongly-supported monophyletic group within the *flavus* clade (Fig. 2). The other two socially parasitic species, L. *fuliginosus* (Latreille) and L. *spathepus* Wheeler, are in the *niger* clade and are sister to one another. Although, we do not have a comprehensive sampling of *Lasius* social parasites and their hosts in the current study, the social parasites do not appear to follow the strict form of Emery's Rule, in which socially parasitic species and their hosts are each other's closest relatives (Emery, 1909). For example, *L. fuliginosus* has been recorded as parasitizing species from the *niger* group (*L. alienus* (Foerster), *L. brunneus* (Latreille) and *L. niger* (Linnaeus)), as well as parasitizing other temporary social parasites from the *flavus* clade, thus making them hyperparasites (Donisthorpe, 1922; Stärcke, 1944; Seifert, 1996). The tendency for *Lasius* temporary social parasites to parasitize species from both major *Lasius* clades holds true for several other taxa in this study. For example, *L. carniolicus* parasitizes *L. flavus* (Fabricius) (*flavus* clade) and *L. alienus* (*niger* clade) (Schmid, 1975; Seifert, 1996), while *L. latipes* parasitizes *L. alienus* (*niger* clade) and *L. interjectus* Mayr (*flavus* clade) (Wing, 1968a; Cover & Sanwald, 1988). These results concur with those of Janda *et al.* (2004), which also did not support Emery's Rule in the strict sense.

A subset of social parasites, here represented by L. 'nr. *subumbratus*', L. *sabularum*, L. *fuliginosus*, and L. *spathepus* are also known to culture fungi to bind walls of their nests (Schlick-Steiner *et al.*, 2008). These species are widely separated on the phylogeny; thus, it appears likely that both social parasitism and fungiculture evolved at least twice within the genus, in agreement with our ancestral state reconstructions (Figs 5, S16, S17).

Taxonomy

Here, we report the taxonomic implications of our study (*Question 6* of Table 1). Note that probable autapomorphies in the context of the Lasiini are *italicized* in the taxon definitions below; the diagnosis of the Lasiini itself is polythetic, as autapomorphies for this clade were not detected at the level of tribe within the Formicinae.

Tribe Lasiini Ashmead, 1905 (Figs 6, 7, 8A–K, 9A–J, 10A–D)

Type genus. Lasius.

Included genus groups. Cladomyrma, *Lasius* group, *Metalasius*, *Prenolepis* group.

Definition (worker).

1. With characters of Formicinae (see Bolton, 2003 and Note 1).
2. Mandible triangular, with 4–11 teeth; third tooth from apex reduced.
3. Dorsal mandibular groove, when present, running along lateral mandibular margin as seen in dorsal view (Note 2).
4. Palp formula usually 6,4, less often 3,4.
5. Frontal protuberance mediad antennal toruli with frontal carinae effaced, becoming broadly rounded posteriorly until continuous with face (Note 3).
6. Frontal protuberance raised above toruli or not.
7. Antennal toruli near or abutting posterior clypeal margin.
8. Antenna 12-, 11-, or 8-merous.
9. Compound eyes not enormous, that is, not longer than half the length of the head; eyes may be reduced to absent; long axis of eyes subparallel.
10. Ocelli present or absent (Note 4).
11. Metanotum differentiated or not.
12. Metapleural gland present, dorsal rim of metapleural gland curved inward.
13. Propodeal spiracle at or near posterolateral margin of propodeum.
14. Propodeal spiracle circular to elliptical, not slit-shaped.
15. Metacoxae wideset: Distance between mesocoxal bases less than between that between bases of metacoxae with mesosoma in ventral view and coxae oriented at right-angles to long axis of body.
16. Metatibiae without double row of ventral (inner) setae.
17. Petiolar foramen in profile view low, not to barely exceeding dorsal margin of metapleural gland, with or without dorsal margin or lip, but lip, when present, inconspicuous (Note 5).
18. Petiolar foramen in ventral view long, anterior margin exceeding metacoxal cavities anteriorly.
19. Petiolar node conspicuously shorter than propodeum, not reaching dorsal surface of propodeum (Note 6).
20. Petiolar apodeme (situated anteriorly on tergum) contiguous or nearly contiguous with petiolar node (Note 7).
21. Petiolar sternum U-shaped in cross-section (Note 8).
22. Abdominal segment III transverse sulcus absent.
23. Base of abdominal segment III with or without complete tergosternal fusion lateral to helcium, free sclerites commencing distantly up segment or near helcium; tergum III overhanging petiole or not.
24. Proventriculus sepalous (Note 9).

Notes on definition:

Note 1. The generic composition of the Lasiini has recently been reassessed following Blaimer *et al.* (2015) and Ward *et al.* (2016). The tribal definition proposed here is thus revised relative to Bolton (2003). It includes new characters and recognizes that several former plagiolepidines belong in the Lasiini.

Note 2. Previous studies have not focused attention on the dorsal mandibular groove. Here it was observed that the groove, as seen with the mandible in dorsal view, runs along the outer margin of the mandible toward the mandibular apex in the Myrmelachistini, Lasiini and most Melophorini. This contrasts with the state observed in the 'formicoform radiation' (i.e., the clade that includes Camponotini, Formicini and Melophorini, along with the monotypic tribes Gesomyrmecini, Gigantiopini, Oecophyllini, and

Fig. 6. Gross phenotypic synopsis of the Lasiini; all images in profile view; scale bars = 1.0 mm. (A) *Cladomyrma hewitti* (CASENT0173906); (B) *Lasius lasioides* (CASENT0906077); (C) *Lasius citrinus* (CASENT0103542); (D) *Myrmecocystus melliger* (CASENT0103518); (E) *Metalasius myrmidon* (CASENT0903666); (F) *Euprenolepis procera* (CASENT0906260); (G) *Nylanderia amblyops* (CASENT0007735); (H) *Paraparatrechina albipes* (CASENT0178759); (I) *Paratrechina ankarana* (CASENT0454372); (J) *Prenolepis imparis* (CASENT0179615); (K) *Pseudolasius amaurops* (CASENT0106005); (L) *Zatania gibberosa* (CASENT0281461). (Image credits, AntWeb: A, C, G, H = April Nobile; B = Shannon Hartman; D = Jen Fogarty; E, Will Ericson; F, Estella Ortega; I, Michele Esposito; J, Erin Prado; K, Michael Branstetter; L, Ziv Lieberman).

Santschiellini; see the section †*Kyromyrma*, an ancestral formicine, under the section '*Incertae sedis* in the Formicinae' below). When the groove is present in the 'formicoform radiation', it is very close to the basal mandibular margin and is shortened, except in various plagiolepidines. The medial and shortened state may have arisen multiple times in the Formicini, Plagiolepidini, and Camponotini clade.

Note 3. The 'frontal protuberance' is the region between the antennal toruli, which is raised relative to the regions of the face laterad the toruli. To some degree, development of this condition accounts for the 'laterally directed' torular condition of Formicidae (Boudinot *et al.*, 2020). In other formicine tribes, including the Melophorini (with *Prolasius* as an exception), the frontal protuberance is carinate above the toruli (*i.e.*, 'frontal carinae are present'), with these carinae continuing as a sharp ridge until their posterior terminus. Within the Lasiini, the frontal carinae are effaced; they are long in all groups except *Cladomyrma*, while in the Plagiolepidini the carinae are short in all genera except *Anoplolepis*.

Note 4. Ocellus presence–absence is a relatively weak character as expression of ocelli may be variable for genera in which ocelli are observed, such as *Lasius* and *Nylanderia*. However, this statement is included as ocellus expression is a traditional character which is easy to evaluate and may have value for future works defining tribes wherein ocelli may be consistently present or absent. Within the Lasiini, ocelli are always absent in *Cladomyrma*, *Euprenolepis*

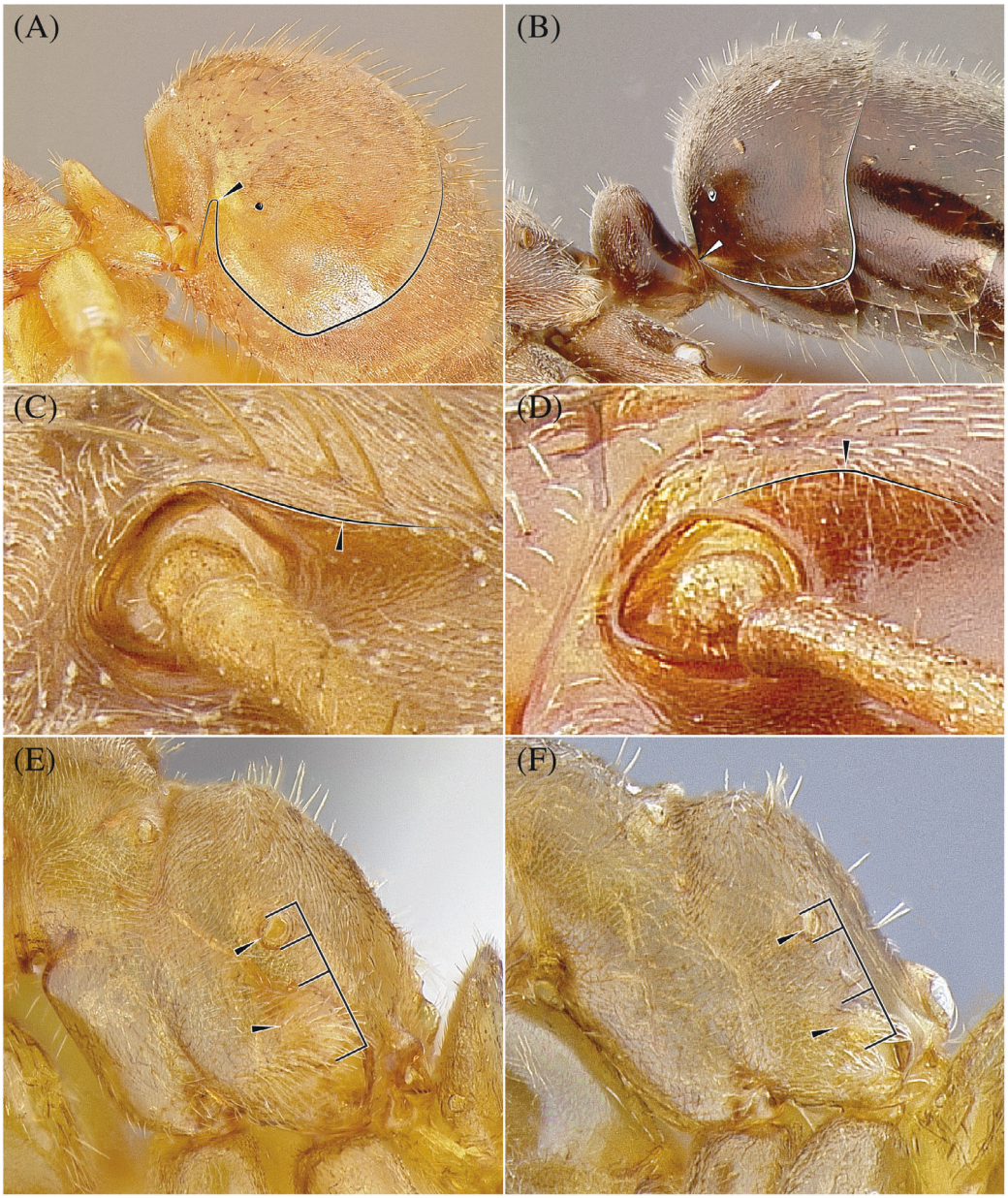

Fig. 7. Some key features of the major clades of the Lasiini. (A) third abdominal tergite modified with dorsoventrally-oriented groove for reception of entire petiole (*Pseudolasius breviceps*); black line indicates contour of tergum and black ellipse the spiracle; (B) third abdominal tergite receiving only posterior base of petiole (*Myrmecocystus mimicus*); white line indicates contour of tergum, and white ellipse the spiracle; (C) frontal protuberance and effaced carinae low relative to face (*P. breviceps*); (D) frontal protuberance and effaced carinae raised dorsally from face (*M. mimicus*); (E) metapleural gland atrium grossly enlarged (*Lasius subumbratus*); black lines show larger size of the metapleural gland bulla (lower indicator) as compared to F, and relative to the propodeal spiracle (upper indicator) and space between the spiracle and bulla (middle portion); (F) metapleural gland atrium small (*Lasius turcicus*); black lines show smaller size of metapleural gland bulla as compared to E, and relative to the propodeal spiracle and space between spiracle and bulla.

Emery, and *Pseudolasius* Emery, variably present among *Lasius*, *Paraparatrechina* Donisthorpe, and *Prenolepis* Mayr species, and consistently present in *Myrmecocystus*, *Paratrechina* Motschoulsky (except *P. kohli*; see comments under *Prenolepis* genus group), and *Zatania* LaPolla *et al.*

Note 5. The conformation of the dorsal region of the petiolar foramen is newly described here. There is complex variation of the form across the subfamily, but it appears at least that the form observed in the Lasiini is consistent; this form is also observed in the Myrmelachistini. In various

Fig. 8. Gross phenotypic synopsis of the extant species groups of *Lasius*, plus two phenotypically similar fossil species; all images in full-face view; scale bars = 0.5 mm. (A) *Lasius brunneus* (CASENT0280440); (B) *Lasius fuliginosus* (CASENT0179898); (C) *Lasius* nr. *niger* (CASENT0106128); (D) *Lasius* nr. *atopus* (CASENT0234858); (E) *Lasius carniolicus* (CASENT0280471); (F) *Lasius claviger* (CASENT0103542); (G) *Lasius brevicornis* (CASENT0280456); (H) *Lasius nearcticus* (CASENT0104774); (I) *Lasius pallitarsis* (CASENT0005405); (J) *Lasius aphidicola* (CASENT0280468); (K) †*Lasius schiefferdeckeri* (MNHNB25217); (L) †*Kyromyrma neffi* (AMNH-NJ1029). (Image credits: D = the authors; AntWeb: A = Will Ericson; B = Erin Prado; C = Michael Branstetter; E, G, J = Shannon Hartman; F, H = April Nobile; I = unknown; K = Vincent Perrichot; L = Dave Grimaldi & Vincent Perrichot.)

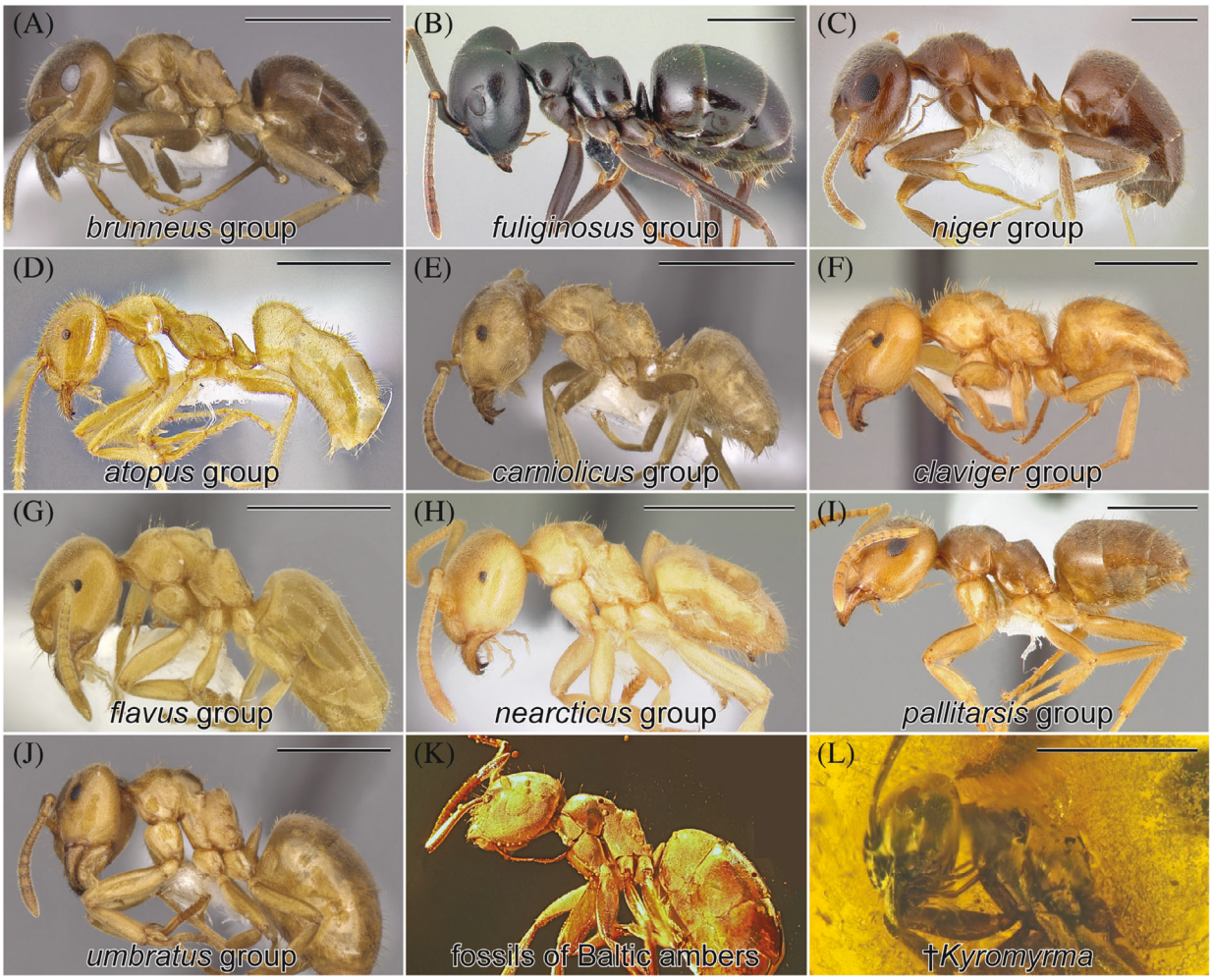

Fig. 9. Gross phenotypic synopsis of the species groups of *Lasius*, plus two phenotypically similar fossil species; all images in profile view; scale bars = 1.0 mm; scale bar unavailable for K. (A) *Lasius brunneus* (CASENT0280440); (B) *Lasius fuliginosus* (CASENT0179898); (C) *Lasius* nr. *niger* (CASENT0106128); (D) *Lasius* nr. *atopus* (CASENT0234858); (E) *Lasius carniolicus* (CASENT0280471); (F) *Lasius claviger* (CASENT0103542); (G) *Lasius brevicornis* (CASENT0280456); (H) *Lasius nearcticus* (CASENT0104774); (I) *Lasius pallitarsis* (CASENT0005405); (J) *Lasius aphidicola* (CASENT0280468); (K) †*Lasius schiefferdeckeri* (HJF013); (L) †*Kyromyrma neffi* (AMNH-NJ1029). (Image credits: D = the authors; AntWeb: A = Will Ericson; B = Erin Prado; C = Michael Branstetter; E, G, J = Shannon Hartman; F, H = April Nobile; I = unknown; K = Vincent Perrichot; L = Dave Grimaldi & Vincent Perrichot.)

lineages within the formicoform radiation, a raised and conspicuously carinate dorsal margin is observed.

Note 6. Short petiolar nodes are also observed in the Myrmelachistini and Plagiolepidini (excluding *Anoplolepis*). The node height is variable in the Melophorini, being short in *Prolasius* and *Myrmecorhynchus* André.

Note 7. The apodeme is clearly separated from the node in most Melophorini, except *Prolasius*.

Note 8. A U-shaped petiolar sternum was used by Bolton (2003) to diagnose the lasiine tribe group. This trait also occurs in the Myrmelachistini, Myrmoteratini Emery, Plagiolepidini, and four Melophorini (*Lasiophanes*, *Prolasius*, *Stigmacros*, *Teratomyrmex*); see 'Ancestral state estimation' results above and Figure S15.

Note 9. The proventriculus is weakly sepalous in *Cladomyrma*. The form of the proventriculus forms a natural division between the Plagiolepidini and the 'plagiolepidiform' *Prenolepis* genus group, as observed by Emery (1925). Due to uncertainty about the polarity of the sepalous condition – and whether this form arose multiple times (Eisner, 1957; Agosti, 1990, 1991) – Bolton (2003) lumped the two plagiolepidiform clades, plus the Myrmelachistini, into the Plagiolepidini.

Exclusion of †*Glaphyromyrmex* from the Lasiini: The Baltic amber formicine, †*Glaphyromyrmex* Wheeler, was placed in the Formicini until recently (Wheeler, 1915, Donisthorpe, 1943, Dlussky, 1967, Dlussky & Fedoseeva 1988, Bolton, 1994), when Dlussky (2008) transferred the genus to the Lasiini.

Fig. 10. Habitus images for the three new genera recognized in this study; scale bars = 0.25 mm. (A, B) *Metalasius myrmidon* **gen.nov. comb.nov.** (CASENT0906115); (C, D) †*Metalasius pumilus* **gen.nov. comb.nov.** (SMFBE1226); (E, F) †*Sussudio* **gen.nov. comb.nov.** (GZG-BST04646). Views: A = full-face; B, E = profile; C = laterally oblique facial; D, F = dorsal. Observe: (1) The compound eyes of *Metalasius myrmidon* and †*M. pumilus* are mid-set, and (2) †*Sussudio* **gen.nov.** has a distinctly-carinate propodeal foramen, vertical petiolar node and nongrooved (lateromedially convex) third abdominal tergite.

Placement of †*Glaphyromyrmex* in the Lasiini is counterintuitive given presence of a ventral double-row of setae on its metatibiae, a state which does not occur in any lasiine. Intuitive placement of †*Glaphyromyrmex* based on morphology is challenging, however. †*Glaphyromyrmex* differs from members of all formicine tribes in which double seta rows occur (Formicini, Camponotini, some Melophorini). Specifically, †*Glaphyromyrmex* differs from the Formicini and most Camponotini in eye position (eyes set at about head midlength), from the Camponotini in having antennal toruli which abut the posterior clypeal margin (vs widely separated), and from the Melophorini, which have well-defined dorsal and ventral flaps surrounding the metapleural gland, a conformation that is apparently absent in †*Glaphyromyrmex*. Recognizing these differences, however, we transfer †*Glaphyromyrmex* back to the Formicini (**tribal transfer**) based on our combined analyses (Fig. 4) and recommend revised study of the fine-scale external anatomy of the fossil taxon.

On the identity of †*Protrechina* Wilson: Wilson (1985) described a genus putatively close to *Paratrechina* sensu lato (~ *Prenolepis* genus group) from mid-Eocene Claiborne amber (Arkansas, 40.4–37.2 Ma; Saunders *et al.*, 1974). This genus, †*Protrechina*, supposedly differs from *Paratrechina s. l.*, *Lepisiota* Santschi and *Brachymyrmex* Mayr – among other, unstated formicines – by the absence of standing macrosetae on the mesosomal dorsum, a state similar to that observed for *Metalasius* **gen.nov.** as noted below. The genus has been variably treated as a lasiine (Bolton, 1994, 1995; LaPolla & Dlussky, 2010), a 'prenolepidine' (Hölldobler & Wilson, 1990), or as *incertae sedis* in the subfamily where it remains at present (Wilson, 1985; Dlussky & Fedoseeva 1988; Bolton, 2003; Ward *et al.*, 2016). The type specimen of †*Protrechina carpenteri* Wilson, at the Museum of Comparative Zoology (Harvard), should be reexamined to evaluate its tribal, and perhaps generic, placement. This would be particularly valuable given the approximately mid-Eocene origin of the *Prenolepis*

genus group here inferred (Fig. 4; Table 5); such a study will be facilitated by use of micro-CT (e.g., Hita-Garcia *et al.*, 2017; Barden *et al.*, 2017b; Boudinot *et al.*, in press), given the poor condition of the specimen reported by LaPolla & Dlussky (2010).

Key to extant genera of Lasiini and primary clades of *Lasius* (workers)

1. Antenna with eight antennomeres. Mesonotum, metanotum, and propodeum more-or-less continuous, and metanotum undifferentiated (Fig. 6A). Propodeal spiracle distinctly situated in dorsal third of propodeum. Frontal carinae inconspicuous, being extremely short (<0.5 × anteroposterior antennal torulus diameter) or absent . . . . . ***Cladomyrma*** (see Agosti, 1991; Agosti *et al.*, 1999).

– Antenna with 11 or 12 antennomeres. Mesonotum, metanotum, and/or propodeum discontinuous, and metanotum differentiated (Fig. 6A–G, I–L), rarely mesosomal dorsum continuous and metanotum undifferentiated (few *Paraparatrechina*) (Fig. 6H). Propodeal spiracle situated somewhat below or above midheight of propodeum, but not in dorsal third. Frontal carinae conspicuous (≥1.0 × anteroposterior antennal torulus diameter) **2**

2. Petiole posteriorly elongated. Node reduced, apex not or barely projecting dorsally above metapleural gland when observed in profile view (Fig. 6F–L). Abdominal tergum IV with anterolateral corners directed anterodorsally from helcium and forming lateral margins of concavity, which receives entire posterior region of petiole when gaster raised (Fig. 7A); petiole largely obscured by abdominal tergum IV in dorsal view. Facial region between antennal toruli flat, effaced frontal carinae not raised above toruli (Fig. 7C) . . . . . ***Prenolepis*** **genus group** (see LaPolla *et al.*, 2012; LaPolla & Fisher, 2014).

– Petiole without posterior elongation. Node squamiform, not reduced, apex projecting dorsally above metapleural gland when observed in profile view (Fig. 6B–E). Abdominal tergum IV with anterolateral corners weakly or not raised anterodorsally from helcium, corners not forming lateral margins of concavity and not concealing entire posterior region of petiole when gaster raised (Fig. 7B); petiole visible in dorsal view, not obscured by abdominal tergum IV. Facial region between antennal toruli bulging to concave, frontal carinae raised above toruli (Fig. 7D) **3**

3. Eyes situated in anterior half of head as measured in full-face view (Fig. 10A). Metapleural gland orifice reduced, with opening directed posteriorly. Propodeal spiracle situated in lower half of propodeum in profile view. Antennomere III broader than long. Hypostoma lacking carina along lateral margins . . . . . ***Metalasius*** **gen.nov.** (not all states observable for †*M. pumilus* **comb. nov.**, see below).

– Eyes situated in posterior half of head as measured in full-face view (Fig. 9). Metapleural gland orifice small to very large, opening laterally as well as posteriorly. Propodeal spiracle situated at or above midheight of propodeum in profile view. Antennomere III usually longer than broad. Hypostoma with carina along lateral margins . . . . . **4 (*Lasius* genus group).**

4. Maxillary palpomeres III and IV strongly flattened and greatly elongated, length of each exceeds length of apical antennomere. Ventral surface of head with psammophore, that is, margined by long setae (Fig. 6D). Mesothorax and metathorax elongated, mesonotum meeting metanotum at very low angle (Fig. 6D). Compound eyes set at or near extreme posterior margin of head in full-face view; eyes often separated from this border by <1 eye diameter . . . . . ***Myrmecocystus*** (see Snelling, 1976, 1982).

– Maxillary palpomeres III and IV circular to elliptical in cross-section and not elongated, length of each is less than length of apical antennomere. Ventral surface of head without psammophore (Fig. 6B, C). Mesothorax not elongated and metathorax very rarely elongated, mesonotum usually meeting metanotum at steep angle (Fig. 6B, C). Compound eyes set further away from posterior head margin in full-face view; eyes usually separated from this border by >1 eye diameter . . . . . **5 (*Lasius*)**.

5. Metapleural gland enlarged internally, atrium (internal chamber of gland) bulging (forming bulla) and conspicuously visible from external view in profile (Fig. 7E)*. Usually, distance between atrium and propodeal spiracle <2 spiracular diameters as viewed with spiracle and gland in same plane of focus (Fig. 7E). Compound eyes usually somewhat- to very-reduced; **if** compound eye large, **then** offset basal tooth present on mandible **and** body yellowish brown . . . . . ***Lasius flavus*** **clade.**

– Metapleural gland small, atrium flat to concave, inconspicuous from external view in profile (Fig. 7F). Usually, distance between atrium and propodeal spiracle >2 spiracular diameters as viewed with spiracle and gland in same plane of focus (Fig. 7F). Compound eyes relatively large **and** offset basal tooth absent; **if** offset basal tooth present, **then** body jet black . . . . . ***Lasius niger*** **clade.**

*Note: The enlarged state of the metapleural gland bulla is a defining synapomorphy of the *flavus* clade. A slightly enlarged bulla is observable in the *fuliginosus* species group, but these jet-coloured ants are otherwise highly distinct.

Genus group of *Lasius* (Figs 6B, C, D, 7B–F, 8A–K, 9A–J)
Included genera. Lasius, *Myrmecocystus*.
Definition (worker).

1. With characters of Lasiini.
2. Mandible with 4–11 teeth.
3. Palp formula 6,4 or 3,4.

4. Basal and masticatory mandibular margins meeting at a weakly oblique angle.
5. Frontal carinae conspicuous, >0.5 × anteroposterior antennal torulus diameter.
6. Frontal region of head between antennal toruli bulging, with frontal carinae raised above toruli (Note 1).
7. Antenna 12-merous.
8. Third antennomere usually longer than broad (Note 2).
9. Compound eye set in posterior half of head (Note 3).
10. Ocelli usually present (Note 4).
11. Dorsum of head with at least some standing setae in addition to those on posterolateral head corners.
12. Mesonotum, metanotum, and/or propodeum discontinuous, metanotum differentiated.
13. Anterolateral margin of mesopleural area, near posteroventral pronotal margin, with longitudinally oriented bosses subtending transverse groove or not (Note 5).
14. Metapleural gland small to very large, orifice opening laterally to posterolaterally, not directed posteriorly.
15. Propodeal spiracle situated in lower 2/3 of propodeum.
16. Petiole with raised squamiform node, without posterior elongation.
17. Abdominal tergum III vertical, without deep groove for receiving petiole; not concealing petiole when gaster raised.
18. Tergosternal suture of abdominal segment III not raised dorsally before unfusing near spiracle, rather anterior margin of abdominal sternum III directed anteriorly away from helcium before narrowly curving posteriorly.
19. Pubescence of abdominal terga VI and VII absent, or present and linear to weakly curved.

Notes on definition:

Note 1. The polarity of the frontal bulge is uncertain. Both the *Lasius* and *Metalasius* genus groups have raised frontal regions, but neither *Cladomyrma* nor the *Prenolepis* genus group do.

Note 2. Antennomere III is longer than broad in most *Lasius*, except for the *flavus* species group (former *Cautolasius*).

Note 3. Although we suspect that posteriorly set eyes are a plesiomorphy for the crown Formicidae, our ancestral state estimation results indicate that the posteriorly set eyes of the *Lasius* genus group are derived and that they are homoplastic with respect to *Prenolepis* + *Zatania* and *Paratrechina* (Figure S10).

Note 4. Ocelli are not expressed in various species of the *flavus* clade. Generally, ocellus presence is a highly variable state, even within species, thus is a weak defining feature for worker ants.

Note 5. The development of the boss subtending the transverse mesosternal groove appears to be an apomorphy of the *Lasius* genus group or *Lasius* itself, with loss in *Myrmecocystus* and reduction in the *L. fuliginosus* group. The groove and shoulder (boss) are present in a reduced form in *Metalasius* and are variable in the *Prenolepis* genus group. Specifically, they are reduced such that no rim is present on the anterior mesosternal margin (e.g., *Nylanderia*), or the groove is elongated (e.g., *Zatania*, *Prenolepis*, *Paratrechina*); some *Paraparatrechina* has either the groove (narrow) or the shoulder.

Genus *Lasius* Fabricius, 1804

= *Donisthorpea* Morice and Durrant, 1915.
= *Acanthomyops* Mayr, 1862 **syn.rev.**
= *Austrolasius* Faber, 1967 **syn.nov.**
= *Cautolasius* Wilson, 1955 **syn.nov.**
= *Chthonolasius* Ruzsky, 1912 **syn.nov.**
= *Dendrolasius* Ruzsky, 1912 **syn.nov.**

Type species. Formica nigra Linnaeus, 1758 (= *L. niger*).

Subgeneric classification remarks. The modern body of taxonomic work on *Lasius* was initiated by Wilson's revision of the genus (Wilson, 1955), which was classified into four subgenera at the time: *Cautolasius*, *Chthonolasius*, *Dendrolasius*, and *Lasius* s. str. In this work, Wilson provided a phylogeny of *Lasius* (Fig. 1A), but this treatment was an intuitive account of what he considered trends in the evolution of the morphology and biogeography of the genus. Subsequently, the subgenus *Austrolasius* was erected for a few socially parasitic species (Faber, 1967), and the former genus *Acanthomyops* was included in *Lasius* as the sixth subgenus (Ward, 2005).

The first phylogenetic inference based on molecular data was presented by Hasegawa (1998), who used COI to investigate relationships of four *Lasius* species (phylogeny not figured here). Since then, two major attempts at resolving the phylogeny were presented by Janda *et al.* (2004) and Maruyama *et al.* (2008) (Fig. 1B, C). Both studies used a combination of morphological characters and molecular data, including mitochondrial markers (COI, COII, tRNA-Leu, 16S). A more recent effort focused on the phylogeny of European species related to *L. niger* (*Lasius* s. str.) and included nuclear genes *LW Rh* and *wg* in addition to 16S and COI (Talavera *et al.*, 2015).

To date, the monophyly of the subgenera has not been questioned except for the nominotypical subgenus (Janda *et al.*, 2004; Maruyama *et al.*, 2008). Recently, Seifert (2020, p. 21) stated that there is clear justification for elevating the subgenera to generic status. Such an action would considerably complicate the classification of the *Lasius* genus group because of the robustly supported paraphyly of the subgenera that we have uncovered here (Figs 1D, 2, S1, Table 4). Specifically, in order to retain monophyly at the genus rank, four new genera would need to be erected for the species groups of *brunneus*, *nearcticus*, *atopus*, and *pallitarsis*. An additional issue would be the placement of the species which have not been sequenced, particularly those of the *niger* species group and, for example, the recently described *L. brevipalpus* Seifert, which is *incertae sedis* in the *niger* clade. The strongest morphological reorganization at the generic or subgeneric levels would be to recognize the reciprocally monophyletic *niger* and *flavus* clades as *Lasius* and *Acanthomyops*, respectively, but we refrain from doing so here (for our rationale, see 'Species group classification of *Lasius*' below).

Comments on extant species. We determine that one species, *Lasius escamole* Reza should be excluded from *Lasius* and considered a junior synonym of the dolichoderine *Liometopum apiculatum* Mayr **syn.nov.** Reza (1925) described *L. escamole*

in the context of a cultural study on the eponymous traditional Mexican dish known to be made from the larvae of *L. apiculatum* (Hoey-Chamberlain *et al.*, 2013). Although Reza's description and illustrations are extremely vague, it is possible to see details that point to a dolichoderine identity. In the figures of the original description, the mandibles have long masticatory margin and small, sharp, even denticles, the ventral metasoma is shown as a slit-like anal opening rather than a formicine-like acidopore, and various figures display the fine, dense, appressed pilosity characteristic of *Liometopum* Mayr, but no erect setae as expected for *Lasius*.

Many species have been added to *Lasius* since Wilson's revision, mostly in Europe and Mediterranean, while North American taxa have largely remained untreated except for a thorough revision of *Acanthomyops* (Wing, 1968a, 1968b). Careful research has revealed multiple Palaearctic *Lasius* species that show only subtle morphological differentiation from close relatives (Seifert, 1983, 1990, 1991, 1992, 2020; Schlick-Steiner *et al.*, 2003). There is no reason to believe that North America does not harbour a diverse fauna of such 'cryptic species'. For example, the question of the putative Holarctically distributed *Lasius* species was resolved by Schär *et al.* (2018) who elevated to species rank the American representatives of *L. alienus*, *L. flavus*, and *L. umbratus* Nylander, recognizing the following revived taxa, in order: *L. americanus* Emery, *L. brevicornis* Emery, and *L. aphidicola* (Walsh). Renewed focus on the Nearctic fauna is necessary, as is expanded sequencing at the global scale.

Comments on extinct species. Without having scored the Baltic *Lasius* fossils other than †*L. schiefferdeckeri*, that is, †*L. punctulatus* Mayr and †*L. nemorivagus* Wheeler, we are unable to quantitatively address their placement. Historically, †*L. punctulatus* and †*L. schiefferdeckeri* were considered to be members of *Lasius* s. str. (Wilson, 1955; Dlussky, 2011), while the queen-based †*L. nemorivagus* was placed in *Chthonolasius* (Wilson, 1955) later to be implicitly considered *incertae sedis* in the genus (Dlussky, 2011).

Our combined-evidence dating analyses recover †*L. schiefferdeckeri* as sister to or within the *Lasius* genus group (Figs 4, S7–S9). As the specific relationship of the fossil to the extant species of the *Lasius* genus group is uncertain, we conservatively consider the fossil *incertae sedis* in *Lasius*. There remains the possibility that †*L. schiefferdeckeri* is ancestral to the extant *niger* clade and is indicative of low rates of phenotypic transformation, as suggested by Mayr (1868), Wheeler (1915), and Wilson (1955). The placement of †*L. schiefferdeckeri* may be refined in future study by scoring characters which are explicitly derived from comparison of the *brunneus* and *niger* groups within the *niger* clade.

The two differentiating traits proposed for the *brunneus* and *niger* groups are, on average, < 8 mandibular teeth in the *brunneus* group (Seifert, 1992; some *niger* group species with <8), and presence of a subapical cleft in the mandibles of *brunneus* group males (Wilson, 1955). While †*L. schiefferdeckeri* demonstrates both a tooth count of <8, and presence of a subapical cleft, the latter character is probably plesiomorphic of the *Lasius* genus group, and the polarity of the former is uncertain. Notably, Wilson (1955) observed that the male mandibles of †*L. schiefferdeckeri* are observed to vary from the '*brunneus* form' to the derived '*niger* form'. With these three traits in mind, it does seem reasonable that †*L. schiefferdeckeri* is stem to or directly ancestral to the *niger* clade.

Note on biology. Despite the interest in this genus, however, basic natural history remains unknown for many species, including the morphologically aberrant *L. atopus* and the species we sequence here, '*L.* nr. *atopus*'. Only a handful of recently published studies have addressed the behaviour of some of the more rarely encountered species (e.g., Raczkowski & Luque, 2011), indicating that more effort is needed to elucidate the biology of *Lasius*.

Species group classification of *Lasius*

To avoid following the undesirable trend where taxonomy is divorced from molecular phylogenetics (Steiner *et al.*, 2009; Ward, 2011), we propose an informal species-group classification of *Lasius*, which reflects the phylogenetic structure within the genus. As the ICZN rules do not apply to informal species groups, this arrangement is also more adaptable to future refinements and new phylogenetic findings, thus contributing to taxonomic stability. Two main clades are recognized, those of *L. niger* (70 spp. + 1 ssp.), and *L. flavus* (54 spp.), with three and seven species groups, respectively. In addition, all 21 valid extinct species are formally considered *incertae sedis* in the genus, while 14 extant species are considered unidentifiable and *incertae sedis* in the genus.

Should the resurrection of subgenera be deemed advisable and desirable, we recommend dividing the genus into *Lasius* s. str. and *Acanthomyops* along the boundaries of the *niger* and *flavus* clade split. Resurrection of *Acanthomyops* may be justified, as it is readily recognizable by the autapomorphic condition of its metapleural gland (see couplet 5 of key to lasiine genera above, Fig. 7E, F, also Appendix S1), and the relatively old split between the *flavus* and *niger* clades (Figs 4, 5). However, we have elected not to do so here because: (i) our molecular sampling is still fractional at the species level (9/70 *niger* clade, 12/54 *flavus* clade); (ii) transfer of *Lasius* subgenera or species groups to *Acanthomyops* may be disruptive to the practicing systematic community; (iii) Sanger data are being rapidly superseded by UCE data for ant systematics; (iv) morphological investigation is necessary to diagnose the newly recovered groups, and (v) the '*Lasius*' gestalt is easy to recognize during field collecting and generally facilitates communication. In either case, the exceptional morphometric data being generated for *Lasius* (e.g., Seifert, 1982, 1992, 2020; Seifert & Galkowski, 2016) will be valuable for model-based phylogenetic analysis combining phenotypic and genotypic data (e.g., Prebus, 2017; Barden *et al.*, 2017a), particularly in the light of the greater information content of continuous trait data relative to discretized characters (Parins-Fukuchi, 2018). Ultimately, our goal is to encourage the consilience of morphological and molecular data, and we view both as critical for a complete understanding of evolution and systematics.

The following inter-group transfers are made: (i) Members of nonmonophyletic former *Lasius* s. str. Are dispersed among *L. brunneus*, *L. niger*, and *L. pallitarsis* groups; (ii) *L. atopus* and *L. humilis* Wheeler are removed from the *L. umbratus* group (former *Chthonolasius*) and placed in the *atopus* and *flavus* groups, respectively and; (iii) *L. nearcticus* Wheeler and *L. sonobei* Yamauchi are removed from the *flavus* group (former *Cautolasius*) and placed in the *nearcticus* group. For diagnosis of the *niger* and *flavus* clades, see the key to extant genera of Lasiini above. The task of morphologically distinguishing two pairs of groups, those of *brunneus* and *niger* and of *flavus* and *nearcticus*, is difficult. Future phylogenetic studies are expected to refine the boundaries of these species-groups. In addition, keys to the species within these groups, and especially that of *umbratus*, are necessary. Diagnostic remarks for each species group are provided to guide such future work.

Note that, in the list below, [e] indicates that specimen(s) of the taxon has/have been examined while empty brackets, [], indicate that specimens were unavailable and placed based on study of the literature. Species that were included in our molecular sampling are **bolded**. Genus group type species are marked with asterisks (*). Overall, with the exclusion of *L. myrmidon* and *L. escamole*, 118 of the 125 valid, extant species (124) and subspecies (1) were examined either directly or indirectly (via AntWeb). For authorities and taxonomic synopses, refer to Bolton (1995) or AntCat (Bolton, 2021). Finally, it should be noted that some groups contain additional, undescribed species.

I. Clade of *niger*

1. Species group of *brunneus* (*L.* s. str. Part 1/3) (Figs 8A, 9A)

Constituent species (11): *austriacus* Schlick-Steiner [e], ***brunneus*** [e], *excavatus* Seifert [e], *himalayanus* Bingham [e], *israelicus* Seifert [e], *lasioides* (Emery) [e], *neglectus* Van Loon *et al.* [e], *precursor* Seifert [e], *silvaticus* Seifert [e], *tapinomoides* Salata & Borowiec [e], ***turcicus*** Santschi [e].

Distribution: Palaearctic.

Identification: Within the *niger* clade, workers of the *brunneus* group differ from the *fuliginosus* group in coloration (brown vs jet black), cuticle surface texture (finely shagreened vs polished), and head shape (more-or-less oval vs cordate); otherwise, apparently without strong or consistent differentiating conditions relative to the *niger* group (Seifert, 2020). Roughly differing from the *niger* group in the combination of mandibles with ≤8 teeth on average within a colony plus scapes and outer (extensor) surface of the metatibia having <8 total standing setae. Species-level identification is provided by Seifert (2020).

Note 1. Within the *brunneus* species group as circumscribed here, two complexes are recognized by Seifert (2020): that of *brunneus* comprises *brunneus*, *excavatus*, *lasioides*, *himalayanus*, and *silvaticus* (five spp. total), and that of *turcicus* comprises *austriacus*, *israelicus*, *neglectus*, *precursor*, *tapinomoides* and *turcicus* (six spp. total).

Note 2. The differentiating features relative to the *niger* group above are intended to be heuristic. See the key in Seifert (2020) for formal identification of *brunneus* group species.

2. Species group of *fuliginosus* (= *Dendrolasius*) (Figs 8B, 9B)

Constituent species (8): *buccatus* Stärcke [], *capitatus* (Kuznetsov-Ugamsky) [e], *fuji* Radchenko [], ***fuliginosus**** [e], *morisitai* Yamauchi [], *nipponensis* Forel [e], *orientalis* Karavaiev [e], ***spathepus*** [e].

Distribution: Palaearctic.

Identification: Universally identifiable among *Lasius* for their jet-black and shining (polished) cuticle, and their weakly to strongly cordate (posteriorly emarginate) heads; unique among the *niger* clade in bearing an offset basal tooth on the mandible. Species-level identification of all *fuliginosus* species is presented in Radchenko (2005a); note that *Lasius buccatus* is known only from the queen and male castes (Stärcke, 1942).

3. Species group of *niger* (*L.* s. str. Part 2/3) (Figs 8C, 9C)

Constituent species (50), subspecies (1): **Holarctic** (1): ***niger**** [e]; **Nearctic** (5): ***americanus*** [e], *crypticus* Wilson [e], *neoniger* Emery [e], *sitiens* Wilson [e], *xerophilus* Mackay and Mackay [e]; **Palaearctic** (45, 1): *alienus* [e], *balearicus* Talavera *et al.* [], *bombycina* Seifert and Galkowski. [e], *casevitzi* Seifert and Galkowski [e], *chinensis* Seifert [e], *cinereus* Seifert [e], *coloratus* Santschi [e], *creticus* Seifert [e], *cyperus* Seifert [e], ***emarginatus*** (Olivier) [e], *flavescens* Forel [e], *flavoniger* Seifert [e], *grandis* Forel [e], *hayashi* Yamauchi and Hayashida [e], *hikosanus* Yamauchi [], *hirsutus* Seifert [], *illyricus* Zimmermann [e], *japonicus* Santschi [e], *kabaki* Seifert [e], *karpinisi* Seifert [e], *koreanus* Seifert [e], *kritikos* Seifert [e], *lawarai* Seifert [e], *longipalpus* Seifert [e], *magnus* Seifert [e], *maltaeus* Seifert [e], *mauretanicus* Seifert [e], *niger pinetorum* Ruzsky [], *nigrescens* Stitz [e], *obscuratus* Stitz [e], *paralienus* Seifert [e], *persicus* Seifert [e], *piliferus* Seifert [e], ***platythorax*** Seifert [e], *productus* Wilson [e], ***psammophilus*** Seifert [e], *sakagamii* Yamauchi and Hayashida [e], *schaeferi* Seifert [e], *schulzi* Seifert [e], *sichuense* Seifert [e], *tebessae* Seifert [e], *tunisius* Seifert [e], *uzbeki* Seifert [e], *vostochni* Seifert [e], *wittmeri* Seifert [e].

Distribution: Holarctic.

Identification: Within the *niger* clade, differing from the *fuliginosus* group similarly to the *brunneus* group (above); otherwise, apparently without strong or consistent differentiating conditions relative to the *brunneus* group (Seifert, 2020). Roughly differing from the *brunneus* group in the combination of mandibles with ≥8 teeth on average within a colony plus scape and outer surface of metatibia with >8 total standing setae. Only *L. niger* is truly Holarctic (Schär *et al.*, 2018); Nearctic and Palaearctic species are otherwise identifiable via Wilson (1955) and Seifert (2020), respectively, although more work is necessary for the American fauna.

Note 1. Our molecular sample for *L. nr. americanus* represents an undescribed species.

Note 2. Within the *niger* species group as circumscribed here, Seifert (2020) recognizes two morphometrically

diagnosable complexes: that of *obscuratus* comprises *criticus*, *obscuratus*, *piliferus*, and *psammophilus*, while that of *paralienus* comprises *bombycina*, *casevitzi*, *kritikos*, and *paralienus*.

Note 3. The differentiating features relative to the *brunneus* group above are intended to be heuristic. See the key in Seifert (2020) for formal identification of *niger* group species.

4. Species *incertae sedis* in the clade of *niger*

Species (1): *brevipalpus* [e].

Note: The species L. *brevipalpus* was described by Seifert (2020) who remarked that its relationship to other 'sensu stricto' *Lasius* is uncertain due to a unique character combination, at least within the Asian fauna. We confirm placement of this species in the *niger* clade.

II. Clade of *flavus*

1. Species group of *atopus* (= *Chthonolasius* part 1/2) (Figs 8D, 9D)

Constituent species (1): ***atopus*** [e].

Distribution: Restricted to western North America (California).

Identification: Among all *Lasius*, *L. atopus* has uniquely elongate scapes and a uniquely slender mesosoma (scapes about as long as anteroposterior head length; metanotum relatively elongate, and mesonotum almost in plane with metanotum). In addition, with dense standing pilosity across the entire body, including appendages. See the definition of this species in Cole (1958).

Notes: This species was previously classified in the former subgenus *Chthonolasius*; our sequenced specimen represents a new species near L. *atopus*.

2. Species group of *carniolicus* (= *Austrolasius*) (Figs 8E, 9E)

Constituent species (2): ***carniolicus**** [e], *reginae* Faber [e].

Distribution: Palaearctic.

Identification: Among groups of the *flavus* clade, most similar to those of *flavus*, *nearcticus*, and *umbratus*, in having relatively small eyes (vs *pallitarsis*), stocky mesosomata (vs *atopus*), and unreduced palpomere count (vs *claviger* group). Clypeus lateromedially narrow relative to head width, thus cheeks in full-face view strongly curving anteriorly to mandibular bases, similar to the condition observed in the *fuliginosus* group. Mandibles with offset basal teeth (variable among groups of *flavus* clade). See Faber (1967) and Seifert (2018) for species-level identification.

Note: *L. carniolicus* and *L. reginae* have been separated from other *Lasius* by their cheeks, which strongly curve toward their mandibular bases (e.g., Faber, 1967; Seifert, 2018). This may be due to the form of their clypei, which appear to be narrow relative to the width of their heads. The width and other quantitative features of the clypeus should be evaluated in future study.

3. Species group of *claviger* (= *Acanthomyops*) (Figs 8G, 9G)

Constituent species (16): *arizonicus* Wheeler [e], *bureni* (Wing) [e], ***californicus*** [e], *claviger** (Roger) [e], *colei* (Wing) [e], *coloradensis* Wheeler [e], *creightoni* (Wing) [e], *interjectus* [e], ***latipes*** [e], *mexicanus* Wheeler [e], *murphyi* Forel [e], *occidentalis* Wheeler [], *plumopilosus* Buren [e], *pogonogynus* Buren [e], *pubescens* Buren [e], *subglaber* Emery [e].

Distribution: Nearctic.

Identification: Unique among *Lasius* in having reduced palpomere counts, ranging from 3,4, 4,4, to 5,4. Offset basal mandibular teeth are present (variable among *flavus* clade groups). Eyes smaller than those of *L. pallitarsis*. Scapes and mesosoma, not elongate as in *L. atopus*. See Wing (1968a) for species-level identification.

4. Species group of *flavus* (= *Cautolasius* part 1/2) (Figs 8G, 9G)

Constituent species (8): **Nearctic** (3): ***brevicornis*** [e], *fallax* Wilson [e], *humilis* [e]; **Palaearctic** (5): *alienoflavus* Bingham [e], *elevatus* Bharti and Gul [e], ***flavus**** [e], ***myops*** Forel [e], *talpa* Wilson [e].

Distribution: Holarctic.

Identification: Among species groups of the *flavus* clade, most similar to those of *carniolicus*, *nearcticus*, and *umbratus* in having relatively small eyes (vs *pallitarsis*), stocky mesosomata and shorter scapes (vs *atopus*), and unreduced palpomere count (vs *claviger* group). At present, not collectively distinguishable from *nearcticus* group; otherwise, identifiable as follows: clypeus broad relative to head width (vs narrow, *carniolicus* group); eyes small, with <35 ommatidia excepting *L. alienoflavus* and *L. flavus*, which lack standing setae on head underside (vs with >35 ommatidia and head underside with distinct, standing setae, *umbratus* group). No key is available to specifically separate all of the species of the *flavus* group as here constituted; the three Nearctic species are keyed in Wilson (1955), with *brevicornis* as '*flavus*'; the two Western European species, *L. flavus* and *L. myops*, are keyed by Seifert (2018); the three species from the Himalayas, *L. alienoflavus*, *L. elevatus*, and *L. talpa* are keyed by Bharti & Gul (2013) and Collingwood (1982), and the easternmost Asian population(s) of *L. talpa* are keyed for North Korea by Radchenko (2005b) and Japan by (Yamauchi, 1979).

Notes: This group corresponds to the former subgenus *Cautolasius*, in part. The inclusion of *L. alienoflavus*, *L. elevatus*, *L. fallax*, *L. humilis*, and *L. talpa* is provisional. Wilson (1955) accepted the placement of *L. humilis* in the former subgenus *Chthonolasius* as proposed by Emery (1925) without stated justification; we observe that this species has very small eyes and lacks standing setae on the ventral head surface, matching the polythetic diagnoses of the *flavus* and *nearcticus* groups. Likewise, the species *L. elevatus* also has very small eyes and lacks postgenal bridge setation, although it was unplaced to subgenus in its original description (Bharti & Gul, 2013). Molecular data should be generated for all species of this group, their relationships relative to the *nearcticus* group tested, and a critical reanalysis of phenotypic traits conducted.

5. Species group of *nearcticus* (= *Cautolasius* part 2/2) (Figs 8H, 9H)

Constituent species (2): ***nearcticus*** [e], ***sonobei*** [e].

Distribution: Holarctic.

Identification: Among groups of the *flavus* clade, most similar to those of *carniolicus*, *flavus*, and *umbratus*, in having relatively small eyes (vs *pallitarsis*), stocky mesosomata and shorter scapes (vs *atopus*), and unreduced palpomere count (vs *claviger* group). At present, not collectively distinguishable from *flavus* group; otherwise, identifiable as follows: clypeus broad relative to head width (vs narrow, *carniolicus* group); eyes small, with <35 ommatidia and underside of head without distinct, standing setae (vs with >35 ommatidia and underside of head with distinct, standing setae, *umbratus* group). No key is available to specifically separate *L. nearcticus* and *L. sonobei*, although the former is Nearctic and keyed in Wilson (1955), the latter Japanese and keyed in Yamauchi (1979).

6. Species group of *pallitarsis* (= *Lasius* s. str. Part 3/3) (Figs 8I, 9I)

Constituent species (1): ***pallitarsis*** [e].

Distribution: Nearctic.

Identification: Among groups of the *flavus* clade, workers are unique in having relatively large eyes (length ≥ 0.2 × head width). Offset basal mandibular tooth present (also *claviger* and *carniolicus* groups among *flavus* clade). Scapes and mesosoma not elongate as in *L. atopus*.

Note: This species was classified in the former subgenus *Lasius* s. str. and has previously been recovered elsewhere in the phylogeny by Janda *et al.* (2004) and Maruyama *et al.* (2008).

7. Species group of *umbratus* (= *Chthonolasius* part 2/2) (Figs 8J, 9J)

Constituent species (24): **Nearctic** (6): *aphidicola* [e], *minutus* Emery [e], *nevadensis* Cole [e], *speculiventris* Emery [e], ***subumbratus*** Viereck [e], *vestitus* Wheeler [e]; **Palaearctic** (18): *balcanicus* Seifert [e], *bicornis* (Foerster) [e], *citrinus* Emery [e], *crinitus* (Smith) [e], *distinguendus* (Emery) [e], *draco* Collingwood [], *jensi* Seifert [e], *longiceps* Seifert [], *meridionalis* (Bondroit) [e], *mikir* Collingwood [e], *mixtus* (Nylander) [e], *nitidigaster* Seifert [e], *przewalskii* Ruzsky [], *rabaudi* (Bondroit) [e], ***sabularum*** [e], *tibialis* Santschi [], *umbratus** [e], *viehmeyeri* Stärcke [e].

Distribution: Holarctic.

Identification: Among groups of the *flavus* clade, most similar to those of *carniolicus*, *flavus*, and *nearcticus* in having relatively small eyes (vs *pallitarsis*), stocky mesosomata (vs *atopus*), and unreduced palpomere count (vs *claviger* group). Among these groups, identifiable by the following combination of traits: clypeus broad relative to head width (vs narrow, *carniolicus* group); eyes larger, with >35 ommatidia, and underside of head with distinct, standing setae (vs with <35 ommatidia except *L. alienoflavus* and *L flavus* which, along with most other *flavus* and *nearcticus* group species, lack distinct standing setae on head underside). No comprehensive key is available for the global fauna of the *umbratus* group; the Nearctic species are keyed in Wilson (1955) where *L. aphidicola* is referred to as *L. umbratus*, and with the addition of *L. nevadensis* by Cole (1956); Wilson (1955) also includes a key to some Palaearctic species, which are also partially covered by Collingwood (1982), Boer (2003) and Seifert (1988, 1990, 1997, 2018). Focused work on this species group, particularly a global key or revision, is necessary.

Note: This group corresponds to the prior subgenus *Chthonolasius*, with the exclusion of *L. atopus*. One of our molecular terminals of this group is an undescribed species near *L. subumbratus*.

III. *Incertae sedis* in genus

1. Impression fossils

Species (18), subspecies (1): **West Palaearctic**: (28.4–23.0 Ma, ***France*, *Aix-en-Provence***): †*epicentrus* Théobald [e]; (12.7–11.6 Ma, ***Croatia*, *Radoboj***): †*anthracinus* (Heer) [e], †*globularis* (Heer) [],†*longaevus* (Heer) [e], †*longipennis* (Heer) [e], †*occultatus* (Heer) [e], †*occultatus parschlugianus* (Heer) [], †*ophthalmicus* (Heer) [e]; (12.7–11.6 Ma, ***Russia*, *Berezovsky***): †*tertiarius* Zalessky []; (11.6–5.3 Ma, ***Poland*, *Schnossnitz***): †*oblongus* Assmann []; (8.7–7.2 Ma, ***France*, *Joursac***): †*crispus* Théobald []; (8.7–2.6 Ma, ***France***, ***Lake Chambon***): †*chambonensis* Théobald [e]; **East Palaearctic**: (20.4–16.0 Ma, ***China*, *Shanwang***): †*inflatus* (Zhang) [], †*mordicus* Zhang [],†*truncatus* Zhang [], †*validus* Zhang []; (16.0–11.6 Ma, ***Russia*, *Vishnevaya***): †*vetulus* Dlussky []; **Nearctic**: (48.6–40.4 Ma, ***USA*, *Kishenehn***): †*glom* LaPolla & Greenwlalt [e]; (37.2–33.9 Ma, ***USA*, *Florissant***): †*peritulus* (Cockerell) [e].

Note 1. All species of *Lasius* based on impression fossils are described from specimens which have some degree of body preservation, with the exception of †*L. oblongus*, †*L. crispus*, and †*L. chambonensis*, which are only represented by wings. The placements of these latter taxa may perhaps be resolved with geometric morphometrics.

Note 2. All impression fossils attributed to *Lasius* are here considered to be *incertae sedis* within the genus. None of the fossils are identifiable to species, given the morphological standards set for extant *Lasius* (e.g., Wilson, 1955; Wing, 1968a, 1968b; Seifert, 2020). However, these fossils do roughly match the gestalt of the genus, thus they represent plausible records of *Lasius* for the geological time periods in which they were discovered. It will be important, therefore, to quantitatively test the placement of †*L. glom* and †*L. peritulus* (for the latter, see also Carpenter, 1930 and Wilson, 1955); together, these two taxa span the late Miocene to early Oligocene, thus possibly representing Nearctic stem lineages. Such a test would require development of male- and queen-specific characters, as none of the impression fossil taxa are represented by workers.

Note 3. The most comprehensive treatment of *Lasius* impression fossils is that of Dlussky & Putyatina (2014), who addressed certain taxa described by Heer (1849, 1867) from Croatia. Other *Lasius* taxa have been described singly by

Théobald (1937), Zalessky (1949), and Dlussky (1981), with the exception of the Chinese fossils of Zhang (1989), who also illustrated Dlussky's species †*L. peritulus*. As for †*L. glom* and †*L. peritulus*, a quantitative test of the placement of these taxa, such as done by Katzke *et al.* (2018), is necessary.

2. Amber fossils

Species (3): †*nemorivagus* [], †*punctulatus* [e], †*schiefferdeckeri* [e].

Deposits: *Palaearctic*: Baltic, Bitterfield, Danish-Scandinavian and Rovno (Ukrainian).

Note: These species, from coniferous ambers (Wolfe *et al.*, 2016), are considered *incertae sedis* in *Lasius* as per the 'Comments on extinct species' section above. Their preservation is sufficient to render species-level identification, in contrast to the impression fossils listed above.

IV. Unidentifiable extant species

Species (14): *alienoniger* Forel, *emeryi* Ruzsky, *exulans* Fabricius, *longicirrus* Chang & He, *minimus* (Kuznetsov-Ugamsky), *monticola* (Buckley), *mixtoumbratus* Forel, *monticola* Buckley, *nigerrimus* (Christ), *nitidus* (Kuznetsov-Ugamsky), *pannonica* Röszler, *rubiginosa* Latreille, *ruficornis* Fabricius, *transylvanicus* Röszler.

Note: The species *exulans*, *monticola*, *rubiginosa* and *ruficornis* were rendered *incertae sedis* by Bolton (1995); we are doubtful that these names will be resolved. Recently, Seifert (2020) considered *alienoniger*, *emeryi*, *longicirrus*, *minimus*, *nigerrimus*, *nitidus*, *pannonica*, and *transylvanicus* to be *nomina nuda*. The species *nigerrimus* is unidentifiable to subfamily (Seifert, 2020). All names listed here are considered unidentifiable.

Genus *Metalasius* gen.nov.

ZooBank LSID. urn:lsid:zoobank.org:act:AC5A1489-C805-4035-A1C0-3DDBC6E1206D.

Type species. Lasius myrmidon Mei, 1998: 177, figs 1–11 (w.). Original designation.

Species included. M. myrmidon (Mei, 1998) **comb.nov.**, †*M. pumilus* (Mayr, 1868) **comb.nov.**

Total clade definition (worker).

1. With characters of Lasiini.
2. Mandible with 6–8 teeth.
3. Palp formula 6,4.
4. Basal and masticatory mandibular margins meeting at a weakly oblique angle.
5. Clypeus modified for reception of labrum (specifically, clypeus with anterolateral notches; Note 1).
6. Frontal carinae conspicuous, >0.5 × anteroposterior antennal torulus diameter.
7. Frontal region of head, between antennal toruli strongly bulging, frontal carinae raised above toruli (Note 2).
8. Antenna 12-merous.
9. *Third antennomere broader than long* (Note 3).
10. Compound eyes set at about head midlength.
11. Ocelli absent.
12. *Dorsum of head completely without standing setae or with only a few small setae around each posterolateral head corner* (Note 4).
13. Mesonotum, metanotum and/or propodeum discontinuous, metanotum undifferentiated medially.
14. Mesopleural anterodorsal margin, near posterolateral region of pronotum, inconspicuously bulging, this weak shoulder a very narrow groove which traverses the mesosternum.
15. Metapleural gland very small, orifice directed almost completely posteriorly (Note 5).
16. Propodeal spiracle situated in lower 2/3 of propodeum.
17. Legs entirely or almost entirely devoid of standing setae.
18. Petiole with raised squamiform node, without posterior elongation.
19. Abdominal tergum III vertical, without deep groove for receiving petiole; not concealing petiole when gaster raised (Note 6).
20. Tergosternal suture of abdominal segment III not raised dorsally before unfusing near spiracle, rather anterior margin of abdominal sternum III directed anteriorly away from helcium before narrowly curving posteriorly (Note 6).
21. Pubescence of abdominal terga VI and VII linear.

Notes on definition:

Note 1. Modification of the anterior clypeal margin for reception of the labrum is here interpreted as a synapomorphy of *Metalasius* plus the core *Prenolepis* genus group. The modification is most easily observed in anterior or anterodorsal view. In most Formicinae, the perceived anterior clypeal margin with the head in full-face view is usually a carina which runs across the clypeus from the lateral clypeal margins. This carina may be raised or otherwise modified; regardless, the carina itself or the anterior region of the clypeus is produced anteriorly, concealing the clypeolabral articulation. In the *Prenolepis* and *Metalasius* genus groups, the clypeolabral articulation is usually exposed or nearly exposed laterally by notches in the anterior clypeal carina, although it may be exposed medially where the anterior clypeal carina is absent.

Note 2. See Note 1 for the *Lasius* genus group.

Note 3. Surprisingly, this distinguishes members of the *Metalasius* genus group from most formicine genera, with the exception of some *Myrmelachista*, various plagiolepidines and the *Lasius flavus group*. *Cladomyrma* species have a cone-shaped third antennomere, which is usually longer than the diameter of its base (and often apex), except in *C. dianeae* Agosti *et al.* for which the length and basal diameter are subequal. Some *Pseudolasius* and *Paraparatrechina* approach having subequal diameter and length.

Note 4. Mei (1998), in his diagnosis of *Metalasius myrmidon*, indicated that these standing setae were absent except for one specimen.

Note 5. This state may be a synapomorphy for the clade consisting of *Metalasius* plus the *Prenolepis* genus group.

It was not possible to evaluate this with confidence for †*M. pumilus*, but from the dorsal view of specimen SMFBE1226 on AntWeb, the gland does appear to be small.

Note 6. These characters could not be evaluated with confidence for †*M. pumilus* with the available material or descriptions.

Etymology. A combination of the Greek 'meta-' (with, across, after) and 'lásios' (hairy), in reference to the former placement of the type species. Homophonously forming 'metal-Asius', invoking the death of the Trojan leader Asius during the assault on the Archaean wall of Troy. Masculine.

Comments. Although, we could not evaluate all of these characters for †*M. pumilus*, this species is consistently recovered as sister to *M. myrmidon* in combined analysis (Figs 4, S7–S9). *Metalasius* is most easily differentiated from both the *Lasius* and *Prenolepis* genus groups by the combination of mid-set eyes, the posteriorly directed and reduced metapleural gland orifice, raised frontal carinae and almost complete lack of standing setae on the head. In addition, both included species of *Metalasius* have broad third antennomeres and unusually small bodies relative to *Lasius*, being <2 mm in total length (Mei, 1998; Dlussky, 2011).

Species *Metalasius myrmidon* (Mei, 1998) **comb.nov.**

Definition (worker).

1. With character states of *Metalasius*.
2. *Dorsal mandibular groove absent* (Note 1).
3. Ventromedial base of mandible without trough or impression (Note 2).
4. Maxillary palps short, exceeding hypostomal margin but not reaching postgenal bridge midlength.
5. Maxillary palpomere 3 longest, 4 shorter but as long as 5 and 6 together (Note 3).
6. Clypeus, in lateral view, convex and weakly bulging anteriorly (Note 3).
7. Anterior tentorial pit situated lateral to midlength of the epistomal suture.
8. *Lateral hypostomal carina absent* (Note 4).
9. *Compound eyes absent*, *reduced or vestigial*, *with at most 9 ommatidia* (Note 5).
10. *Propodeal spiracle situated distinctly in lower half of propodeum* (Note 6).
11. Legs almost entirely devoid of standing setae (Note 3).
12. Petiolar node weakly inclined anteriorly, node well-developed, squamiform (Note 7).

Notes on definition:

Note 1. The dorsal mandibular groove is discernable in all examined *Lasius* and *Prenolepis* genus group taxa.

Note 2. Presence of a trough on the ventromedial base of the mandible is a newly detected synapomorphy of the core *Prenolepis* genus group. The impression is enhanced when the ventromedial mandibular margin is carinate and/or produced medially, and best seen when the mandibles are open and with the head in lateral anteroventral view. The trough may be reduced or absent in some species.

Note 3. Previously included in the original diagnosis of the species *M. myrmidon* by Mei (1998).

Note 4. The lateral hypostoma is usually delimited by a carina, which is discontinuous with the medial hypostomal lamina. Among formicines, the lateral hypostomal carina is absent only in *Acropyga* (some species) and *Brachymyrmex*, both genera outside of Lasiini.

Note 5. The specimens, which were available for examination had 5–8 ommatidia; the maximum ommatidium count is from Mei (1998, p. 178).

Note 6. A lowered propodeal spiracle appears sporadically replicated in only a few *Prenolepis* genus group members.

Note 7. The petiolar node is strongly inclined anteriorly in the core *Prenolepis* genus group.

Comments. Metalasius myrmidon is uniquely identified among the Lasiini by absence of the dorsal mandibular groove and lateral hypostomal carina, short and broad third antennomere, mid-set compound eyes (when present), which are reduced to at most 9 ommatidia and near complete absence of standing setae on the head. High magnification may be required to evaluate the lateral hypostoma.

Species †*Metalasius pumilus* (Mayr, 1868) **comb.nov.**

Definition (worker).

1. With character states of *Metalasius* (Note 1).
2. Maxillary palps long, reaching occipital foramen (Note 2).
3. Compound eyes well-developed, with >20 ommatidia.
4. Mesosomal dorsum devoid of setae.
5. Legs entirely devoid of standing setae.
6. Petiolar node weakly inclined anteriorly, node squamiform.

Notes on definition:

Note 1. Several characters could not be evaluated for †*M. pumilus*, including the ventromedial mandibular groove, palpomere proportions, clypeal profile, and lateral hypostomal carina.

Note 2. From Dlussky (2011).

Comments. We place †*M. pumilus* and *M. myrmidon* together based on the results of our phylogenetic analyses, and we interpret presence of the broad third antennomere and highly reduced cranial setation as synapomorphies of this clade. †*Metalasius pumilus* differs from *M. myrmidon* by the following: (i) compound eyes large; (ii) maxillary palps long, reaching occipital foramen, and (iii) standing setae completely absent from head dorsum and mesosoma.

Although, we have not examined the neotype of †*M. pumilus*, designated by Dlussky (2011) and deposited in Muzeum Ziemi Polskiej Akademii Nauk in Warsaw, the specimen we have studied is unlikely to be misidentified as it exhibits unique diagnostic traits of the species among the Lasiini, let alone of the Baltic amber fauna, including absence of setae on the head dorsum, well-developed eyes, short and broad third antennomere, and very small body size (<2 mm). Dlussky (2011) describes the eyes of both †*L. schiefferdeckeri* and †*M. pumilus* as 'shifted somewhat posteriorly so that the length of [the] gena [is] more than [that of the] maximum diameter of [the] eyes'. This very general statement is true of both species, however, the eyes of †*L. schiefferdeckeri* are distinctly set in the posterior head half whereas those of †*M. pumilus* and *M. myrmidon* are situated

at head midlength, distinguishing them from all *Lasius* genus group members.

Genus group of *Prenolepis*

Genera included. Euprenolepis, *Nylanderia*, *Paraparatrechina*, *Paratrechina*, *Prenolepis*, *Zatania*.

Definition (worker).

1. With characters of Lasiini.
2. Mandible with 4–7 teeth.
3. Palp formula variable: 6,4; 4,4 3,4; 5,3; 4,3; 3,3; 2,3; 2,2 (Note 1).
4. *Basal and masticatory mandibular margins usually meeting at a strongly oblique angle*.
5. Clypeus modified for reception of labrum (specifically, clypeus with anterolateral notches; Note 1 of *Metalasius*).
6. Frontal carinae conspicuous, >0.5 × anteroposterior antennal torulus diameter.
7. Frontal region of head between antennal toruli flat, frontal carinae not raised above toruli.
8. Antenna 11- or 12-merous.
9. Third antennomere usually longer than broad (see Note 3 of *Metalasius*).
10. Compound eyes usually at about head midlength, sometimes set posteriorly (see Note 3 of *Lasius* genus group).
11. Ocelli present or absent.
12. Dorsum of head with standing setae.
13. Mesonotum, metanotum and/or propodeum discontinuous, metanotum usually differentiated (Note 2).
14. Mesopleuron anterodorsal margin, near posterolateral region of pronotum, usually without raised boss nor with narrow or broad groove traversing the mesosternum (Note 5 of *Lasius* genus group).
15. Metapleural gland very small, orifice directed completely to nearly completely posteriorly (Note 5 of *Metalasius*).
16. Propodeal spiracle situated in lower 2/3 of propodeum.
17. Legs with or without standing setae.
18. *Petiole with very low node and posteriorly elongated*.
19. *Abdominal tergum III inclined anteriorly*, *with deep groove for reception of petiole*, *concealing most of petiole in dorsal view when gaster raised*.
20. *Abdominal tergum III with complete tergosternal fusion adjacent to helcium*, *and fusion raised anterodorsally*, *with sclerites becoming free high up on segment*.
21. *Pubescence of abdominal terga VI and VII often dense*, *forming a uniform layer of short and strongly curved setae* (Note 3).

Notes on definition:

Note 1. The palp formula of most genera is 6,4. Most *Euprenolepis*, however, have a palpomere count of 3,4, with the exception of *E. negrosensis* (Wheeler), which has a 4,4 count. The count is variable in *Pseudolasius*, while the count in *Paraparatrechina*, particularly the *weissi* species group, is also reduced (LaPolla *et al.*, 2010).

Note 2. The metanotum of many but not all *Paraparatrechina* is undifferentiated.

Note 3. These setae may or may not completely cover tergum VI. Absence of this characteristic pubescence occurs in and may be a synapomorphy of *Euprenolepis* and *Paratrechina*.

Comments. Paratrechina has recently expanded from a single species to six (LaPolla *et al.*, 2010, 2013; LaPolla & Fisher, 2014; Williams & LaPolla, 2016). One of these recently added species, *P. kohli*, was originally described in *Prenolepis*, transferred to *Nylanderia* (as a subgenus of *Paratrechina*), back to *Prenolepis*, and finally to *Paratrechina* (sensu stricto) (LaPolla & Fisher, 2014). This species stood out from the remainder in its surface sculpturing, eye positioning, color, and mandibular dentition. It was observed during this study that *P. kohli* has a petiolar node which exceeds propodeal spiracle height, lacks the raised tergosternal fusion of abdominal segment III and posterior elongation of the petiole, and closely resembles species of *Anoplolepis*, specifically *A. carinata* (Emery) and *A. tenella* (Santschi). In addition, *P. kohli* has 11-merous antennae, an undifferentiated metanotum, posteriorly set eyes, and lacks ocelli, as is characteristic of *Anoplolepis* (Fisher & Bolton, 2016). We find in combined analyses that *P. kohli* always falls outside of the Lasiini (Figs 4, S7–S9). For these morphological and phylogenetic reasons, we transfer the species *P. kohli* to *Anoplolepis* in the Plagiolepidini, forming *A. kohli* (Forel, 1916) **comb.nov.** (tribal transfer). Expanded sampling of male characters may improve placement of the fossil taxon †*P. henschei*, with respect to the remainder of the genus group.

***Incertae sedis* in the Formicinae**

Genus †*Kyromyrma*. Comparative morphological study of †*Kyromyrma* (~92 Ma, New Jersey amber; Grimaldi & Agosti, 2000) at the gross (Figs 8L, 9K) and fine scales reveals considerable morphological affinity to *Lasius* (holotype examined at AMNH). In the original description of †*Kyromyrma*, the authors did not address the problem of within-subfamily placement, merely noting that 'the fossil bears an overall resemblance to *Prolasius*, mostly by virtue of the generalized morphology' (Grimaldi & Agosti, 2000, p. 13681). Our combined evidence analyses resulted in ambiguous support for the placement of †*Kyromyrma*, with the genus being recovered as sister to the *Lasius* genus group (Figure S5), sister to the core Lasiini (Figures S8, S9), sister to all Lasiini (Figure S7), or sister to Formicinae exclusive of Myrmelachistini (Fig. 4). Statistical support for these placements was uniformly low.

Genus †*Sussudio* gen.nov.

Type and included species. †*P. boreus* Wheeler, 1915. Original designation.

ZooBank LSID. http://zoobank.org/urn:lsid:zoobank.org:act:BFF515E7-9966-443F-8A34-555A4B41906B

Definition (worker).

1. With characters of the Formicinae (Note 1).
2. *Cranium size variable*, *width somewhat broader than to about twice that of mesosoma* (Note 2).
3. Mandible triangular, with 7–8 teeth.
4. Dorsal mandibular groove extending along lateral mandibular margin in dorsal view.
5. Palps reduced, not reaching midlength of postgenal bridge.

6. Frontal carinae raised above antennal toruli.
7. Antennal toruli abutting posterior clypeal margin.
8. Antennomere count unknown (Note 3).
9. Antennomere III longer than broad.
10. Compound eyes situated posterior to head midlength.
11. Compound eyes not enormous and long axes subparallel.
12. Ocelli minutely present or absent.
13. Promesonotum domed, raised well above propodeum.
14. Metanotal groove well-developed.
15. Petiolar foramen in profile view clearly raised and margined with conspicuous thickened carina or lip.
16. Petiolar node squamiform, tall; dorsoventral height equal to or possibly exceeding dorsum of propodeum.
17. Abdominal segment III without raised tergosternal fusion.

Notes on definition:

Note 1. Several characters were not possible to evaluate. These include the following: Reduction of third tooth from mandibular apex, palp formula, the metapleural gland, ventral length of the petiolar foramen, relative separation of the meso- and metacoxae, presence or absence of setal double-row on ventral tibial surfaces, petiolar apodeme conformation, cross-sectional shape of the petiolar sternum, and presence or absence of the posthelcial sulcus.

Note 2. The massive head of †*P. boreus* led Wheeler (1915) to erroneously assume that the specimens were majors of *Pseudolasius*; Wheeler did note the posteriorly set eyes of †*P. boreus*, one of the distinctions between it and *Pseudolasius*, but vacillated based on the insufficient knowledge of the latter genus at that time.

Note 3. The examined specimens are missing their terminal antennomeres, and no previous descriptions of †*P. boreus* include an antennomere count.

Etymology. A simplification of 'pseudo-*Pseudolasius*' inspired by the musician Phil Collins. Masculine.

Comments. †*Sussudio boreus* **comb.nov.** was previously placed in the Lasiini (Emery, 1925, Dlussky & Fedoseeva 1988, Bolton, 1994), and has been considered to be a member of the genus *Pseudolasius* (Wheeler, 1915; LaPolla & Dlussky, 2010). Based on an examination of a syntype (GZG-BST04646) and a nontype (NHMW1984-31-211) worker, as well as the original description from Wheeler (1915), we reject both placements. Neither specimen can be mistaken due to the unique combination of characters they display, including setation, high petiolar nodes, massive crania, and mesosomal form. †*Sussudio boreus* does not display the modifications of the third abdominal segment characteristic of the *Prenolepis* genus group, also rejecting its original placement in *Pseudolasius* (see diagnostic Note 2 above). †*Sussudio* is excluded from the Lasiini overall by two additional characters: (i) The petiolar node, which is completely vertical and very tall dorsoventrally, is as tall as or possibly taller than the propodeum; and (ii) the raised and conspicuously lipped petiolar foramen. No lasiine, extant or extinct, has such a tall petiolar node, nor do any species display the petiolar foramen conformation observed in †*Sussudio*. We cannot confidently place †*Sussudio* in any extant tribe, therefore, we consider †*Sussudio incertae sedis* in the Formicinae. As with other fossil taxa, which are of uncertain placement in the Formicinae, micro-CT scanning could be used to evaluate the form of the helcium and third abdominal sternum.

Conclusion

Revisionary works have traditionally scrutinized morphological systems for the systematic classification of a given group of interest. Here, we integrate traditional morphology with molecular phylogeny to understand the ant tribe Lasiini in the context of the subfamily Formicinae. Of particular interest to us are the suite of phenotypic characteristics which are used to define taxa. After reevaluating the fossil record of the Formicinae, we were able to estimate the geological age of phylogenetic branching events in the subfamily; with this chronogram, we formally estimated the probability that key diagnostic characters are ancestral or derived for any given clade. To this end, we have tested polarity hypotheses for traits used by Bolton in his crucial morphological reclassification of the Formicidae (Bolton, 2003), as well as the form of the proventriculus – a structure used by taxonomists for well over a century to classify the Formicinae and other subfamilies (e.g., Forel, 1874, 1878; Emery, 1888, 1925). We found that the sepalous proventriculi and 'lasiine' wide-set coxae are synapomorphies of the Formicinae, and that the 'plagiolepidiform' condition of the third abdominal segment originated three times independently in the subfamily. In addition, we found that two life history traits, temporary social parasitism and fungiculture, have both evolved twice in the genus.

One key question arising from our work is how to treat the two genera of the *Lasius* genus group relative to the fossils of *Lasius*, given the problem of anagenesis and the apparent high degree of morphological conservativism of the nominotypical genus. This conservativism is evidenced by the striking similarity of the *niger* clade with the Baltic amber fossils and the Cretaceous genus †*Kyromyrma*. Should the Baltic amber taxa be split, even though there are not enough morphological features to differentiate them from *Lasius* as currently delimited? Or should the phenotypically distinct genus *Myrmecocystus*, like *Acanthomyops* before it, be synonymized with *Lasius*? Perhaps it will be necessary to split the Baltic taxa and to revive *Acanthomyops* for the *flavus* clade. For now, we acknowledge the difficulty of justifying our choice to retain the Baltic amber fossils in the genus *Lasius* given the principle that all higher taxa are to be monophyletic. We also emphasize that the unexpectedly young age of the crown *Lasius* genus group is not likely to be an artefact of dating method or taxon sampling. We hypothesize that the overall short branch lengths of the *Lasius* genus group are a result of increased species turnover associated with colonization of and radiation into the recently emerged North temperate ecosystems (Economo *et al.*, 2018). The young crown group age of *Lasius* and *Myrmecocystus* in turn likely contributes to lack of morphological divergence and makes these ants known examples of taxonomically difficult genera (e.g., Snelling, 1976; Seifert & Galkowski, 2016).

With respect to our evolutionary questions, we reconceive the ancestral formicine as having originated around the end

of the Early Cretaceous or beginning of the Late Cretaceous with anteriorly set eyes, narrowly set coxae, circular propodeal spiracles, lacking a sulcus posterad the helcial sternite, and having low anterolateral corners of abdominal tergum III. We find support for the 'sepalous' condition of the proventriculus as an autapomorphy of the Formicinae, suggesting that greater control of the crop valve may have been a key innovation in the origin and subsequent radiation of the subfamily during the Mesozoic, albeit with a number of reversals. In this evolutionary morphological context, the Lasiini derived wide-set coxae and raised gastral corners independently of the Plagiolepidini and some Melophorini, the former in the Late Cretaceous and the latter probably during the Tertiary period. We find that the new genus, *Metalasius*, is a probable relict of an ancient clade which split from its common ancestor with the tropicopolitan radiation of the *Prenolepis* genus group during the Late Cretaceous.

To date, our study provides the best-supported hypothesis of phylogenetic relationships among the major lineages of *Lasius* and, in addition to revising the classification of the Lasiini, contributes to a greater understanding of the tempo and mode of formicine evolution. From the phylogenetic perspective, we conclude that inclusion of a clock model in analyses of morphology results in substantial topological improvement, and that divergence dating analyses should, if possible, include both morphological and molecular data in the tip-dating framework. Despite the advances we propose, much work remains to be done for the Lasiini. Extended morphological data are required to resolve the placements of fossils more completely. Such analyses may benefit from the inclusion of males (e.g., Barden *et al.*, 2017a) and characters specific to the *Prenolepis* genus group. Our work has revealed that two fossil taxa were misplaced at genus rank (†*L. pumilus*, now †*M. pumilus* **comb.nov.** and †*P. boreus*, now †*Sussudio boreus* **gen.nov. comb.nov.**), as were two fossil taxa misplaced to tribe rank (†*Glaphyromyrmex* and †*Sussudio* **gen.nov.**). We have great hope for the future of holistic phylogenetic studies as ever more genomic and phenomic data are made available.

Supporting Information

Additional supporting information may be found online in the Supporting Information section at the end of the article.

Appendix S1. Morphometric differentiation of *Lasius, Metalasius myrmidon*, and †*M. pumilus*.

Appendix S2. Morphological state definitions used for the 114-character matrices.

Figure S1. Schematics of the constraints used in the topology tests for Bayes factor analysis of the Lasiini_55t dataset. (A) H_0: *Metalasius* and *Lasius* genus group monophyletic; H_1: *Metalasius* and *Prenolepis* genus group monophyletic (B) H_0: *Lasius* s. str. Monophyletic; H_1: *Lasius* s. str. Paraphyletic (C) H_0: *Chthonolasius* monophyletic; H_1: *Chthonolasius* polyphyletic (D) H_0: *Cautolasius* monophyletic; H_1: *Cautolasius* paraphyletic.

Figure S2. Results of the concordance factor analysis inferred from the Lasius_55t dataset in IQTREE. Node support values are reported as gene concordance factor (gCF) versus site concordance factor (sCF).

Figure S3. Results of analysis of the Lasiini_w_outgroups_w_fossils_morphology_154t dataset in MrBayes. Node support values are reported as Bayesian posterior probabilities (PP).

Figure S4. Results of analysis of the Lasiini_w_outgroups_135t dataset in MrBayes. Node support values are reported as Bayesian posterior probabilities (PP).

Figure S5. Results of analysis of the Lasiini_w_outgroups_135t dataset in IQTREE. Node support values are reported as maximum likelihood bootstrap (BS).

Figure S6. Results of analysis of the Lasiini_w_outgroups_w_fossils_154t dataset in MrBayes without a clock model. Node support values are reported as Bayesian posterior probabilities (PP).

Figure S7. Results of analysis of the Lasiini_w_outgroups_w_fossils_154t dataset in MrBayes with a uniform branch length prior and IGR clock rate prior. Node support values are reported as Bayesian posterior probabilities (PP). Horizontal blue bars at nodes are 95% highest posterior density (HPD) intervals.

Figure S8. Results of analysis of the Lasiini_w_outgroups_w_fossils_154t dataset in MrBayes with a uniform branch length prior and TK02 clock rate prior. Node support values are reported as Bayesian posterior probabilities (PP). Horizontal blue bars at nodes are 95% highest posterior density (HPD) intervals.

Figure S9. Results of analysis of the Lasiini_w_outgroups_w_fossils_154t dataset in MrBayes with an FBD branch length prior and TK02 clock rate prior. Node support values are reported as Bayesian posterior probabilities (PP). Horizontal blue bars at nodes are 95% highest posterior density (HPD) intervals.

Figure S10. Ancestral state estimation (*ace*) results from analysis of a 135-taxon chronogram for compound eye location under the equal rates assumption. In the pie charts, red = eyes anteriorly set and blue = eyes set at or posterior to head midlength.

Figure S11. Ancestral state estimation (*ace*) results from analysis of a 135-taxon chronogram for coxal separation under the equal rates assumption. In the pie charts, red = close-set and blue = wide-set.

Figure S12. Ancestral state estimation (*ace*) results from analysis of a 135-taxon chronogram for sulcus presence

posteroventral to the helcium. In the pie charts, red = sulcus absent and blue = sulcus present.

Figure S13. Ancestral state estimation (*ace*) results from analysis of a 135-taxon chronogram for propodeal spiracle shape. In the pie charts, red = spiracle circular to elliptical and blue = spiracle slit-shaped.

Figure S14. Ancestral state estimation (*ace*) results from analysis of a 135-taxon chronogram for proventricular form. In the pie charts, red = asepalous, blue = sepalous.

Figure S15. Ancestral state estimation (*ace*) results from analysis of a 135-taxon chronogram for tergosternal suture conformation of abdominal segment III. In the pie charts, pink = without narrow shoulder, blue = low narrow shoulder, red = high narrow shoulder.

Figure S16. Ancestral state estimation (*ace*) results from analysis of a 21-taxon chronogram representing *Lasius* for temporary social parasitism. In the pie charts, red = absence, blue = presence.

Figure S17. Ancestral state estimation (*ace*) results from analysis of a 21-taxon chronogram representing *Lasius* for fungiculture. In the pie charts, red = absence, blue = presence.

Figure S18. Dot plot of longitudinal distance from anterolateral corners of clypeus to posterior margins of compound eyes (ED2) by maximum head length (HL2) contrasting the two primary clades of *Lasius* with the species *Metalasius myrmidon* and †*M. pumilus* and demonstrating that the compound eyes of the latter two taxa are clearly set more-anteriorly than those of *Lasius*.

Figure S19. Box and whisker plots of values for six eye position indices, showing differentiation among *Lasius*, *Metalasius myrmidon*, and †*M. pumilus*.

Figure S20. Box and whisker plot of relative eye size (ESI), the index of average eye length (ELx) proportional to maximum head length (HL2), contrasting the two primary clades of *Lasius* with the species *Metalasius myrmidon* and †*Metalasius pumilus*.

Table S1. Primers used for amplification and sequencing *abdominal-A* (*abdA*), *Arginine Kinase* (*ArgK*), *rudimentary* (*CAD*), *elongation factor 1 α F2 copy* (*EF1αF2*), *long-wavelength rhodopsin* (*LW Rh*), *Topoisomerase I* (*Top1*), *Ultrabithorax* (*Ub*), *wingless* (*wg*). Blank spaces every three nucleotides delimit codons, except for intronic sequences, which are arbitrarily presented with spaces every three nucleotides. Most frequently used primers are denoted by asterisk.

Table S2. GenBank data for all sequences used in this study.

Table S3. PartitionFinder best schemes for the Lasiini_w_outgroups_135t and Lasiini_55t datasets.

Acknowledgements

We extend our primary gratitude to Phil Ward. Phil provided us with funding, specimens, sequences, constructive discussion, and attention to the manuscript; as well, he recommended the name *Metalasius*, which we appreciate. We thank the three anonymous reviewers of the present work, as their comments improved the study. We also appreciate the critique of an anonymous reviewer of our first manuscript on *Lasius* phylogeny, as this led to our discovery of the placement of *M. myrmidon* and morphological reevaluation of the Lasiini. Thanks to Dave Grimaldi for granting access to the amber collection at the AMNH. For his exquisite automontage images of Baltic amber material and for sharing his insights into the fossil record of the Formicidae, we thank Vincent Perrichot. Brian Fisher and Michele Esposito: Thank you for AntWeb and for maintaining Bolton's catalog and Ward *et al.*'s AntBib on AntCat. We thank Barry Bolton and Brian Fisher for commenting on the manuscript prior to submission. We thank Bonnie Blaimer for discussion of the Formicinae and for sending us the UCE single-locus gene trees for coalescence analysis. We thank Adrian Richter for discussing head characters and the classification of *Lasius*. Jill Oberski caught some mistakes in the manuscript and translated Mayr's writing for us; thank you. Thank you to Christian Rabeling and Daniela Mera Rodriguez for providing feedback on an early version of the manuscript. Finally, we thank Lech Borowiec and Sebastian Salata for contributing specimens of *Metalasius myrmidon* and *L. carniolicus*, respectively. MMP and MLB were supported by NSF DEB-1943626 while working on this study. The authors declare no conflict of interest.

Data availability statement

The data that support the findings of this study are openly available on Dryad at https://doi.org/10.25338/B8B645.

References

Adams, R.H. & Castoe, T.A. (2019) Statistical binning leads to profound model violation due to gene tree error incurred by trying to avoid gene tree error. *Molecular Phylogenetics and Evolution*, **134**, 164–171.

Agosti, D. (1990) What makes the Formicini the Formicini? *Actes Colloques Insectes Sociaux*, **6**, 295–303.

Agosti, D. (1991) Revision of the oriental ant genus *Cladomyrma*, with an outline of the higher classification of the Formicinae (Hymenoptera: Formicidae). *Systematic Entomology*, **16**, 293–310.

Agosti, D., Moog, J. & Maschwitz, U. (1999) Revision of the oriental plant-ant genus *Cladomyrma*. *American Museum Novitates*, **3283**, 1–24.

Ashmead, W.H. (1905) A skeleton of a new arrangement of the families, subfamilies, tribes and genera of the ants, or the superfamily Formicoidea. *The Canadian Entomologist*, **37**, 381–384.

Astruc, C., Julien, J.F., Errard, C. & Lenoir, A. (2004) Phylogeny of ants (Formicidae) based on morphology and DNA sequence data. *Molecular Phylogenetics & Evolution*, **31**, 880–893.

Barden, P., Boudinot, B.E. & Lucky, A. (2017a) Where fossils dare and males matter: combined morphological and molecular analysis untangles the evolutionary history of the spider ant genus *Leptomyrmex* Mayr (Hymenoptera: Dolichoderinae). *Invertebrate Systematics*, **31**, 765–780. https://doi.org/10.1071/IS16067.

Barden, P., Herhold, H.W. & Grimaldi, D.A. (2017b) A new genus of hell ants from the Cretaceous (Hymenoptera: Formicidae: Haidomyrmecini) with a novel head structure. *Systematic Entomology*, **42**, 837–846.

Baroni Urbani, C., Bolton, B. & Ward, P.S. (1992) The internal phylogeny of ants (Hymenoptera: Formicidae). *Systematic Entomology*, **17**, 301–329.

Bayzid, M.S., Mirarab, S., Boussau, B. & Warnow, T. (2015) Weighted statistical binning: enabling statistically consistent genome-scale phylogenetic analyses. *PLoS One*, **10**, e0129183.

Bergsten, J., Nilsson, A.N. & Ronquist, F. (2013) Bayesian tests of topology hypotheses with an example from diving beetles. *Systematic Biology*, **65**, 660–673.

Bergström, G. & Löfqvist, J. (1970) Chemical basis for odour communication in four species of *Lasius* ants. *Journal of Insect Physiology*, **16**, 2353–2375.

Bharti, H. & Gul, I. (2013) *Lasius elevatus*, a new ant species of the subgenus *Cautolasius* (Hymenoptera: Formicidae) from the Indian Himalayas. *Asian Myrmecology*, **5**, 53–58.

Blaimer, B.B., Brady, S.G., Schultz, T.R., Lloyd, M.W., Fisher, B.L. & Ward, P.S. (2015) Phylogenomic methods outperform traditional multi-locus approaches in resolving deep evolutionary history: a case study of formicine ants. *BMC Evolutionary Biology*, **15**, 257.

Blaimer, B.B., LaPolla, J.S., Branstetter, M.G., Lloyd, M.W. & Brady, S.G. (2016) Phylogenomics, biogeography and diversification of obligate mealybug-tending ants in the genus *Acropyga*. *Molecular Phylogenetics & Evolution*, **102**, 20–29.

Blaimer, B.B., Ward, P.S., Schultz, T.R., Fisher, B.L. & Brady, S.G. (2018) Paleotropical diversification dominates the evolution of the hyperdiverse ant tribe Crematogastrini (Hymenoptera: Formicidae). *Insect Systematics & Diversity*, **2**, 1–14.

Boer, P. (2003) First description of the worker caste of *Lasius viehmeyeri* Emery (Hymenoptera: Formicidae). *Zoologische Mededelingen*, **77**, 321–323.

Bolton, B. (1990a) Abdominal characters and status of the cerapachyine ants (Hymenoptera, Formicidae). *Journal of Natural History*, **24**, 53–68.

Bolton, B. (1990b) Army ants reassessed: the phylogeny and classification of the doryline section (Hymenoptera, Formicidae). *Journal of Natural History*, **24**, 1339–1364.

Bolton, B. (1990c) The higher classification of the ant subfamily Leptanillinae (Hymenoptera: Formicidae). *Systematic Entomology*, **15**, 267–282.

Bolton, B. (1994) *Identification Guide to the Ant Genera of the World*, p. 222. Harvard University Press, Cambridge.

Bolton, B. (1995) *A New General Catalogue of the Ants of the World*, p. 504. Harvard University Press, Cambridge.

Bolton, B. (2003) Synopsis and classification of Formicidae. *Memoirs of the American Entomological Institute*, **71**, 1–370.

Bolton, B. (2021) *AntCat: An Online Catalog of the Ants of the World*. URL http://antcat.org [accessed on 5 July 2021].

Borowiec, M.L. (2016a) Generic revision of the ant subfamily Dorylinae (Hymenoptera, Formicidae). *ZooKeys*, **608**, 1–280.

Borowiec, M.L. (2016b) AMAS: a fast tool for alignment manipulation and computing of summary statistics. *PeerJ*, **4**, e1660. https://doi.org/10.7717/peerj.1660.

Borowiec, M.L. (2019) Convergent evolution of the army ant syndrome and congruence in big-data phylogenetics. *Systematic Biology*, **68**, 642–656.

Borowiec, M.L., Cover, S.P. & Rabeling, C. (2021) The evolution of social parasitism in Formica ants revealed by a global phylogeny. *Proceedings of the National Academy of Sciences*, **118**, e2026029118. https://doi.org/10.1073/pnas.2026029118.

Borowiec, M.L., Rabeling, C., Brady, S.G., Fisher, B.L., Schultz, T.R. & Ward, P.S. (2019) Compositional heterogeneity and outgroup choice influence the internal phylogeny of the ants. *Molecular Phylogenetics & Evolution*, **134**, 111–121.

Bouckaert, R., Heled, J., Kühnert, D. *et al.* (2014) BEAST 2: a software platform for Bayesian evolutionary analysis. *PLoS Computational Biology*, **10**, e1003537. https://doi.org/10.1371/journal.pcbi.1003537.

Boudinot, B.E., Perrichot, V. & Chaul, J.C.M. (2020) †Camelosphecia gen. nov., lost ant-wasp intermediates from the mid-Cretaceous (Hymenoptera, Formicidae). *ZooKeys*, **1005**, 21–55.

Boudinot, B.E., Richter, A., Katzke, J., Chaul, J.C.M., Keller, R.A., Economo, E.P., Beutel, R.G. & Yamamoto, S. (in press) Evidence for the evolution of eusociality in stem ants and a systematic revision of †Gerontoformica (Hymenoptera, Formicidae). Zoological Journal of the Linnaean Society.

Brady, S.G., Fisher, B.L., Schultz, T.R. & Ward, P.S. (2014) The rise of army ants and their relatives: diversification of specialized predatory doryline ants. *BMC Evolutionary Biology 2014*, **14**, 1–14. https://doi.org/10.1186/1471-2148-14-93.

Brady, S.G., Schultz, T.R., Fisher, B.L. & Ward, P.S. (2006) Evaluating alternative hypotheses for the early evolution and diversification of ants. *Proceedings of the National Academy of Sciences*, **103**, 18172–18177.

Branstetter, M.G. (2012) Origin and diversification of the cryptic ant genus *Stenamma* Westwood (Hymenoptera: Formicidae), inferred from multilocus molecular data, biogeography and natural history. *Systematic Entomology*, **37**, 478–496.

Branstetter, M.G., Danforth, B.N., Pitts, J.P. *et al.* (2017b) Phylogenomic insights into the evolution of stinging wasps and the origins of ants and bees. *Current Biology*, **27**, 1019–1025.

Branstetter, M.G., Jesovnik, A., Sosa-Calvo, J., Lloyd, M.W., Faircloth, B.C., Brady, S.G. & Schultz, T.R. (2017c) Dry habitats were crucibles of domestication in the evolution of agriculture in ants. *Proceedings of the Royal Society, Series B*, **284**, 20170095.

Branstetter, M.G. & Longino, J.T. (2019) Ultra-conserved element phylogenomics of New World *Ponera* (Hymenoptera: Formicidae) illuminates the origin and phylogeographic history of the endemic exotic ant *Ponera exotica*. *Insect Systematics & Diversity*, **2**, 1–13.

Branstetter, M.G., Longino, J.T., Ward, P.S. & Faircloth, B.C. (2017a) Enriching the ant tree of life: enhanced UCE bait set for genome-scale phylogenetics of ants and other Hymenoptera. *Methods in Ecology and Evolution*, **8**, 768–776. https://doi.org/10.1111/20141-210X.12742.

Brown, W.L. Jr (1954) Remarks on the internal phylogeny and subfamily classification of the family Formicidae. *Insectes Sociaux*, **1**, 21–31.

Buckley, T.R., Simon, C. & Chambers, G.K. (2001) Exploring among-site rate variation models in a maximum likelihood framework using empirical data: effects of model assumptions on estimates of topology, branch lengths, and bootstrap support. *Systematic Biology*, **50**, 67–86.

Buschinger, A. (2009) Social parasitism among ants: a review (Hymenoptera: Formicidae). *Myrmecological News*, **12**, 219–235.

Carpenter, F.M. (1930) The fossil ants of North America. *Bulletin of the Museum of Comparative Zoology*, **70**, 1–66.

Castresana, J. (2000) Selection of conserved blocks from multiple alignments for their use in phylogenetic analysis. *Molecular Biology and Evolution*, **17**, 540–552.

Chomicki, G., Ward, P.S. & Renner, S.S. (2015) Macroevolutionary assembly of ant/plant symbioses: *Pseudomyrmex* ants and their ant-housing plants in the Neotropics. *Proceedings of the Royal Society. Series B*, **282**, 20152200. https://doi.org/10.1098/rspb.2015.2200.

Cole, A.C. Jr (1956) Studies of Nevada ants. II. A new species of *Lasius* (*Chthonolasius*) (Hymenoptera: Formicidae). *Journal of the Tennessee Academy of Science*, **31**, 26–27.

Cole, A.C. Jr (1958) A remarkable new species of *Lasius* (*Chthonolasius*) from California (Hymenoptera: Formicidae). *Journal of the Tennessee Academy of Science*, **38**, 75–77.

Collingwood, C.A. (1982) Himalayan ants of the genus *Lasius* (Hymenoptera: Formicidae). *Systematic Entomology*, **7**, 283–296.

Cover, S.P. & Sanwald, R. (1988) Colony founding in *Acanthomyops murphyi*. *Advances in Myrmecology* (ed. by J.C. Trager), pp. 405–417. Brill, New York, New York.

Darwell, C.T., Fischer, G., Sarnat, E.M. *et al.* (2019) Genomic and phenomic analysis of Island ant community assembly. *Molecular Ecology*, **29**, 1611–1627. https://doi.org/10.1111/mec.15326.

Dlussky, G.M. (1967) Ants of the genus *Formica* from the Baltic Amber. *Paleontological Journal*, **1**, 69–77.

Dlussky, G.M. (1981, 1981) Miocene ants (Hymenoptera, Formicidae) of the USSR. [In Russian.]. *New Fossil Insects from the Territories of the USSR. [in Russian.] Trudy Paleontologicheskogo Instituta*, Vol. **183** (ed. by V.N. Vishnyakova, G.M. Dlussky and L.N. Pritykina), pp. 64, 1–83, 87. Moscow: Nauka: *Akademiya Nauk SSR*.

Dlussky, G.M. & Fedoseeva, E.B. (1988) Origin and early stages of evolution in ants [in Russian]. Pp. 70–144 in: Ponomarenko, A. G. (ed.) *Cretaceous Biocenotic Crisis and Insect Evolution. [in Russian.]*. Moskva: Nauka, 232 pp.

Dlussky, G.M. (2008) Ants of the tribe Formicini (hymenoptera, Formicidae) from late Eocene amber of Europe. *Paleontological Journal*, **42**, 500–513.

Dlussky, G.M. (2011) The ants of the genus *Lasius* (hymenoptera, Formicidae) from late Eocene European ambers. *Vestnik Zoologii*, **45**, 209–222.

Dlussky, G.M. & Putyatina, T.S. (2014) Early Miocene ants (Hymenoptera: Formicidae) from Radoboj, Croatia. *Neues Jahrbuch für Geologie und Paläontologie Abhandlungen*, **272**, 237–285.

Donisthorpe, H. (1922) The colony founding of *Acanthomyops (Dendrolasius) fuliginosus* Latr. *The Biological Bulletin*, **42**, 173–184.

Donisthorpe, H. (1943) A list of the type-species of the genera and subgenera of the Formicidae. [part]. *Annals and Magazine of Natural History*, **10**, 617–688.

Economo, E.P., Narula, N., Friedman, N.R., Weiser, M.D. & Guénard, B. (2018) Macroecology and macroevolution of the latitudinal diversity gradient in ants. *Nature Communications*, **9**, 1778. https://doi.org/10.1038/s41467-018-04218-4.

Eisner, T. (1957) A comparative morphological study of the proventriculus of ants (Hymenoptera: Formicidae). *Bulletin of the Museum of Comparative Zoology*, **8**, 439–490.

Eisner, T. & Brown, W.L. Jr (1958) The evolution and social significance of the ant proventriculus. *Proceedings Tenth International Congress of Entomology*, **2**, 503–508.

Emery, C. (1888) Über den sogennanten Kaumagen einiger Ameisen. *Zeitschrift für Wissenschaftliche Zoologie*, **46**, 378–412.

Emery, C. (1895) Die Gattung *Dorylus* Fab. Und die systematische Eintheilung der Formiciden. *Abteilung für Systematik, Geographie und Biologie der Tiere*, **8**, 685–778.

Emery, C. (1909) Über den Ursprung der dulotischen, parasitischen und myrmekophilen Ameisen. *Biologischen Centralblatt*, **19**, 352–362.

Emery, C. (1925) Hymenoptera. Fam. Formicidae. Subfam. Formicinae. *Genera Insectorum*, **183**, 1–302.

Faber, W. (1967) Beiträge zur Kenntnis sozialparasitischer Ameisen. I. *Lasius* (*Austrolasius* n. sg.) *reginae* n. sp., eine neue temporär sozialparasitische Erdameise aus Österreich (Hym. Formicidae). *Pflanzenschultz Berichte*, **36**, 73–107.

Fabricius, J.C. (1804) *Systema Piezatorum Secundum Ordines, Genera, Species, Adjectis Synonymis, Locis, Observationibus, Descriptionibus*. Brunswick: C. Reichard. xiv + 15–439 + 30 pp.

Faircloth, B.C., Branstetter, M.G., White, N.D. & Brady, S.G. (2015) Target enrichment of ultraconserved elements from arthropods provides a genomic perspective on relationships among Hymenoptera. *Molecular Ecology Resources*, **15**, 489–501.

Felsenstein, J. (1983) Methods for inferring phylogenies: a statistical view. *Numerical Taxonomy* (ed. by J. Felsenstein), pp. 315–316. Springer-Verlag, Berlin, Heidelberg.

Felsenstein, J. (1988) Phylogenies from molecular sequences: inference and reliability. *Annual Review of Genetics*, **22**, 521–565.

Felsenstein, J. (2001) The troubled growth of statistical phylogenetics. *Systematic Biology*, **50**, 465–467.

Felsenstein, J. (2003) *Inferring Phylogenies*, p. 664. Sinauer Associates, Inc., Sunderland, Massachusetts.

Fischer, G., Azorsa, F., Garcia, F.H., Mikheyev, A.S. & Economo, E.P. (2015) Two new phragmotic ant species from Africa: morphology and next-generation sequencing solve a caste association problem in the genus Carebara Westwood. *ZooKeys*, **525**, 77.

Fisher, B.L. & Bolton, B. (2016) *Ants of Africa and Madagascar, a Guide to the Genera*, p. 503. University of California Press, Oakland.

Forel, A. (1874) Les fourmis de la Suisse. Systématique, notices anatomiques et physiologiques, architecture, distribution géographique, nouvelles expériences et observations de moeurs. *Neue Denkschriften der Allgemeinen Schweizerischen Gesellschaft für die Gesammten Naturwissenschaften*, **26**, 1–452.

Forel, A. (1878) Études myrmécologiques en 1878 (première partie) avec l'anatomie du gésier des fourmis. *Bulletin de la Société Vandoise des Sciences Naturelles*, **15**, 337–392.

Forel, A. (1886) Études myrmécologiques en 1886. *Annales de la Société Entomologique de Belgique*, **30**, 131–215.

Forel, A. (1912) Formicides néotropiques. Part VI. 5me sous-famille Camponotinae Forel. *Mémoires de la Société Entomologique de Belgique*, **20**, 59–92.

Forel, A. (1916) Fourmis du Congo et d'autres provenances rècoltées par MM. Hermann Kohl, Luja, Mayné, etc. *Revue Suisse de Zoologie*, **24**, 397–460.

Grimaldi, D. & Agosti, D. (2000) A formicine in New Jersey Cretaceous amber (Hymenoptera: Formicidae) and early evolution of the ants. *Proceedings of the National Academy of Sciences of The United States of America*, **97**, 13678–13683.

Grimaldi, D., Agosti, D. & Carpenter, J.M. (1997) New and rediscovered primitive ants (Hymenoptera: Formicidae) in Cretaceous amber from New Jersey, and their phylogenetic implications. *American Museum Novitates*, **3208**, 1–24.

Hansen, J., Sato, M., Russel, G. & Pushker, K. (2013) Climate sensitivity, sea level and atmospheric carbon dioxide. *Philosophical Transaction of the Royal Society A*, **371**, 20120294. https://doi.org/10.1098/rsta.2012.0294.

Hasegawa, E. (1998) Phylogeny and host-parasite relationships in social parasitism in *Lasius* ants. *Entomological Science*, **1**, 133–135.

Hashimoto, Y. (1996) Skeletomuscular modifications associated with the formation of an additional petiole and on the anterior abdominal segments in aculeate Hymenoptera. *Japanese Journal of Entomology*, **64**, 340–356.

Heath, T.A., Huelsenbeck, J.P. & Stadler, T. (2014) The fossilized birth–death process for coherent calibration of divergence-time

estimates. *Proceedings of the National Academy of Sciences*, **111**, E2957–E2966. https://doi.org/10.1073/pnas.1319091111.

Heer, O. (1849) Die Insektenfauna der Tertiärgebilde von Oenigen und von Radoboj in Croatien. Zweiter Theil: Heuschrecken, Florfliegen, Aderflügler, Schmetterlinge und Fliegen. Lepzig: W. Engelmann, vi +264 pp.

Heer, O. (1867) Fossile Hymenopteren aus Oeningen und Radoboj. *Neue Denkschriften der Allgemeinen Sschweizerischen Gesellschaft für die Gesammten Naturwissenschaften*, **22**, 1–42.

Hita-Garcia, F., Fischer, G., Liu, C., Audisio, T.L. & Economo, E.P. (2017) Next-generation morphological character discovery and evaluation: an X-ray micro-CT enhanced revision of the ant genus *Zasphinctus* Wheeler (Hymenoptera: Formicidae: Dorylinae) in the Afrotropics. *ZooKeys*, **693**, 33–93.

Hoey-Chamberlain, R., Rust, M.K. & Klotz, J.H. (2013) A review of the biology, ecology and behavior of velvety tree ants of North America. *Sociobiology*, **60**, 1–10.

Hölldobler, B. & Wilson, E.O. (1990) *The Ants*. Harvard University Press, Cambridge, Massachusetts. xii + 732 pp.

Holman, L., Lanfear, R. & d'Ettorre, P. (2013) The evolution of queen pheromones in the ant genus *Lasius*. *Journal of Evolutionary Biology*, **26**, 1549–1558.

Janda, M., Folková, D. & Zrzavý, J. (2004) Phylogeny of *Lasius* ants based on mitochondrial DNA and morphology, and the evolution of social parasitism in the Lasiini (Hymenoptera: Formicidae). *Molecular Phylogenetics and Evolution*, **33**, 595–614.

Jansen, G., Savolainen, R. & Vepsäläinen, K. (2010) Phylogeny, divergence-time estimation, biogeography and social parasite–host relationships of the Holarctic ant genus *Myrmica* (Hymenoptera: Formicidae). *Molecular Phylogenetics and Evolution*, **56**, 294–304.

Jesovnik, A., González, V.L. & Schultz, T.R. (2016) Phylogenomics and divergence dating of fungus-farming ants (Hymenoptera: Formicidae) of the genera *Sericomyrmex* and *Apterostigma*. *PLoS One*, **11**, e0151059.

Jesovnik, A., Sosa-Calvo, J., Lloyd, M.W., Branstetter, M.G., Fernández, F. & Schultz, T.R. (2017) Phylogenomic species delimitation and host-symbiont coevolution in the fungus-farming ant genus *Sericomyrmex* Mayr (Hymenoptera: Formicidae): ultraconserved elements (UCEs) resolve a recent radiation. *Systematic Entomology*, **42**, 523–542.

Kass, R.E. & Raftery, A.E. (1995) Bayes factors. *Journal of the American Statistical Association*, **90**, 773–795.

Katoh, K., Misawa, K., Kuma, K.I. & Miyata, T. (2002) MAFFT: a novel method for rapid multiple sequence alignment based on fast Fourier transform. *Nucleic Acids Research*, **30**, 3059–3066.

Katoh, K. & Standley, D.M. (2013) MAFFT multiple sequence alignment software version 7: improvements in performance and usability. *Molecular Biology and Evolution*, **30**, 772–780.

Katzke, J., Barden, P., Dehon, M., Michez, D. & Wappler, T. (2018) Giant ants and their shape: revealing relationships in the genus *Titanomyrma* with geometric morphometrics. *PeerJ*, **6**, 36 pp., e4242. https://doi.org/10.7717/peerj.4242.

Keller, R.A. (2000) Cladistics of the tribe Ectatommini (Hymenoptera: Formicidae): a reappraisal. *Insect Systematics & Evolution*, **31**, 59–69.

Keller, R.A. (2011) A phylogenetic analysis of ant morphology (Hymenoptera: Formicidae) with special reference to the poneromorph subfamilies. *Bulletin of the American Museum of Natural History*, **355**, 1–90.

Klopfstein, S., Ryer, R., Coiro, M. & Spasojevic, T. (2019) Mismatch of the morphological model is mostly unproblematic in total-evidence dating: insights from an extensive simulation study. *bioRxiv*. https://doi.org/10.1101/679084.

Klopfstein, S. & Spasojevic, T. (2019) Illustrating phylogenetic placement of fossils using RoguePlots: an example from ichneumonid parasitoid wasps (Hymenoptera, Ichneumonidae) and an extensive morphological matrix. *PLoS One*, **14**, e212942.

Lanfear, R., Frandsen, P. B., Wright, A. M., Senfeld, T., Calcott, B. (2016) PartitionFinder 2: New Methods for Selecting Partitioned Models of Evolution for Molecular and Morphological Phylogenetic Analyses. *Molecular Biology and Evolution*. https://doi.org/10.1093/molbev/msw260

LaPolla, J.S., Brady, S.G. & Shattuck, S.O. (2010) Phylogeny and taxonomy of the *Prenolepis* genus-group of ants (Hymenoptera: Formicidae). *Systematic Entomology*, **35**, 118–131.

LaPolla, J.S. & Dlussky, G.M. (2010) Review of fossil *Prenolepis* genus-group species (Hymenoptera: Formicidae). *Proceedings of the Entomological Society of Washington*, **112**, 258–273.

LaPolla, J.S. & Fisher, B.L. (2014) Then there were five: a reexamination of the ant genus *Paratrechina* (Hymenoptera, Formicidae). *ZooKeys*, **422**, 35–48.

LaPolla, J.S., Hawkes, P.G. & Fisher, J.N. (2013) Taxonomic review of the ant genus *Paratrechina*, with a description of a new species from Africa. *Journal of Hymenoptera Research*, **35**, 71–82.

LaPolla, J.S., Kallal, R.J. & Brady, S.G. (2012) A new ant genus from the greater Antilles and Central America, *Zatania* (Hymenoptera: Formicidae), exemplifies the utility of male and molecular character systems. *Systematic Entomology*, **37**, 200–214.

Larsson, A. (2014) AliView: a fast and lightweight alignment viewer and editor for large datasets. *Bioinformatics*, **30**, 3276–3278.

Latreille, P.A. (1809) *Genera crustaceorum et insectorum secundum ordinem naturalem in familias disposita, iconibus exemplisque plurimus explicata. Tomus 4*. Parisiis et Argentorati [= Paris and Strasbourg]: A. Koenig, 399.

Lattke, J. (1994) Phylogenetic relationships and classification of ectatommine ants (Hymenoptera: Formicidae). *Entomologica Scandinavica*, **25**, 105–119.

Lepeletier de Saint-Fargeau, A. (1835 1836) *Histoire naturelle des insectes. Hyménoptères. Tome I*, p. 547. *Roret*, Paris.

Lepeletier de Saint-Fargeau, A. (1836) *Histoire naturelle des insectes. Hyménoptères. Atlas*. Roret, Paris. 16 pp. + 47 plates.

Lewis, P.O. (2001) A likelihood approach to estimating phylogeny from discrete morphological character data. *Systematic Biology*, **50**, 913–925.

Linnaeus, C. (1758) *Systema naturae per regna tria naturae, secundum classes, ordines, genera, species, cum characteribus, differentiis, synonymis, locis. Tomus I. Editio decima, reformata. Holmiae [= Stockholm]: L. Salvii*, 824 pp.

Liu, C., Sarnat, E.M., Friedman, N.R. *et al.* (2020) Colonize, radiate, decline: unraveling the dynamics of Island community assembly with Fijian trap-jaw ants. *Evolution*, **74**, 1082–1097. https://doi.org/10.1111/evo.13983.

Markó, B. & Czechowski, W. (2004) *Lasius psammophilus* Seifert and *Formica cinerea* Mayr (Hymenoptera: Formicidae) on sand dunes: conflicts and coexistence. *Annales Zoologici*, **54**, 365–378.

Maruyama, M., Steiner, F.M., Stauffer, C., Akino, T., Crozier, R.H. & Schlick-Steiner, B.C. (2008) A DNA and morphology based phylogenetic framework of the ant genus *Lasius* with hypotheses for the evolution of social parasitism and fungiculture. *BMC Evolutionary Biology*, **8**, 1–15. Article 237. https://doi.org/10.1186/1471-2148-8-237.

Matos-Maraví, P., Clouse, R.M., Sarnat, E.M. *et al.* (2018) An ant genus-group (*Prenolepis*) illuminates the biogeography and drivers of insect diversification in the Indo-Pacific. *Molecular Phylogenetics & Evolution*, **123**, 16–25. https://doi.org/10.1016/j.ympev.2018.02.007.

Matzke, N.J. (2013) Probabilistic historical biogeography: new models for founder-event speciation, imperfect detection, and fossils allow

improved accuracy and model-testing. *Frontiers of Biogeography*, **5**, 242–248.
Mayr, G. (1868) Die Ameisen des baltischen Bernsteins. *Beiträge zur Naturkunde Preussens*, **1**, 1–102.
Mei, M. (1998) Lasius (Cautolasius) myrmidon n. sp.: a new hypogaeic ant from Greece (Hymenoptera Formicidae). *Bollettino della Società Entomologica Italiana*, **130**, 177–182.
Miller M.A., Pfeiffer W. & Schwartz T. (2010) Creating the CIPRES Science Gateway for inference of large phylogenetic trees. *Proceedings of the Gateway Computing Environments Workshop* (GCE), 14 Nov. 2010, New Orleans, LA pp. 1–8.
Minh, B.Q., Schmidt, H.A., Chernomor, O., Schrempf, D., Woodhams, M.D., von Haeseler, A. & Lanfear, R. (2020) IQ-TREE 2: new models and efficient methods for phylogenetic inference in the genomic era. *Molecular Biology and Evolution*, **37**, 1530–1534. https://doi.org/10.1093/molbev/msaa015.
Mirarab, S., Bayzid, M.S., Boussau, B. & Warnow, T. (2014) Statistical binning enables an accurate coalescent-based estimation of the avian tree. *Science*, **346**, 1250463.
Mirarab, S. & Warnow, T. (2015) ASTRAL-II: coalescent-based species tree estimation with many hundreds of taxa and thousands of genes. *Bioinformatics*, **31**, i44–i52.
Moreau, C.S., Bell, C.D., Vila, R., Archibald, S.B. & Pierce, N.E. (2006) Phylogeny of the ants: diversification in the age of angiosperms. *Science*, **312**, 101–104.
Paradis, E., Claude, J. & Strimmer, K. (2004) APE: analysis of phylogenetics and evolution in R language. *Bioinformatics*, **20**, 289–290.
Paradis, E. & Schliep, K. (2018) ape 5.0: an environment for modern phylogenetics and evolutionary analyses in R. *Bioinformatics*, **2018**, 1–3. https://doi.org/10.1093/bioinformatics/bty633.
Parins-Fukuchi, C. (2018) Use of continuous traits can improve morphological phylogenetics. *Systematic Biology*, **67**, 328–339. https://doi.org/10.1093/sysbio/syx072.
Parr, C.L. & Gibb, H. (2010) Competition and the role of dominant ants. *Ant Ecology* (ed. by L. Lach, C.L. Parr and K.L. Abbott), pp. 77–96. Oxford University Press, Oxford.
Perrault, G.H. (2004) Étude morphoanatomique et biométrique du métasoma antérieur des ouvrières. Contribution à la systématique et à la phylogénie des fourmis (Hymenoptera: Formicidae). *Annales de la Société Entomologique de France (n.s.)*, **40**, 291–371.
Perrichot, V., Wang, B. & Barden, P. (2020) New remarkable hell ants (Formicidae: Haidomyrmecinae stat. nov.) from mid-Cretaceous amber of northern Myanmar. *Cretaceous Research*, **109**, 104381. https://doi.org/10.1016/j.cretres.2020.104381.
Pontin, A.J. (1961) Population stabilization and competition between the ants *Lasius flavus* (F.) and *L. niger* (L.). *The Journal of Animal Ecology*, **30**, 47–54.
Prebus, M.M. (2017) Insights into the evolution, biogeography and natural history of the acorn ants, genus *Temnothorax* Mayr (Hymenoptera: Formicidae). *BMC Evolutionary Biology*, **17**, 22. https://doi.org/10.1186/s12862-017-1095-8.
Prebus, M.M. (2021) Phylogenetic species delimitation in the ants of the *Temnothorax salvini* group (Hymenoptera: Formicidae): an integrative approach. *Systematic Entomology*, **46**, 307–326.
Prins, A.J. (1983) A new ant genus from southern Africa (Hymenoptera, Formicidae). *Annals of the South African Museum*, **94**, 1–11.
Quque, M. & Bles, O. (2020) Lasius. *Encyclopedia of Social Insects* (ed. by C. Starr). Springer, Cham. https://doi.org/10.1007/978-3-319-90306-4_169-1.
Raczkowski, J.M. & Luque, G.M. (2011) Colony founding and social parasitism in *Lasius* (*Acanthomyops*). *Insectes Sociaux*, **58**, 237–244.
Radchenko, A. (2005a) A review of the ants of the genus *Lasius*, 1804, subgenus *Dendrolasius* Ruzsky, 1912 (Hymenoptera: Formicidae) from East Palaearctic. *Annales Zoologici*, **55**, 83–94.
Radchenko, A. (2005b) Monographic revision of the ants (Hymenoptera: Formicidae) of North Korea. *Annales Zoologici (Warsaw)*, **55**, 127–221.
Rambaut, A. & Drummond, A. (2014) *FigTree Version* 1.4.2 [WWW document]. URL http://beast.bio.ed.ac.uk/software/figree [accessed on 2 February 2015].
Rambaut, A., Suchard, M.A., Xie, D. & Drummond, A.J. (2014) *Tracer* v1.6 [WWW document]. URL http://beast.bio.ed.ac.uk/Tracer [accessed on 2 February 2015].
Ree, R.H. & Sanmartín, I. (2018) Conceptual and statistical problems with the DEC+J model of founder-event speciation and its comparison with DEC via model selection. *Journal of Biogeography*, **45**, 741–749. https://doi.org/10.1111/jbi.13173.
Revell, L.J. (2012) phytools: an R package for phylogenetic comparative biology (and other things). *Methods in Ecology and Evolution*, **3**, 217–223.
Reza, A. (1925) Recursos alimentícios de México de origen animal poco conocidos. *Memorias y Revista de la Sociedad Científica "Antonio Alzate"*, **44**, 1–22.
Romiguier, J., Rolland, J., Morandin, C. & Keller, L. (2018) Phylogenomics of palearctic Formica species suggests a single origin of temporary parasitism and gives insights to the evolutionary pathway toward slave-making behaviour. *BMC Ecology and Evolution*, **18**(40), 1–8.
Ronquist, F., Klopfstein, S., Vilhelmsen, L., Schulmeister, S., Murray, D.L. & Rasnitsyn, A.P. (2012a) A total-evidence approach to dating with fossils, applied to the early radiation of the Hymenoptera. *Systematic Biology*, **61**, 973–999.
Ronquist, F., Lartillot, N. & Phillips, M.J. (2016) Closing the gap between rocks and clocks using total-evidence dating. *Philosophical Transactions of the Royal Society, Series B*, **371**, 20150136.
Ronquist, F., Teslenko, M., van der Mark, P. *et al.* (2012b) MrBayes 3.2: efficient Bayesian phylogenetic inference and model choice across a large model space. *Systematic Biology*, **61**, 539–542.
Royer, D.L., Berner, R.A., Montañez, I.P., Tabor, N.J. & Beerling, D.J. (2004) CO_2 as a primary driver of Phanerozoic climate. *GSA Today*, **14**, 4–10.
O'Meara, B. (2008) Using Trees: Myrmecocystus Phylogeny and Character Evolution and New Methods for Investigating Trait Evolution and Species Delimitation (PhD Dissertation). Nature Precedings, 1–1.
Saunders, W.B., Mapes, R.H., Carpenter, F.M. & Elsik, W.C. (1974) Fossiliferous amber from the Eocene (Claiborne) of the Gulf coastal plain. *GSA Bulletin*, **85**, 979–984.
Schär, S., Talavera, G., Espadaler, X., Rana, J.D., Anderson, A.A., Cover, S.P. & Vila, R. (2018) Do Holarctic ant species exist? Trans-Beringian dispersal and homoplasy in the Formicidae. *Journal of Biogeography*, **45**, 1–12. https://doi.org/10.1111/jbi.13380.
Schlick-Steiner, B.C., Steiner, F.M., Konrad, H. *et al.* (2008) Specificity and transmission mosaic of ant nest-wall fungi. *Proceedings of the National Academy of Sciences*, **105**, 940–943.
Schlick-Steiner, B.C., Steiner, F.M., Schödl, S. & Seifert, B. (2003) *Lasius austriacus* sp. n., a central European ant related to the invasive species *Lasius neglectus*. *Sociobiology*, **41**, 725–736.
Schmid, F.R. (1975) Über den *Lasius carniolicus* Mayr, eine seltene Ameisenart in der Schweiz. 9. Wettbewerb Schweizer Jugend forscht.
Scotese, C.R. (1998) The PALEOMAP Project: paleogeographic atlas and plate tectonic software. *Oceanographic Literature Review*, **3**, 606–607. http://www.scotese.com/ [accessed on 4 November 2016].
Seifert, B. (1982) *Lasius* (*Chthonolasius*) *jensi* n. sp. - eine neue temporär sozialparasitische Erdameise aus Mitteleuropa (Hymenoptera, Formicidae). *Reichenbachia*, **20**, 85–96.
Seifert, B. (1983) The taxonomical and ecological status of *Lasius myops* Forel (Hymenoptera, Formicidae) and first description of its males.

Abhandlungen und Berichte des Naturkundemuseums Görlitz, **57**, 1–16.
Seifert, B. (1988) A revision of the European species of the ant subgenus *Chthonolasius* (Insecta, Hymenoptera, Formicidae). *Entomologische Abhandlungen, Staatliches Museum für Tierkunde Dresden*, **51**, 143–180.
Seifert, B. (1990) Supplementation to the revision of European species of the ant subgenus *Chthonolasius* Ruzsky, 1913 (Hymenoptera, Formicidae). *Doriana*, *Supplemento agli Annali del Museo Civico di Storia Naturale "G. Doria"*. *GEN*, **6**, 1–13.
Seifert, B. (1991) *Lasius platythorax* n. sp., a widespread sibling species of *Lasius niger* (Hymenoptera: Formicidae). *Entomologia Generalis*, **16**, 69–81.
Seifert, B. (1992) A taxonomic revision of the Palaearctic members of the ant subgenus *Lasius* s. str. (Hymenoptera: Formicidae). *Abhandlungen und Berichte des Naturkundemuseums Görlitz*, **66**, 1–67.
Seifert, B. (1996) *Ameisen: Beobachten, Bestimmen*. Naturbuch Verlag, Augsburg.
Seifert, B. (1997) *Lasius nitidigaster* n. sp. – a new ant of the subgenus *Chthonolasius* Ruzsky (Hymenoptera: Formicidae). *Annales Zoologici*, **46**, 201–205.
Seifert, B. (2018) *The Ants of Central and North Europe*, p. 408. Lutra Verlags- und Vertriebsgesellschaft, Tauer.
Seifert, B. (2020) A taxonomic revision of the Palaearctic members of the subgenus *Lasius* s. str. (Hymenoptera, Formicidae). *Soil Organisms*, **92**, 15–86.
Seifert, B. & Galkowski, C. (2016) The Westpalaearctic *Lasius paralienus* complex (Hymenoptera: Formicidae) contains three species. *Zootaxa*, **4132**, 44–58.
Shattuck, S. (1992) Higher classification of the ant subfamilies Aneuretinae, Dolichoderinae and Formicinae (Hymenoptera: Formicidae). *Systematic Entomology*, **17**, 199–206.
Shattuck, S.O. (1995) Generic-level relationships within the ant subfamily Dolichoderinae (Hymenoptera: Formicidae). *Systematic Entomology*, **20**, 217–228.
Snelling, R.R. (1976) A Revision of the Honey Ants, Genus *Myrmecocystus* (Hymenoptera: Formicidae). *Natural History Museum of Los Angeles County Science Bulletin*, **24**, 1–163.
Snelling, R.R. (1982) A revision of the honey ants, genus *Myrmecocystus*, first supplement (Hymenoptera: Formicidae). *Bulletin of the Southern California Academy of Sciences*, **81**, 69–86.
Sosa-Calvo, J.E., Schultz, T.R., Jesovnik, A., Dahan, R.A. & Rabeling, C. (2018) Evolution, systematics, and natural history of a new genus of cryptobiotic fungus-growing ants. *Systematic Entomology*, **43**, 549–567.
Stärcke, A. (1942) Drie nog onbeschreven Europeesche miervormen. *Tijdschrift voor Entomologie*, **85**, xxiv–xxix.
Stärcke, A. (1944) Retouches sur quelques fourmis d'Europe. 3. Autres *Lasius*. *Entomologische Berichten*, **11**, 153–158.
Steiner, F.M., Schlick-Steiner, B.C. & Seifert, B. (2009) Morphology-based taxonomy is essential to link molecular research to nomenclature. *Contributions to Natural History*, **12**, 1295–1315.
Strong, E.E. & Lipscomb, D. (1999) Character coding and inapplicable data. *Cladistics*, **15**, 363–371.
Sullivan, J. & Swofford, D.L. (2001) Should we use model-based methods for phylogenetic inference when we know assumptions about among-site rate variation and nucleotide substitution pattern are violated? *Systematic Biology*, **50**, 723–729.
Talavera, G., Espadaler, X. & Vila, R. (2015 2014) Discovered just before extinction? The first endemic ant from the Balearic Islands (*Lasius balearicus* sp. nov.) is endangered by climate change. *Journal of Biogeography*, **42**, 589–601. https://doi.org/10.1111/jbi.12438.
Théobald, N. (1937) *Les insectes fossiles des terrains oligocènes de France Nancy*, p. 473. Nancy, France: G. Thomas.
Traniello, J.F.A. & Levings, S.C. (1986) Intra- and intercolony patterns of nest dispersion in the ant *Lasius neoniger*: correlations with territoriality and foraging ecology. *Oecologia*, **69**, 413–419.
van Elst, T., Eriksson, T.H., Gadau, J., Johnson, R.A., Rabeling, C., Taylor, J.E. & Borowiec, M.L. (2021) Comprehensive phylogeny of *Myrmecocystus* honey ants highlights cryptic diversity and infers evolution during aridification of the American southwest. *Molecular Phylogenetics and Evolution*, **155**, 107036.
Ward, P.S. (1990) The ant subfamily Pseudomyrmecinae (Hymenoptera: Formicidae): generic revision and relationship to other formicids. *Systematic Entomology*, **15**, 449–489.
Ward, P.S. (1994) *Adetomyrma*, an enigmatic new ant genus from Madagascar (Hymenoptera: Formicidae), and its implications for ant phylogeny. *Systematic Entomology*, **19**, 159–175.
Ward, P.S. (2005) A synoptic review of the ants of California (Hymenoptera: Formicidae). *Zootaxa*, **936**, 1–68.
Ward, P.S. (2011) Integrating molecular phylogenetic results into ant taxonomy (Hymenoptera: Formicidae). *Myrmecological News*, **15**, 21–29.
Ward, P.S., Blaimer, B.B. & Fisher, B.L. (2016) A revised phylogenetic classification of the ant subfamily Formicinae (Hymenoptera: Formicidae), with resurrection of the genera *Colobopsis* and *Dinoponera*. *Zootaxa*, **4072**, 343–357. https://doi.org/10.11646/Zootaxa.4072.3.4.
Ward, P.S. & Boudinot, B.E. (2021) Grappling with homoplasy: taxonomic refinements and reassignments in the ant genera *Camponotus* and *Colobopsis* (Hymenoptera: Formicidae). *Arthropod Systematics & Phylogeny*, **79**, 37–56.
Ward, P.S. & Brady, S.G. (2003) Phylogeny and biogeography of the ant subfamily Myrmeciinae (Hymenoptera: Formicidae). *Invertebrate Systematics*, **17**, 361–386.
Ward, P.S., Brady, S.G., Fisher, B.L. & Schultz, T.R. (2010) Phylogeny and biogeography of dolichoderine ants: effects of data partitioning and relict taxa on historical inference. *Systematic Biology*, **59**, 342–362.
Ward, P.S., Brady, S.G., Fisher, B.L. & Schultz, T.R. (2015) The evolution of myrmicine ants: phylogeny and biogeography of a hyperdiverse ant clade (Hymenoptera: Formicidae). *Systematic Entomology*, **40**, 61–81.
Ward, P.S. & Downie, D.A. (2005) The ant subfamily Pseudomyrmecinae (Hymenoptera: Formicidae): phylogeny and evolution of big-eyed arboreal ants. *Systematic Entomology*, **30**, 310–335.
Ward, P.S. & Fisher, B.L. (2016) Tales of dracula ants: the evolutionary history of the ant subfamily Amblyoponinae (Hymenoptera: Formicidae). *Systematic Entomology*, **41**, 683–693.
Weisrock, D.W., Smith, S.D., Chan, L.M., Biebouw, K., Kappeler, P.M. & Yoder, A.D. (2012) Concatenation and concordance in the reconstruction of mouse lemur phylogeny: an empirical demonstration of the effect of allele sampling in phylogenetics. *Molecular Biology and Evolution*, **29**, 1615–1630.
Wheeler, W.M. (1915 1914) The ants of the Baltic Amber. *Schriften der Physikalisch-Ökonomischen Gesellschaft zu Königsberg*, **55**, 1–142.
Williams, J.L. & LaPolla, J.S. (2016) Taxonomic revision and phylogeny of the ant genus *Prenolepis* (Hymenoptera: Formicidae). *Zootaxa*, **4200**, 201–258.
Williams, J.L., Zhang, Y.M., Lloyd, M.W., LaPolla, J.S., Schultz, T.R. & Lucky, A. (2020) Global domination by crazy ants: phylogenomics reveals biogeographical history and invasive species relationships in the genus *Nylanderia* (Hymenoptera: Formicidae). *Systematic Entomology*, **45**, 730–744.
Wilson, E.O. (1955) A monographic revision of the ant genus *Lasius*. *Bulletin of the Museum of Comparative Zoology*, **113**, 1–201.
Wilson, E.O. (1971) *The Insect Societies*, p. 548. The Belknap Press of Harvard University Press, Cambridge, Massachusetts.

Wilson, E.O. (1985) Ants from the Cretaceous and Eocene amber of North America. *Psyche*, **92**, 205–216.

Wing, M.W. (1968a) Taxonomic revision of the Nearctic genus *Acanthomyops* (Hymenoptera: Formicidae). *Memoirs of the Cornell University Agricultural Experiment Station*, **405**, 1–173.

Wing, M.W. (1968b) *A taxonomic revision of the Nearctic genus Acanthomyops Mayr (Hymenoptera: Formicidae)*. [Abstract.]. Dissertation Abstracts. B. Sciences and Engineering, **28**, 3934.

Wolfe, A.P., McKellar, R.C., Tappert, R., Rana, N.S.S. & Muehlenbachs, K. (2016) Bitterfield amber is not Baltic amber: three geochemical tests and further constraints on the botanical affinities of succinite. *Review of Palaeobotany and Palynology*, **225**, 21–32.

Wright, A.M., Lloyd, G.T. & Hillis, D.M. (2016) Modeling character change heterogeneity in phylogenetic analyses of morphology through the use of priors. *Systematic Biology*, **65**, 602–611.

Xie, W., Lewis, P.O., Fan, Y., Kuo, L. & Chen, M.H. (2011) Improving marginal likelihood estimation for Bayesian phylogenetic model selection. *Systematic Biology*, **60**(2), 150–160.

Yamauchi, K. (1979, 1978) Taxonomical and ecological studies on the ant genus *Lasius* in Japan (Hymenoptera: Formicidae). I. Taxonomy. *Science Report of the Faculty of Education Gifu University (Natural Science)*, **6**, 147–181.

Yang, Z. (2006) *Computational Molecular Evolution*, p. 376. Oxford University Press, Oxford.

Zachos, J.C., Dickens, G.R. & Zeebe, R.E. (2008) An early Cenozoic perspective on greenhouse warming and carbon-cycle dynamics. *Nature*, **451**, 279–283. https://doi.org/10.1038/nature06588.

Zalessky, Y.M. (1949) A new tertiary ant. [in Russian.]. *Sovetskaya Geologiya*, **40**, 50–54.

Zhang, C., Stadler, T., Klopfstein, S., Heath, T.A. & Ronquist, F. (2016) Total-evidence dating under the fossilized birth-death process. *Systematic Biology*, **65**, 228–249.

Accepted 22 September 2021